Studying the Transition from Fossil Fuel to Renewable Generation in Hydro Dominant Electricity Systems

Luke Schwartfeger

A thesis presented for the degree of
Doctor of Philosophy
in
Electrical and Computer Engineering
at the
University of Canterbury,
Christchurch, New Zealand.

February 2021

ABSTRACT

Climate change is a significant and ever-growing threat to societies around the world. To reduce its consequences, immediate changes to reduce anthropogenic greenhouse gas emissions (GHGs) are needed. A major contribution to global GHGs is from fossil fuel thermal generation supplying a majority of the world's electricity. Its extensive use is due to a variety of reasons including its controllability, enabling it to fulfil a range of roles to maintain security of supply for electricity systems (e.g. peaking, baseload and load following). To transition to a low-to-zero emission system, thermal generation needs to be replaced with renewable generation such as wind and solar. Wind and solar generation production is intermittent and has limited controllability. As a result, it can only reliably provide energy (not capacity) and cannot fulfil the same roles as thermal generation, hence other assets will be required to maintain security of supply.

Systems with established hydro generation and reservoir storage have an advantage when integrating renewable generation. In conjunction with hydro reservoir storage, wind and solar generation intermittency is largely mitigated as water can be conserved in reservoirs during high renewable production periods, effectively storing this energy. Hydro generation itself has no operational GHG emissions and is more controllable than thermal generation, hence it can take the security of supply roles.

However, hydro generation comes with its own risks. Low inflow years (droughts) can threaten security of supply, which in New Zealand is often managed with thermal generation. Also, managing a hydro electric system is complex, in part due to reservoirs linking the current generation dispatch decision to all future dispatch decisions. As such, specialist hydro scheduling optimisation methodologies have been developed to assist with hydro system management.

To study the renewable generation transition of hydro-thermal electricity systems, a hydro scheduling modelling tool is developed for system studies[1]. It consists of two sub-tools: a Price Discovery and System Operation Simulation (SOS). The Price Discovery uses a deterministic Dynamic Programming based approach to produce optimal water

[1] i.e it is not intended for operational purposes

value functions, one for each reservoir in the system model. The SOS simulates the operation of the system using these water value functions to determine the hydro generation prices. Time series it produces include storage trajectories, generation dispatch and transmission power flow. A deterministic Price Discovery is deem sufficient for the system studies particularly for New Zealand, although in future work, it can be extended to consider the stochastic nature of inflows.

To accompany the hydro scheduling modelling tool, a New Zealand system model is developed. It is a two-transmission-node, two-reservoir model representing New Zealand's North and South Islands. Although simple, the model sufficiently represents New Zealand system's major constraints and dynamics. These include the transmission constraint between the North and South Island, the geographical mismatch between demand (majority in the North Island) and hydro resource (generation, storage and inflows, majority in the South Island) and the temporal mismatch between hydro inflows (high in spring and summer) and demand (high during winter). These issues are evident in New Zealand's system given its limited hydro storage, being only 9% of annual demand.

A unique aspect of the hydro scheduling modelling tool is that it uses a high temporal resolution (half hourly to daily) over a medium term time horizon (one year). This allows an investigation into the impact of generation and transmission capacity constraints on the water value functions and system operation. A high temporal resolution is valuable given wind and solar generation's intermittency.

To demonstrate the modelling tool's capability for quantifying the impacts of the renewable generation transition, it is applied to a 2030 scenario variant of the New Zealand system model. This model has increased demand and two of the thermal generators are considered decommissioned. The study determines the amount of additional renewable generation require to avoid empty reservoirs and consequential demand curtailment and the value of additional hydro storage and generation capacity and transmission capacity. The value of diversifying between additional wind and solar generation is also investigated.

Deputy Vice-Chancellor's Office
Postgraduate Office

UNIVERSITY OF CANTERBURY
Te Whare Wānanga o Waitaha
CHRISTCHURCH NEW ZEALAND

Co-Authorship Form

This form is to accompany the submission of any thesis that contains research reported in co-authored work that has been published, accepted for publication, or submitted for publication. A copy of this form should be included for each co-authored work that is included in the thesis. Completed forms should be included at the front (after the thesis abstract) of each copy of the thesis submitted for examination and library deposit.

Please indicate the chapter/section/pages of this thesis that are extracted from co-authored work and provide details of the publication or submission from the extract comes:
N/A

Please detail the nature and extent (%) of contribution by the candidate:
The PhD candidate did the research and wrote all sections of the published manuscript. The co-authoring supervisory team suggested research directions and offered criticisms which the candidate worked into the manuscript.

Certification by co-authors

If there is more than one co-author then a single co-author can sign on behalf of all. The undersigned certifies that:

- The above statement correctly reflects the nature and extent of the PhD candidate's contribution to this co-authored work
- In cases where the candidate was the lead author of the co-authored work, he or she wrote the text.

Name: - Signature: Date: -

CONTENTS

ACKNOWLEDGEMENTS

Through my PhD journey, I have received so much support from many people.

First of all, I would like to thank my supervisors, past and present. Allan Miller for securing the GREEN Grid project funding that enabled me to undertake this PhD, Gari Bickers for providing an expert industry perspective and Radnya Mukhedkar for keeping me focused and keeping me focused and calm through advice and direction. And to Alan Wood, who was incredibly supportive, whom has devoted significant time to discuss my research, providing clarity when I most needed it and being patient with my rambling. Thank you very much for your dedication and belief in me.

Thank you to the Electrical and Computer Engineering Department as a whole for their support. In particular, Neville Watson who provided some early contacts that helped me and Deborah Erueti who is an excellent postgraduate administrator who answered many-a-random inquiry from me. Thank you to the technicians who assisted me with everything computer related: Florin Predan, Mike Shurety and David Van Leeuwen. A particular thank you to Florin for my pestering regarding the computer lab.

Thank you to Jeffrey Burl who give me an introduction to multi-stage decision problems and dynamic programming, starting my learning process. Also thank you to Grant Read, Greg Sise, Mark Nelson and Tom Halliburton for their time educating me on the hydro scheduling problem in New Zealand. Also, thanks Ian Mason for hallway chats about renewable generation and New Zealand's energy future.

Thank you to the EPECentre for providing so many presenting, travel and learning opportunities. I apologies for the amount of paper I have used from the stationary cupboard, the sudden rearrangement of computers in the office and, when applicable, my pacing when I was in deep thought. Thank you to Shreejan Pandey for discussions on productivity and developing a career and David Santos-Martin for entrepreneurship perspective and assisting with my first conference paper. Thank you to all of the administrators and managers: Sue Bradley, Danica Nel, Ruth Payne, Kirsten Marsh, Linsey Mackenzie, Susannah Hawtin, Marie-Claire Brehaut, Shreejan Pandey and Isabelle Le Quellec; You have all enabled not only the opportunities I have been fortunate to have, but for many students. Thank you to the researchers and engineers

for the knowledge and conversations: Bill Heffernan, Richard Strahan, Sharee McNab, Ryan Van Herel and Nurzhan Nursultanov.

Thank you to the EPECentre postgrads, some of you I've shared an office with: Josh Schipper, Michael Campbell, Thomas Smart, Euan McGill, Parash Acharya, Dougal McQueen and Scott Lemon. The intermittent discussion on everything and anything and the odd beer provided a great level of distraction when needed. A particular thanks to Josh for lending me his mathematical knowledge when I was teasing out problems and Scott for his advanced understanding of algorithms and coding.

Thank you to my friends and flatmates who have mostly put up with my random behaviours and long radio-silence periods - I look forward to reconnecting with you.

Thank you to Generation Zero, in particular the Christchurch crew when I was actively volunteering. Through working with you all on climate change action advocacy, you broadened my perspective how to be involved in the change we need which gave me validation for my work.

Thank you to my partner Chrissy. You have provide solutions to problems where I had already conceded, reminded me of my efforts that I had discounted and moved on from, and shown me life outside of the PhD-centric realm I had placed myself into. I love you very much.

Lastly, thank you to my Mum, Dad and brother, Daniel. You have been very sympathetic and mindful of me as I've been working on my PhD, consistently caring about what I'm doing and how it is going. A major part of me being able to pursue this has been because of your support. Mum, thank you for your compassion when I simply needed to discuss the difficulties I've faced, your empathy is immense. Dad, thank you for your immediate understand of my situation and your help with my random math problems I approached you with, you are the best teacher. Daniel, thank you for the random chill out sessions gaming and your quick wit always making me laugh, time with you is truly relaxing. I look forward to spending more time with you all.

Chapter 1

INTRODUCTION

Electricity systems are an integral part of modern society in the developed world and a key objective for developing nations to establish, given that they provide the energy that powers our lives. As society has developed, electricity systems have been grown to cater to everyone's needs and wants, when and where it is required. The primary operational objective of the electricity system and the organisations that participate in its operation is to maintain security of supply.

Maintaining security of supply involves ensuring that adequate electricity will be available over the foreseeable future and can be thought of in different time horizons. Pérez-Arriaga [2007] provides a useful conceptual breakdown of electricity system operation, management, investment and strategy:

- Security (Real-Time): The readiness of the available electricity system assets (generation and transmission) to supply demand at each instant through the system dispatch

- Firmness (Short- to Medium-Term): Ensure adequate energy and capacity resources are available over the period. Energy resources include stored energy (hydro reservoir storage and fossil fuel stockpile) and forecast renewable generation. Capacity resources include dispatchable generation, demand response and fast acting storage (batteries). This involves securing fuel contracts and reasonable hydro storage management.

- Adequacy (Long Term): System expansion planning and constructing new generation and transmission infrastructure to meet forecast long-term demand (energy and capacity).

- Strategic Energy Policy (Long to Very Long-term): Monitoring the long-term availability of energy resources (e.g. geothermal reservoir health, impacts of climate change on system dynamics).

Strict definitions of the length of the time horizons do not exist but general spans are:

- Real-Time: Instantaneous to less than an hour
- Short-Term: One hour to one week
- Medium-Term: One week to one year
- Long-Term: One to five years
- Very Long-Term: Beyond five years

Historically, demand growth has been the major driver behind electricity system development. However, environmental constraints also influence development of electricity systems. Examples of constraints are avoiding damage to ecosystems and limiting pollution, both of which can restrict the construction of generation. Undoubtedly, the environmental concern with the highest priority is climate change. Although fossil fuels have played a primary role in the development of many countries, they have also contributed to global warming which is resulting in many negative effects including increased frequency of extreme weather events and sea level rise and promises more severe impacts unless immediate action is taken to reduce Greenhouse Gas (GHG) emissions.

In order to combat climate change, electricity systems will need to transition to low or net zero emissions. This primarily involves minimising the use of fossil fuel thermal generation (henceforth referred to as conventional thermal generation) to reduce GHG emissions. An issue with this is that conventional thermal generation fulfils several important security of supply roles in electricity systems including peaking, load following and baseload supply. As thermal generation production is reduced, investment into other energy and capacity resources will need to occur to cover these roles. One such resource will be renewable generation (wind, solar and geothermal) which fortunately have zero or minimal operational GHG emissions. Electricity systems will also need to supply demand which is expected to increase as other fossil fuel uses such as transportation, process heat and space heating shift to being electric [Transpower New Zealand 2018b].

The climate friendly transition of electricity systems will be accompanied with a variety of challenges affecting security of supply and efficiencies. One such challenge is that wind, solar and geothermal generation are non-dispatchable, that is their output is not able to be readily controlled. The production of wind and solar generation is variable as they depend on location, climatic conditions, weather, season and other time variant factors. Given this, they cannot be depended upon to provide capacity when needed, such as during the critical peak demand times in evenings and mornings. Although

they are variable, their output is reasonably predictable on a short time horizon (one to two hours, refer to Chapter 3) so other controllable generation can be coordinated with non-dispatchable generation. Geothermal generation is an excellent supplier of baseload demand but it is restricted to this mode of operation as only very slow variations in output are possible to limit plant degradation mechanisms.

An inefficiency with wind and solar generation is that periods of high production can occur requiring energy to be spilt by throttling the wind turbines or altering the operation mode of solar inverters. This excess can only be utilised if there is sufficient storage or dispatchable demand. The risk of spilling energy means there is a trade-off between the amount of wind and solar capacity installed and the economical cost of doing so, which introduces an economic limitation on the total capacity of installed renewable generation.

The locations of renewable generation sites are dictated by where the natural resource is available, whereas thermal generation has far more location-based flexibility. The disadvantage of this geographical constraint is two-fold. Firstly, connecting renewable generation requires unique extensions to the transmission system, adding to capital costs. Secondly, transmitting the distantly produced renewable generation results in transmission losses, reducing the system's overall efficiency.

In aggregate, managing these challenges involves utilising other resources. Locational issues can be overcome by constructing new transmission assets and reinforcing the existing grid. To mitigate the issues with non-dispatchability, other dispatchable generation needs to be available to ensure that demand can always be met. Reducing the use of conventional thermal generation makes this more difficult as it fulfils all the generation roles (peaking capacity, load following and baseload supply). Fortunately, hydro generation, can also perform these roles. Hydro generation is highly flexible as the water flow propelling the turbine is fully controllable. Often hydro generation also has an upstream reservoir to store water to release in the future which can perform the same function as thermal fuel storage. Also, the flexibility of reservoir storage means hydro generation can be coordinated with wind and solar generation to capture excess production that would otherwise be spilt, increasing the economic renewable generation penetration level.

Unfortunately hydro generation is not free of difficulties. One of these is that the inflows of water into upstream reservoirs that hydro generation use are variable and uncertain in a similar manner to wind and solar resources. This in combination with limited reservoir storage leads to the storage management challenge, where the operator

must have storage at an appropriate level to capture any incoming inflows over the forecast future, have adequate water available of the hydro generators to supply demand, and avoid the minimum and maximum storage levels to avoid shortages and spill respectively. Avoiding shortages is a major concern as this can threaten security of supply. In New Zealand, during periods of low inflows and high demand, conventional thermal generation has been dispatched ahead of hydro generation to conserve stored water, which is a role called hydro (storage) firming. A challenge with transitioning to a low emissions electricity system is that conventional thermal generation will not be able to perform this function. This shifts hydro storage management from being predominantly an operational problem, where conventional thermal generation could be relied on, to a planning problem, where ensuring that sufficient renewable generation (wind, solar and geothermal) is planned and constructed to mitigate shortage risks. In storage situations, some conventional thermal generation may have to be held in reserve.

1.1 OBJECTIVES

The primary objective is to develop a modelling tool that is capable of:

1. Identifying and quantifying potential issues for maintaining security of supply with hydro dependent electricity systems reducing conventional thermal generation and increasing renewable generation (wind, solar and geothermal) penetration as a part of transitioning to low emissions electricity systems.

2. Investigate the value of system investment options in maintaining security of supply. These options include generation, hydro storage and transmission capacity.

To achieve this, a medium term, high temporal resolution deterministic Dynamic Programming based modelling tool is developed, and to demonstrate its usefulness it is applied to a future system scenario of a New Zealand system model.

1.2 THESIS OUTLINE

This thesis is organised as follows:

Chapter 2 Hydro Scheduling Theory and Literature Review:
Discusses the hydro scheduling problem highlighting its complexity that makes it a unique and difficult problem to solve. The hydro scheduling problem's multi-stage decision problem formulation is presented followed by the theory of the solution methodologies and corresponding literature. This provides an overview of the consistent practices in the field.

Chapter 3 New Zealand System Model Design:
The model of New Zealand's electricity system is presented. A simple two-node, two reservoir representation is opted for to impose minimal computational load while still capturing the impact of generation, storage and transmission capacity constraints. The components of the New Zealand electricity system model are discussed, outlining constraints and dynamics that are accounted for. Two versions of the system model are shown: circa 2015 and a 2030 scenario system.

Chapter 4 Hydro Scheduling Tool:
This chapter presents the development of the hydro scheduling tool. It consists of two sub-tools: a Price Discovery, which is a deterministic Dynamic Programming based tool that produces water value functions for each hydro reservoir over a year-long horizon with a time interval of a half hour to one day, and System Operation Simulation, which takes these water value functions and simulates the operation of the system. As a part of the Price Discovery development, an alternative convergence criteria is presented and justified, as well as an examination of the effect of boundary conditions imposed on the water value functions when the modelling tool uses a high temporal resolution.

Chapter 5 Sensitivity Studies:
There are two sensitivity studies performed. The first study examines a range of time interval spans (half hour to daily) in order to determine the differences in the water value functions and system operation. The second study compares a range of storage discretisation resolutions. The impact on the water value functions, system operation and computation times are clarified.

Chapter 6 Evaluating System Investments:
This chapter demonstrates the capability of the modelling tool to achieve the objectives. Three system studies were carried out with the 2030 New Zealand system model scenario:

1. Exploring a range of additional renewable generation to cater for demand growth and the decommissioning of a portion of thermal generation

2. Determining the value of increased hydro generation and storage capacity and additional transmission capacity

3. Finding the impact of different combinations of wind and solar renewable generation

1.3 CONTRIBUTIONS

The contributions of this thesis are:

- Development of a simple New Zealand hydro thermal electric power system model that captures the key constraints of the system while imposing the minimal computational load that allows the study of renewable generation transitions
- Development of a deterministic Dynamic Programming based hydro scheduling modelling tool with a high temporal resolution (half hour to daily). This feature allows the electricity system capacity constraints to be captured.
- The value and computational cost of a range of high temporal resolutions in a medium term tool are quantified, identifying the difference in the water value functions and storage trajectories.
- Provides an in-depth examination of the dynamics behind the calculation of the water value functions. This includes an investigation into the water value function boundary conditions and how temporal resolution can impact the condition's influence. A time interval invariant option is implemented.
- Determination of representative inflow sequences (from dry to wet years) from the historical available data through simulation rather than total annual inflow, a common practice in New Zealand
- A clear overview of the major hydro scheduling methodologies and their development from a literary environment that spans a relatively long time frame and many variants.
- Creation of a simple water value function to hydro price function procedure that is scalable with the number of reservoirs and able to incorporate any one dimensional interpolation method
- Produces a preliminary value for the ratio between wind and solar generation for New Zealand that takes advantage of their combined temporal diversity

Chapter 2

HYDRO SCHEDULING THEORY AND LITERATURE REVIEW

The earliest published hydro scheduling methodology dates back as early as 1946 [Wallace and Fleten 2003]. From then, there has been extensive development of a range of approaches and variations in those approaches and applying them to conduct studies of the systematic changes in electricity systems. This chapter discusses the two major branches of hydro scheduling methodologies and their descendent methods:

- Dynamic Programming:
  - Stochastic Dynamic Programming
  - Constructive Dual Dynamic Programming
- Stochastic Programming (Optimisation):
  - Stochastic Dual Dynamic Programming

Implicit Stochastic Optimisation is also discussed. Prior to presenting this methodology discussion, a brief overview on hydro electric power systems is given followed by an overview of the hydro scheduling problem and its formulation as a multistage decision problem.

Hydro scheduling methodologies are applied to a variety of situations outside of hydro generation, such as irrigation and waterway management, for which the decision variable is water release. Note that, given the focus here is on electricity systems, water release and hydro generation will be used interchangeably.

2.1 HYDRO ELECTRIC POWER SYSTEM OVERVIEW

An electric power system can be broadly broken down into four components: Generation, Transmission, Distribution and Demand. Generation injects ac (alternating current) electric power into the transmission system which carries electricity via high and medium

voltage (HV, MV) power lines and transformers to distribution networks and direct-connect major consumers. Distribution networks consist of medium and low voltage lines and transformers that supply demand. A variety of generation types include fossil fuel thermal, wind, solar, geothermal and hydro.

The manner in which an electric power system is operated varies from system-to-system around the world. However they can be broadly categorised into centrally controlled or market operated. A centrally controlled system is coordinated typically by a state authority charged with maintaining security of supply and maximising public utility. Through market operation, generation companies offer electricity onto one or more markets (e.g. spot market) from which retail companies bid into, purchase and on-sell to consumers, with the objective to maximise profit. A system operator uses the offers and system data to optimise the generation dispatch and coordinates with the generation companies and transmission system operator to achieve it. The system operator also procures reserves and other services from the market to manage real time variation and contingent events.

A hydro scheme refers to one or more reservoirs that could be controlled or uncontrolled, waterways that carry water between these reservoirs, and hydro generators which are either situated on or divert water from waterways and produce electrical energy from the water flow. Some reservoirs directly preceding hydro generators are headponds which maintain the water pressure. The inflows into the reservoirs are sourced through rainfall or snow melt within their catchment areas. The operation of a hydro scheme involves the hydro operator coordinating the water throughout the scheme to meet the dispatch level allocated to them by the system operator.

A hydro electric power system refers to an electric power system that has a high proportion of hydro generation and storage. A hydro electric power system that also relies on thermal generation is often referred to as a hydro-thermal (electric) system.

2.2 HYDRO SCHEDULING PROBLEM

In simple terms, the hydro scheduling problem refers to the determination of the optimal generation dispatch which includes the hydro generation with reservoir storage. In an electric power system comprised of mainly conventional thermal generation, operating the system is a time interval to time interval affair; there is no need to consider the impact of the current dispatch decision on the next, except for real-time (e.g. ramp rates) and long-term (e.g. fuel management) dynamics. With the inclusion of reservoir storage and hydro generation, the current dispatch decision is a major factor in determining the amount of hydro storage available for subsequent decisions. This temporal coupling

between decisions expands the decision space, increasing the complexity of determining the optimal decision for the current decision stage.

The main benefit of hydro generation is that stored water is free fuel which, when released through a hydro generator, displaces costly thermal generation resulting in cheaper electricity production. However, operating hydro generation is not devoid of risk, and poor management can lead to unfavourable situations such as a shortage or excess of water. When a shortage occurs more expensive thermal generation units need to be dispatched to cover electricity demand. In the extreme case hydro generation capacity may be constrained by the lack of water, leading to demand curtailment as there is inadequate generation capacity to supply demand. A shortage could occur if hydro generation was heavily dispatched prior to a low inflow period. An excess of water occurs when the maximum storage (water level) is breached. A reservoir's storage capacity is set for environmental and societal reasons by a regulatory entity. If the water stored exceeds this level, it is required to be spilt from the reservoir. Spilt water does not flow through a hydro generator, and is a waste of resource, and increases the amount of thermal generation required.

The other variable in determining the available water at any decision stage are water inflows into the hydro schemes. Inflows are the aggregation of precipitation flowing through waterways in a hydro scheme's catchment. When precipitation falls as rain, the amount of water entering the scheme's reservoirs is coincident, whereas during cold winter months, some or the majority of the precipitation may fall as snow. This snow later melts typically during spring, adding water to the scheme. This results in a seasonal inflow pattern. However, the volumes of snow-melt and the timing of rainfall (otherwise called inflow events) is uncertain. Further, there is year-to-year variation in inflow volumes leading to dry and wet inflow years (low and high inflows respectively). For hydro reliant systems, inflow uncertainty is a major source of risk when operating a hydro electric system as there is no guarantee that if water is released at present that inflows will replenish it in the near future. One of the challenges of the hydro scheduling problem is to optimally manage hydro reservoirs under this uncertainty while providing a cost effective and reliable electricity supply.

An electrical power system can have multiple hydro schemes geographically distributed with a range of storage and generation capacities. This adds an extra level of coordination ensuring storage is distributed such that energy is not stranded in one area of the network due to transmission system constraints. Also, a hydro reservoir system consists of a network of hydro generation plants and reservoirs connected by waterways (rivers or man-made canals) called a hydro scheme. A hydro scheme has constraints including maximum and minimum water levels for each reservoir and maximum or minimum

flows through some of the waterways. All of these constraints need to be abided by when operating a hydro scheme.

The hydro scheduling problem is classed as a multi-stage decision problem which the next section outlines. This includes its mathematical formulation and an introduction of its associated terminology.

2.3 MUTLI-STAGE DECISION PROBLEM

A multi-stage decision problem consists of [Kirk 1970]:

- A dynamic equation which relates the system's current state (x_t), control decision (u_t) and disturbances (b_t) to the future state (x_{t+1})
- A performance measure which evaluates how well the system is operated, either by a cost function ($C_{t,T}(x_t, u_t)$) or benefit function ($B_{t,T}(x_t, u_t)$). Both are functions of decisions and system states over the problem's time horizon, t to T where t indexes the time (or decision stage) and T is the end-of-horizon time step. The time horizon is also referred to as a planning horizon.
- Constraint equations which define relationships between the system's variables (such as those in the dynamic equation) and the limits on the state and decision variables.

The general cost function of a multi-stage decision problem is shown in Equation (2.1), and consists of two parts. $C^x(x_T, T)$ is the cost function for the system existing in the state x_T at the end of the horizon ($t = 1, ..., T$) and $C^u(x_t, u_t)$ is the cost function of the control decision u_t from the state x_t.

$$C_{t,T}(x_t, u_t) \;=\; C^x(x_T, T) + \sum_{t=t_0}^{T} C^u(x_t, u_t) \tag{2.1}$$

The decision and state variables are bounded by constraints shown in Equation (2.2). The first constraint is the form of the dynamic equation and other system constraints, and the latter two are bounds on the states and control decisions.

$$\begin{aligned} x_{t+1} &= B_t^x x_t + B_t^u u_t + b_t \\ \underline{x}_t &\leq x_t \leq \bar{x}_t \\ \underline{u}_t &\leq u_t \leq \bar{u}_t \end{aligned} \tag{2.2}$$

For a hydro electric system, the variable vectors typically represent:

- State variables, $x(t)$: Hydro reservoir storage,
- Decision variables, $u(t)$: Dispatched hydro and thermal generation, and spill from reservoirs and transmission system power flows.
- Disturbances, b_t : Inflows into the hydro reservoirs and electricity demand.

Stochastic multi-stage decision problems also regard inflows at earlier time intervals (e.g. $t-1$) as state variables. For simplicity of the remaining formulation, the only state variable represented will be hydro storage. Typically constraints of the hydro electric system include:

- the dynamic equation which is the water balance for the hydro schemes
- demand satisfaction, and
- the power flow between electricity system nodes.

Equation (2.3) shows the water balance equation where $s_t \in x_t$ is the hydro storage vector, $f_t \in b_t$ is the inflow vector, $g_t^h \in u_t$ is the vector of hydro generation water releases and $w_t \in u_t$ is the spill vector. Henceforth, x_t will be replaced by s_t.

$$s_{t+1} = s_t + f_t - g_t^h - w_t \tag{2.3}$$

The performance measure of a hydro thermal electric system (Equation (2.4)) includes the cost of thermal generation at each stage and a penalty if demand is curtailed (typically the value of lost load). A cost is not allocated to the state of the system or other control decisions.

$$\begin{aligned} C^u(s_t, u_t) \Rightarrow C^u(u_t) &= c_t \cdot u_t \\ C_{t,T}(u_t) &= \sum_{\tau=t}^{T} c_\tau \cdot u_\tau \end{aligned} \tag{2.4}$$

c_* is the cost per unit vector. A series of control decisions spanning a time horizon $t = 1, ..., T$ is known as a policy, $U_{t,T}$. A policy will direct the system along a storage trajectory ($S_{t,T}$) from an initial storage s_1. If the policy and trajectory abide by system constraints, they are deemed admissible. $U_{t,T}$ and $S_{t,T}$ are present in Equation (2.5).

$$\begin{aligned} U_{t,T} &= \{u_t : t = 1, ..., T\} \\ S_{t,T} &= \{s_t : t = 1, ..., T\} \end{aligned} \tag{2.5}$$

The admissible policy that minimises the cost function is the optimal policy, $U^*_{t,T}$ and guides the system along the optimal trajectory $S^*_{t,T}$. Multi-stage decision problem methodologies are used to solve the hydro scheduling problem. The remainder of the chapter covers these.

2.4 DYNAMIC PROGRAMMING

Bellman [1954] presents Dynamic Programming (DP) as a means to solve multi-stage decision problems. Instead of considering all decisions over the time horizon at once, as the native multi-stage formulation implies, Dynamic Programming considers each stage one at a time, transforming the problem from a single problem with one large search space of T decisions into a problem of T smaller search spaces each concerned with a single stage's decision. For this reason, DP is referred to as a decomposition approach.

At each stage, the impact of the present decision on future decisions still needs to be accounted for. Dynamic Programming achieves this with two cost components, an immediate cost ($C_{t,t+1}(x_t, u_t) = c_t \cdot u_t$) and a future cost ($C_{t+1,T}(s_{t+1}) = \alpha_{t+1}(s_{t+1})$ as shown in Equation (2.6). The immediate cost corresponds to the cost of the decision at present, which is generally the cost of dispatched thermal generation. The future cost is the total cost of all future decisions over the time horizon as a consequence of the decision at present. Note that the future cost is a function of the $t+1$ storage vector (s_{t+1}) determined with the water balance equation (Equation (2.3)) which is dependent on the state at t (s_t) and the decision at t (u_t).

$$\begin{aligned} C_{t,T}(s_t, u_t) &= C_{t,t+1}(s_t, u_t) + C_{t+1,T}(s_{t+1}) \\ &= c_t \cdot u_t + \sum_{\tau=t+1}^{T} c_\tau \cdot u_\tau \\ &= c_t \cdot u_t + \alpha_{t+1}(s_{t+1}) \end{aligned} \tag{2.6}$$

The basis of the decomposition between the immediate and future cost elements in a multi-stage decision problem is the *Principle of Optimality* [Bellman 1954]:

> *An optimal policy has the property that whatever the initial state and initial decision are, the remaining decisions must constitute an optimal policy with regard to the state resulting from the first decision.*

In other words, the validity of the decomposition to immediate and future cost components depends on the future cost function ($\alpha_{t+1}(s_{t+1})$) representing the cost of the optimal policy from $t+1$ to T while the system is at the current storage state (s_t). Given this, solving the multi-stage decision problem involves optimising the single stage problem's cost function for each time step:

$$\min_{u_t} C_{t,T}(s_t, u_t) = \min_{u_t} \left[c_t \cdot u_t + \alpha^*_{t+1}(s_{t+1}) \right] \tag{2.7}$$

subject to the system constraints (Equation (2.2)). When optimising for the current stage, the optimal decision balances the immediate and future costs of the decision. For the hydro scheduling problem, the decision is the amount of hydro and thermal generation to dispatch to supply demand. The greater the hydro generation dispatched, the lower the immediate cost since hydro generation has no fuel cost. However, the water released will not be available later and thermal generation may need to be dispatched in the future instead, hence the future cost is higher. In the opposite case, the greater the amount of thermal generation dispatched, the lesser the future cost due to the conservation of water but the greater the immediate cost.

An issue with solving the single stage problem at t is that the future cost function representing the costs for decisions u^*_{t+1} to u^*_T from $t+1$ to T is needed, effectively before they occur. An approach to manage this is to solve the problem backwards $(t = T, T-1, ..., 1)$ which makes the future cost function readily available at any time t. This is called *Backwards Recursion*. In its native form Dynamic Programming is deterministic, so has perfect foresight of system inputs such as hydro inflows and electric power demand over the time horizon. Stochastic Dynamic Programming accounts for inflow uncertainty and is covered later.

The key relationship between $\alpha^*_{t+1}(s_{t+1})$ and $\alpha^*_t(s_t)$ is described by the recurrence equation:

$$\begin{aligned} \alpha^*_t(s_t) &= \min_{u_t} \left[c_t \cdot u_t + \alpha^*_{t+1}(s_{t+1}) \right] \\ &= c_t \cdot u^*_t + \alpha^*_{t+1}(s_{t+1}) \end{aligned} \tag{2.8}$$

Using Equation (2.8), $\alpha^*_t(s_t)$ (left-hand side) can be constructed from the optimal decision vector u^*_t determined by optimising the single stage problem with the future cost component $(\alpha^*_{t+1}(s_{t+1}))$. However, to do this on a continuous state space would require both an optimal policy function $(u^*_t(s_t))$ and future cost function $(\alpha^*_{t+1}(s_{t+1}))$ defined on $\underline{s}_t \leq s_t \leq \bar{s}_t$. At the very least, this requires assumptions about the form of these functions, for concessions on the representation of the optimal policy over the time horizon to be made, or both. Instead of this, with Dynamic Programming the state space is discretised (Equation (2.9)) and the single stage optimisation (Equation (2.8)) is evaluated at each discrete state vector, $s_{t,j}$, producing an approximate future cost function at discretised storage vectors, $\widetilde{\alpha}_t(s_{t,j})$. An optimal dispatch decision is not guaranteed to result in a storage vector (s_{t+1}) coincident with the discretised storage state vector so the value of $\alpha^*_{t+1}(s_{t+1})$ is determined with interpolation.

$$\begin{aligned} \underline{s} \leq s \leq \bar{s} \quad &\Longrightarrow \quad \{\hat{s}_k \quad \text{for} \quad k = 1, ..., M\} \\ \alpha_t(s_t) \quad &\Longrightarrow \quad \widetilde{\alpha}_t(s_{t,k}) = c \cdot u^*_t(s_{t,k}) + \widetilde{\alpha}^*_{t+1}(s_{t+1}) \end{aligned} \tag{2.9}$$

where:

- $\{\hat{s}_k \; \forall \; k\}$ is the discretised state space and $\hat{s}_k$ is the k'th discretised state vector
- M is the total number of discretised state vectors
- $\widetilde{\alpha}^*_t(s_{t,k})$ is the approximate future cost function

A part of the initialisation of a DP methodology is to set a future cost function at the end of the time horizon (i.e. $t = T + 1$ and $\widetilde{\alpha}^*_{T+1}(s_{T+1})$) so the backwards recursion can be implemented. A method to generate the *optimal* end-of-horizon cost function is to successively conduct the DP optimisation backward over the horizon. Upon reaching the beginning of horizon ($t = 1$), $\widetilde{\alpha}^*_{T+1}(s_{T+1})$ is set to $\widetilde{\alpha}^*_1(s_1)$ and the optimisation is repeated. This is conducted until a steady state is reached [Côté and Leconte 2016, Read 2014]. For the first DP run, $\widetilde{\alpha}^*_{T+1}(s_{T+1})$ is set to an arbitrarily defined approximate function.

Three factors that influence the time required to solve a DP problem are the number of system states, discrete levels to represent each state, and time stages. The influence of the numbers of system states and discretisation levels is specifically referred to as the *Curse of Dimensionality*. The curse of dimensionality introduces a decision where the representation of the physical system needs to be balanced against the computation time required. For a hydro electric system which has a number of hydro schemes, each with multiple reservoirs, attempting to perfectly represent this would lead to significant computation times. Common measures to manage the dimensionality include aggregating the reservoirs and schemes together or applying the hydro scheduling methodology to the system in a spatially decomposed manner. Both of these techniques are presented in literature based examples below.

The calculation of the $\widetilde{\alpha}^*_t(s_{t,k})$ involves $\widetilde{\alpha}^*_{t+1}(s_{t+1})$ which is on the continuous state space even though is is only defined on the discrete state space. It is possible to use the discretised state space, but this would impose the discretisation of u_t as well. Instead, if the state transition from s_t to s_{t+1} results in s_{t+1} being between the discretised state vectors, then $\widetilde{\alpha}^*_{t+1}(s_{t+1})$ is determined by interpolating from the surrounding future cost function values. Interpolation options include linear [Young 1967] and cubic spline interpolation [Tejada-Guibert et al. 1993].

Upon completing the single stage optimisations backwards over the time horizon, the optimal policy function ($U^*_t(s_{t,k})$) is available to produce the operating rules. At any time t in the time horizon and with the current state, $s_{t,k}$, the optimal hydro generation dispatch can be found. This is specific to the inflow and electric power system conditions (e.g. demand profile) imposed.

A common and likely more popular alternative to producing optimal policy functions is to store water value functions, $v_t^*(s_{t,k})$. A water value is effectively the fuel price for hydro generation and can serve as the hydro generation price function in a typical generation dispatch cost function.

In a similar manner to the optimal policy function, the water value function spans the time horizon and is in terms of the storage state space ($s_{t,k}$). The recurrence equation relating the future cost functions at t and $t+1$ (Equation (2.8)) is substituted with Equation (2.10). This is also based on the Principle of Optimality but applied to the water value function.

$$v_t^*(s_t) = v_{t+1}^*(s_{t+1}) \tag{2.10}$$

The optimal water value function is produced by projecting an end-of-horizon arbitrarily defined water value function ($v_{T+1}^*(x_j) \forall j$) backwards for which Equation (2.10) provides the basis. Equation (2.10) states that the t optimal water value function at t storage (s_t) is equal to the $t+1$ water value at reservoir storage at $t+1$ (s_{t+1}). s_{t+1} is determined with the water balance equation (Equation (2.3)) using the optimal decision found with the single stage optimisation. As with the future cost function, given that v_{t+1}^* is defined on the discretised storage state space and s_{t+1} may be between these, $v_{t+1}^*(s_{t+1})$ may need to be interpolated.

With the water value function approach, the single stage problem objective function changes from minimising the immediate and future cost to a generation dispatch optimisation (Equation (2.11)). Examining the original cost function (Equation (2.6)), the future cost function is analogous to a hydro generation cost. The higher the hydro generation production, the high the future cost (thermal generation) and vice versa. With the water value approach, the water value function can serve as a hydro generation price function, and the integral of its product with the hydro generation dispatch replaces the future cost function.

$$\min_{u_t} \left[c_t \bullet u_t + \alpha_{t+1}^*(s_{t+1}) \right] \Longrightarrow \min_{u_t} \left[c_t \bullet u_t + \int_0^{u_t} v_{t+1}^*(s_{t+1}) \cdot q_t d(q_t) \right] \tag{2.11}$$

With the optimal water value function, at any t in the time horizon and storage (s_t), the optimal hydro generation prices can be found then used in a generation dispatch optimisation.

2.4.1 Dynamic Programming Literature

Typically DP approaches discretise the storage state space and perform an optimisation or search procedure (e.g. LP) to determine the optimal policy or water value at each point. In an era when computational resources were far more scarce, Becker and Yeh [1974] presented an early DP variant wherein the LP solution determined the water release for discrete levels of possible demand, referred to as LP-DP. With the resultant operating function, a DP algorithm is applied to find the optimal releases obeying the operating rules and producing the storage trajectory. This effectively focuses on a feasible operational storage region by proxy hence somewhat avoids the curse of dimensionality. However, the observation from Grygier and Stedinger [1985] is that Bellman's Principle of Optimality is not valid for the solution since the storage and inflow state space is not captured. Regardless of this, LP-DP was implemented in a handful of cases. Becker and Yeh [1974] and Mariño and Mohammadi [1983] both applied LP-DP to two reservoirs of the California Central Valley Project, while Yeh et al. [1992] studied a hydro-thermal system in China.

Due to the computational burden of DP (and hydro scheduling methodologies overall), problem or system decompositions are often implemented. Yeh et al. [1992] presents a temporal decomposition, having separate tools for monthly, daily and hourly time intervals such that the seasonality, daily variation in demand and hourly constraints could be separately accounted for while maintaining reasonable computational load. The tools are coupled through the optimal policy function of the lower temporal resolution being used by higher temporal resolution tools as the boundary conditions.

Srdjević [1985] implements a spatial decomposition where they consider each reservoir in the system separately, iterating over each reservoir and updating its entry in the decision vector. This decomposition approach is called Successive Approximations (DP-SA). This transforms the problem from a single optimisation encompassing N number of water releases to N number of single reservoir optimisations.

Johnson et al. [1993] conducts a comparison between multi-linear and cubic spline interpolation when determining values from the future cost function. The issue with linear interpolation is that it will typically over-estimate the cost, particularly at state vectors that are distant from the discretised state space points. Although spline interpolation requires more computational effort, the state space discretisation can be coarser than for linear interpolation. They performed both deterministic and stochastic DP on a 4-reservoir system with a range of 3 to 17 discrete levels per reservoir. The error was determined by comparing the future cost function of the 17 level spline interpolation and the other future cost functions. Broadly speaking

the spline interpolation outperformed the linear interpolation in terms of error and computation time. The computation time of the spline interpolation was similar due to a specialist algorithm they implemented.

2.5 STOCHASTIC DYNAMIC PROGRAMMING

Stochastic Dynamic Programming (SDP) method applies the dynamic programming algorithm while accounting for the uncertainty of inflows. SDP models inflows with a Markov Chain [Stedinger et al. 1984]. A Markov Chain model has of a variety of states which the system can transition between. Each transition has an associated conditional probability of occurring (also called a transition probability). For an inflow model, each state is an inflow amount and the transition probabilities can be derived from historical inflow data.

The SDP recurrence equation for producing an optimal policy function is [Côté and Leconte 2016, Stedinger et al. 1984]:

$$\alpha_t^*(x_t, f_{t-1}) = \underset{f_t|f_{t-1}}{\mathbb{E}} \left(\min_{u_t} C_t(u_t) + \alpha_{t+1}^*(s_{t+1}, f_t) \right) \tag{2.12}$$

where the $t-1$ inflow is regarded as a state variable along with the discretised storage levels. The expectation in Equation (2.12) is resolved with Equation (2.13). The single stage problem is solved for each inflow state transition (indexed by l) producing an optimal cost for each. The product of each conditional probability of f_t^l occurring given f_{t-1} happening and its associated optimal cost is calculated and the average of these products is taken as $\alpha_t^*(x_t, f_{t-1})$. This is conducted at each discretised storage vector. Note in Equation (2.13), the particular inflow states belonging to the l'th transition is omitted for clarity.

$$\alpha_t^*(s_t, f_{t-1}) = \sum_{l=1}^{L} \left[\left\{ \min_{u_t} C_t(u_t) + \alpha_{t+1}^*(s_{t+1}, f_t) \right\} \times P^l(f_t = f_{t,k}|f_{t-1}) \right] \tag{2.13}$$

$P^l(f_t = f_{t,k}|f_{t-1})$ is the conditional probability of the l'th transition. The inclusion of f_{t-1} as a state variable in the future cost function allows a lag-1 auto-correlation to be built in but also adds a dimension to the state space, increasing the computation required to produce the future cost function.

SDP can be solved with a variety of methods including Linear Programming, Policy Iteration and Value Iteration [Littman et al. 1995]. Policy Iteration, presented by Howard [1960], is an iterative convergence method that consists of a value determination

step and a policy improvement step. The former step evaluates the cost for each decision. The latter step compares these costs to costs of other admissible decisions. The least cost decision is placed in the policy. Once the policy reaches a steady state, the process terminates and the policy is deemed the optimal policy. Value Iteration is similar, but evaluates and attempts to converge to the total optimal cost. Once solved, the output of SDP is a function of decisions for a given state x_t and previous inflow f_{t-1}.

2.5.1 Stochastic Dynamic Programming Literature

An early implementation of SDP was by Little [1955] although they themselves did not use the SDP terminology as it was not common at the time. Little applies Bellman's stochastic variant of dynamic programming and models the inflow variable with a lag-1 Markov chain. Discretising the inflow probability distribution produced the inflow states for the Markov Chain model. They were included with the discretised storage vectors as a part of the state space, adding to the dimensionality. When determining the operating policy with the optimal policy function, both the current storage and either previous or forecast inflow can be used.

Kelman et al. [1990] presents a SDP variant called Sampling SDP which aims to capture the temporal and spatial structure of inflow sequences. Kelman notes that the Markov Chain model of inflows, usually implemented in SDP, utilise a single inflow state to represent all reservoirs in the lag-1 model. As such these SDP tools did not account for the cross-correlation between reservoirs and the auto-correlation over multiple decision stages, which was done to limit the number of state space dimensions. Sampling SDP selects a number of sample inflow sequences to represent the joint distribution of reservoir and tributary inflows. Also, Kelman et al. [1990] substitutes the previous inflow with a forecast inflow for the state variable. This requires the probability of the forecast inflow given the inflow sequences' values to be calculated. Along with capturing the correlations, Sampling SDP avoids error due to the discretisation of the inflow probability distribution required by SDP.

Another variation on SDP's representation of inflows was implemented by Turgeon [2005]. Instead of a range of $t-1$ inflows being the Markov chain states, they were replaced by a weighted sum of the previous time intervals' inflows in an attempt to capture the inflow's previous behaviour over a longer period of time. The tool was applied with daily and weekly time intervals to an example system with the weighted sum having a range of spans (0 to 16 days, 0 to 4 weeks) and showed that both the benefit and spill improved with increasing span. Turgeon raised an issue with the statistical representation of long spans given that only 84 years of inflow sequences were available.

Tejada-Guibert et al. [1993] carried out an extensive study into some internal aspects of SDP. Their conclusions were:

1. By comparing the use of the optimal policy versus the future cost function to simulate the system operation, they found that on average the future cost function resulted in higher benefit.

2. Using Linear or Spline Interpolation when determining values from the future cost function made no discernible difference to the benefit derived from the system operation

3. With these interpolation approaches, a range of storage level discretisations were explored for both linear and spline interpolation. Overall, linear interpolation performed worse than spline but approached similar benefits at higher resolutions of discretisation.

During the 1990s, many electricity systems were deregulated resulting in a shift from centralised control to multiple separate entities trading via an electricity market. For systems with hydro generation and storage, it highlighted the desire to value water rather than determine optimal operation. With water values, entities can compare the value of their hydro resource to the market price and engage in energy arbitrage; purchasing electricity from the market when it is cheap and conserving water for high priced periods. Turgeon and Charbonneau [1998] provided an example of this where they calculated the marginal production cost (water value) for Hydro-Quebec (a Canadian hydro operator). They also conducted an aggregation-disaggregation approach given that the system had 26 reservoirs.

Another consequence of deregulation is that hydro system operation optimisation went from one global optimisation, minimising the societal cost of electricity, to multiple optimisations conducted by separate entities focused on profit maximisation, which resulted in somewhat different operation. Such a difference was investigated by Wolfgang et al. [2009] where they reported that the average reservoir levels post-deregulation had reduced by 4.6%. Modelling the collective behaviour of multiple hydro operators in a market situation is difficult, particularly when their strategies are not publicly known. Instead, they attempt to deduce reasons outside of the market as to why the reservoir operation differed. They considered curtailment costs, transmission constraints, power exchange with others in the Nordic Pool, variation in the stochastic variable distributions and climate change. They found that none of these elements seemed to contribute to the change in average reservoir level reduction implying that it is related to the deregulation.

Dias et al. [2010] presented an alternative approach to integrating the future cost function into the single stage problem. They applied a Convex Hull algorithm to the future cost function to produce a compact piecewise linear function (i.e. minimum number of hyperplanes). Convex Hull algorithms take a set of points, such as future cost at each discretised storage (and inflow) vector, and iteratively adds hyperplanes until the points are adequately represented. They also refer to a variety of Convex Hull algorithm literature. Brandi et al. [2015] also implement SDP with Convex Hull.

Deterministic treatment of hydro system operation provides a much simpler approach to modelling and is far less computationally intensive. However, Philbrick Jr. and Kitanidis [1999] stress that deterministic optimisation for hydro system operation can lead to poor performance particularly under low probability, high cost events such as droughts and floods. To illustrate this, they apply a deterministic optimisation and SDP based tools. The deterministic optimisation is simply the SDP tool but instead of a Markov Chain model of inflows, they use forecast inflows. They find that the deterministic optimisation resulted in significantly higher mean operating costs, up to 79.9% worse. Côté and Leconte [2016] also conduct a study comparing deterministic optimisation, SDP, Sampling SDP and SP with Scenario Tree (SP-ST, described later). They modelled the Rio Tinto's Alcan system (4 reservoir and 3125 MW of hydro generation capacity) on a weekly time interval with 54 years of inflow sequences, finding that Sampling SDP and SP-ST were superior in how they operated the reservoirs based on the total energy produced by hydro generation.

2.6 CONSTRUCTIVE DUAL DYNAMIC PROGRAMMING

Constructive Dual Dynamic Programming (CDDP) is a variant of Dynamic Programming developed largely by Read and other associates [Read and Hindsberger 2010]. CDDP is similar to the water value DP method (WV-DP) in that it projects the $t+1$ water value function backward over the time horizon. Where CDDP differs is the manner in which it conducts these projections.

The WV-DP backwards projection determines the water values at t for each of the discretised storage levels ($s_t^k \; \forall \; k$) by solving the single stage problem for each and then finding the $t+1$ water values at s_{t+1}^*. Instead of this, CDDP finds the storage levels (s_t) of a select set of water values relying on the same recurrence equation as WV-DP (Equation (2.10)). Typically these water values correspond to the prices of thermal generation. Note that in CDDP, the storage state space is not discretised.

The thermal generation prices (c_i^{tg} where i indexes thermal generators) are taken as the set of values given that their price relative to the water value determines whether

they are dispatched ahead of or after hydro generation for a least cost dispatch. By extension, this determines the amount of hydro generation that occurs as well. The storage levels at t that correspond to the thermal prices are determined by:

1. For each c_i^{tg}, determine the corresponding hydro generation dispatch (g_i^h) that would occur
2. Using Equation (2.14) calculate the s_t with the s_{t+1} storage associated with c_i^{tg} (known), g_i^h and the inflows (f_t) $\forall\ i$

$$\begin{aligned} s_{t+1} &= s_t + f_t - g_t^h \\ s_t &= s_{t+1} - f_t + g_t^h \end{aligned} \tag{2.14}$$

This process is conducted over the time horizon producing a storage series for each thermal price. Collectively, these form the water value functions, albeit in a different form to that of the WV-DP approach.

2.6.1 Constructive Dual Dynamic Programming Literature

Read and Hindsberger [2010] cover a range of CDDP based tools and their applications. SPECTRA is well known in New Zealand given its use prior to deregulation for the centralised operation of its hydrothermal system. Other tools include RAGE/DUBLIN and ECON-BID. RAGE/DUBLIN was used to study the market dynamics of New Zealand's hydrothermal system. The last explicit tool was ECON-BID which was applied to study the impacts of inter-region transmission connection in Western Europe and the Nordic region.

Scott and Read [1996] applied a CDDP tool to study the potential behaviour of electricity market participants in New Zealand's electricity system. There were two companies with one controlling the major storage reservoirs and one thermal generator (the price maker) and the other controlling the remaining thermal and other generators (the price taker). They conducted simulations investigating the impact of contracts between consumers and generation companies, comparing the resultant market behaviour to a perfect competition simulation. Given that contracted supply is effectively outside of the spot market trading, they found that contracts distort a market's behaviour relative to perfect competition, resulting in higher cost to consumers.

2.7 STOCHASTIC PROGRAMMING

Stochastic Programming is concerned with solving optimisation problems with uncertainty, so is well suited to account for uncertain inflows. Stochastic Programming's two stage problem illustrates the basics of the methodology.

The two stage problem considers the decision in the first stage ($t = 1$) under uncertainty that is resolved in the second stage ($t = 2$) [Wallace and Fleten 2003]. From a hydro scheduling context, the decision is the amount of hydro generation to dispatch and the uncertainty lies in the incoming inflows. Equation (2.15) shows the general formulation of the first stage:

$$\min_{u_1} \; g_1(u_1) + \mathbb{E}\Big[Q(u_1, \xi)\Big] \text{ s.t. } A_1(u_1) \tag{2.15}$$

where u_1 is the first stage decision, $g_1(u_1)$ is the cost of u_1 and $Q(u_1, \xi)$ is the optimal second stage cost which is dependent on the first stage decision and the resolution of the stochastic component represented by ξ. A_1 represents the constraints on the first stage, whatever their form.

Equation (2.16) represents the minimisation to determine $Q(u_1, \xi)$:

$$\begin{aligned} Q(u_1, \xi) = \min_{u_2} \; & g_2(u_2, \xi) \\ \text{s.t. } & A_2(u_1, u_2, \xi) \end{aligned} \tag{2.16}$$

where $g_2(u_2, \xi)$ represents the second stage cost. The second stage problem is constrained by the consequences of u_1 on the system, any limitations imposed by the stochastic variable(s) and the pre-existing constraints on u_2. These are collectively represented by $A_2(u_1, u_2, \xi)$. In order to make the first stage decision, the range of potential situations that could result from the first stage and the resolution of the stochastic component need to be considered. The expectation can be found with:

$$\mathbb{E}\Big[Q(u_1, \xi)\Big] = \sum_{\gamma=1}^{\Gamma} p_\gamma \, Q(u_1, \xi_\gamma) \tag{2.17}$$

where there are Γ number of scenarios indexed by γ, p_γ is the probability of γ scenario and ξ_γ represents a particular instance of the stochastic component. The inflows and their probabilities can be determined by discretising the inflow probability distribution based on historical data or can be synthetically generated. Equation (2.17) can be substituted into Equation (2.15), giving a single problem formulation which can be solved by a classical optimisation approach (e.g. linear programming) known as the deterministic equivalent:

$$\begin{aligned} \min_{u_1} \; & g_1(u_1) + \sum_{\gamma=1}^{\Gamma} p_\gamma \, Q(u_1, \xi_\gamma) \\ \text{s.t. } & A_1(u_1) \\ & A_{2,\gamma}(u_1, u_{2,\gamma}, \xi_\gamma) \end{aligned} \tag{2.18}$$

Obviously, the hydro scheduling problem is concerned with multiple sequential decision stages. The multi-stage version can be represented as a repeatedly nested two stage problem formulation for stages $t = 1$ to T:

$$\min\ g_1(u_1) + \mathbb{E}\Big[\min\ g_2(u_2) + \mathbb{E}\Big[... + \mathbb{E}\Big[\min\ g_T(u_T)\Big]\Big]...\Big] \tag{2.19}$$

The constraint representation has been omitted for clarity but is still applicable. Obviously Equation (2.19) has a significant number of possible instances at each stage, effectively covering a large probability tree. To ensure computational tractability with multi-stage stochastic programming problems, specific paths from the root node ($t = 1$) to the end node ($t = T$) are selected to be a sample of the probability tree, referred to as a scenario tree.

The literature of Stochastic Programming and Stochastic Dual Dynamic Programming is discussed after the Stochastic Dual Dynamic Programming description.

2.8 STOCHASTIC DUAL DYNAMIC PROGRAMMING

Stochastic Dual Dynamic Programming (SDDP) is a multi-stage stochastic optimisation solution methodology that has been extensively applied to the hydro scheduling problem since its creation and application by Pereira and Pinto [1991]. In a similar manner to Dynamic Programming, SDDP considers each decision stage separately and links them through a future cost function. Equation (2.20) presents this as a deterministic linear programming formulation:

$$\begin{aligned} \min\ & c_t \cdot x_t + \alpha_{t+1}(x_{t+1}) \\ \text{s.t.}\quad & A_t x_t \leq b_t \end{aligned} \tag{2.20}$$

where x_t represents the decision and state variables (such as storage and hydro generation), c_t is the cost vector and α_{t+1} represents the future cost function. A_t and b_t are the constraint matrix and vector. SDDP differs from DP in that it represents $\alpha_{t+1}(x_{t+1})$ as an analytical piecewise linear function rather than constructing it on a discretised state space.

The piecewise linear functions are built with Benders Cuts as SDDP can be interpreted as an extension of Benders decomposition [Pereira and Pinto 1991]. The SDDP algorithm involves performing a forward simulation ($t = 1, 2, ..., T$) to produce an approximate operating policy ($x_t;\ t = 1, 2, ..., T$) and then conducting a backwards recursion over the time horizon ($t = T, T-1, ..., 2$) and adding hyperplanes (Benders Cuts) to the $\alpha_{t+1}(x_{t+1})$ improving their approximation of the future cost functions. This is repeated until convergence has been achieved [Pereira and Pinto 1991]). The extension to the

stochastic case involves examining a range of scenarios and determining the expected hyperplanes to use for the future cost functions.

An advantage of SDDP over DP based methods is that it avoids the need to discretise the state space hence does not suffer from the curse of dimensionality. However this comes at the cost of emphasising the $t = 1$ decision as Pereira and Pinto [1991] focus on convergence only at this decision stage. This is a significant difference between SP and DP based methods as DP, SDP and CDDP all produce steady state optimal functions for the entire time horizon. By focusing on the current decision stage convergence only, SP methods reduce the computational burden and as a consequence of this, SP methods must be run at each decision stage which aligns with real world system operation as the optimisation inputs can be updated.

2.8.1 Stochastic Programming and Stochastic Dual Dynamic Programming Literature

Wallace and Fleten [2003] discuss the application of Stochastic Programming to hydro scheduling since its inception. An interesting element is their content on the earliest published hydro scheduling literature by Massé [1947][1]. Massé developed a stochastic optimisation methodology for the operation of hydro schemes prior to the formalisation of that terminology. Accompanying this is a discussion on the issues with deterministic tools being too optimistic and the concept of water values.

An early variant of temporal decomposition is presented by Pereira and Pinto [1983]. Instead of the two-stage problem referring to two subsequent decision intervals, Pereira and Pinto treat the first stage as the medium-term problem (MT, weekly) and the second stage as the short-term problem (ST, hourly). The ST constraints are coupled to the MT problem through Benders Cuts forming the future cost function. The benefit of this coupling is to avoid the MT solutions being infeasible in the ST as the ST constraints such as generation and transmission capacity are translated back to the MT problem. The MT problem is concerned with hydrological dynamics and balancing production and demand. This decomposition was likely a precursor to the SDDP presented by Pereira and Pinto [1991].

Flatabø et al. [2002] implements a more traditional temporal decomposition to study how Norwegian hydro generation operates in the Nordic Pool under different risk management scenarios including future contracts. The decomposition consists of long,

[1]Les Réserves et la régulation de l'avenir dans la vie économique. II, Avenir aléatoire. Hermann, Paris, vol I and II. All content pertaining Massé (1947) was taken from Wallace and Fleten [2003] as the two books are in French hence were not read.

medium and short term (LT, MT and ST) tools. The LT and MT tools use SDDP with the LT water value function being used by the MT tool. The ST tool is deterministic and represents hydro and thermal generation at the unit level, hydro efficiency and thermal efficiency.

Warland and Mo [2016] present an alternative to the typical Stochastic (Linear) Programming and SDDP approaches called Scenario Fan. Scenario Fan could be viewed as adjacent to Sampling SDP or an extension to Pereira and Pinto [1983] temporal decomposition. The structure of the Scenario Fan approach is the two-stage problem where the first stage is the immediate time interval ahead (t) and the second stage is a multistage problem covering the remaining time horizon ($t+1$ to T). The similarity with Sampling SDP is that the second multistage problem is solved for a range of inflow scenarios. Warland and Mo compare this Scenario Fan tool to an SDP tool and the former results in less thermal generation and spill.

Philpott et al. [2010] conduct a study into the inefficiency of the electricity market in New Zealand by comparing market opeartion with a modelled centrally controlled operation. The modelled operation was conducted with an SDDP based tool with an 18 node and six reservoir representation of New Zealand's system over a week. Broadly the centrally controlled operation resulted in less thermal generation production, hence fuel cost, largely due to the flexibility granted by a single operator.

Duenas et al. [2018] is an example of a contemporary study examining high renewable generation penetration and its effects on a hydro dominant electricity system. The tool used was Stochastic (Linear) Programming based with Scenario Tree along with a DC power flow transmission model with 20 nodes, which Duenas et al. points out is an expansion on the traditional hydro scheduling tools. They consider a range of generation (wind and hydro) and transmission expansion scenarios broadly confirming the importance of the transmission system in integrating more renewable generation and, for Iceland's situation, that returning to fossil fuel generation would be more expensive than renewable generation.

Fredo et al. [2019] compares the impact of integrating hydro generation efficiency function in a SDDP with Scenario Tree tool versus a constant factor, with the latter being the typical practice. This study is an example of examining the implicit assumption made with solving the hydro scheduling problem for real world systems. Accounting for the efficiency resulted in 7-11% lower production costs but took 11 times longer to solve than the constant factor.

de Matos and Finardi [2012] outline the SMETA tool implemented in the Brazilian system. The Brazilian system has considerable storage relative to many systems around the world. As such SMETA is an example of a multi-year time horizon tool, on the order of 5 to 10 years at a monthly time interval. The complete tool consists of three components: Hydro Scheme Aggregation, Inflow Scenario Production and an SDDP with Scenario Tree based tool to produce the operating policy.

2.9 IMPLICIT STOCHASTIC OPTIMISATION

Stochastic Dynamic Programming and Stochastic Dual Dynamic Programming are both known as explicit stochastic optimisation methods where uncertainty is considered at each decision stage. Implicit Stochastic Optimisation (ISO) is an alternative method.

ISO is a Monte Carlo approach to incorporate uncertainty with any deterministic optimisation and was initially applied to a hydro scheduling problem by Young [1967]. ISO consists of two steps:

1. A deterministic optimisation is applied to a variety of inflow scenarios which are based on historical data or synthetically generated. For the hydro scheduling problem this would be a variety of inflow sequences. For example, if the optimisation used Dynamic Programming, this would produce an optimal policy function for each scenario. The optimal policy function describes the optimal generation dispatch for a given system state (storage) at a time interval within the time horizon.

2. Regression analysis on the collection of deterministic optimal policy functions is conducted to produce a function that provides the optimal decision for a given time t, system state (storage) and value of the random variable (inflow)

2.9.1 Implicit Stochastic Optimisation Literature

Willis et al. [1984] provides an overview of the early development of ISO and presents their ISO-LP approach. The LP determines the optimal monthly releases over a 64 year horizon. A second-order autoregressive model was used to produce the reservoir operating rules dependent on storage and a forecast inflow.

In a review of hydro scheduling methodologies, Labadie [2004] expressed a concern with ISO, stating that regression may lead to poor correlations that invalidate the operating rules. For example, if the current inflows have low correlations with those implemented in the scenarios, the regression analysis may produce a poor regressed policy. They also comment on other methods requiring extensive trial and error. Other methods may

include evolutionary methodologies such as artificial neural networks which have been applied successfully (Farias et al. [2006]). There are a handful of studies comparing ISO and other explicit stochastic optimisation approaches.

Lee and Labadie [2007] use ISO-DP along with Sampling SDP and Deterministic DP as comparisons for a Reinforcement Learning (RL) approach. The attraction of RL is that it learns the stochastic nature of the inflows rather than being given an explicit probability distribution. A RL algorithm performs a pseudo-search of the decision space through an iterative process that evaluates and adjusts the operating policy until the performance measure converges. The tools are applied to the Geum River Basin (South Korea) using the October 1998 to September 2002 inflow sequence for the operation simulation. The performance measure used to judge all the tools was a weighted sum of satisfying demand, avoiding spill and abiding by water flow constraints. They found that Reinforcement Learning had the best performance.

Celeste and Billib [2009] compare the performance of ISO with Quadratic Programming (ISO-QP), Parametrisation-Simulation-Optimisation (PSO) and SDP tools. A PSO algorithm begins with a predefined policy function, operates the system according to this policy function under a variety of inflow scenarios and then adjusts the parameters of the policy function formulation. This process is repeated until the policy function converges. They use a vulnerability index which is the average of the absolute percentage difference between water release and demand. It is implied that vulnerability here is used as a risk-of spill and curtailment measure. They find that ISO-QP and PSO have lower vulnerability indexes than SDP for the single reservoir system.

Another ISO-centered comparison was presented by Moreira and Celeste [2017]. The ISO tool differed in that the current time interval's (month) forecast inflow was replaced by a forecast long-term mean reservoir inflow as a regression variable. The horizon of the forecast mean inflow was from 0 to 36 months. The ISO tool with a 9 month forecast horizon had comparible vulnerability to SDP, both of which performed better than the deterministic optimisation.

Henao et al. [2019] presents a study in which an ISO based tool is applied to Columbia's hydro dominant system transitioning from thermal generation to more renewable generation, in particular to wind and solar. They simulate a range of wind and solar generation scenarios from 2016 to 2030 with an increasing demand trend and a monthly time interval. An interesting result was that in the high wind generation scenarios, coal and natural gas generation was still required in years after 2024 but, with solar generation making up the majority of added renewable generation, all thermal generation

is eliminated over the time horizon.

Yang et al. [2018] also investigates renewable generation transition, modelling the coordination of hydro and solar generation with a ISO based tool. They also compare the effect of using a linear fitting method and PSO approach to produce the operating rules from the deterministic optimisations.

As an alternative to applying regression to derive operating rules, Celeste et al. [2009] instead interpolate them from the collection of the deterministic optimal policy functions across all inflow scenarios. The interpolated ISO operating policy was non-monotonic as it was heavily influenced by local data points. Even with this, the vulnerability measures between regression and interpolation based policies were indifferent.

2.10 CONCLUDING REMARKS

A major driving factor behind the development of hydro scheduling methodologies is achieving computational tractability while capturing the real world system dynamic adequately. This is in part due to the problem's spatial and temporal dimensional breadth. The hydro systems range from small single schemes to interconnected multi-national systems, the time horizons span from a number of days at a sub-hourly interval to many-year spans and monthly steps. To manage this, the problem is decomposed in a variety of ways:

- Stage-wise: Dynamic Programming and Dual Dynamic Programming approaches separate each decision stage
- Time horizon: Having long-, medium- and short-term coupled tools
- Element-wise: Successive Approximations approach considering reservoirs separately

Another technique to reduce the computational intensity is to aggregate the hydro schemes and systems.

A key difference between Dynamic Programming and Stochastic Programming based approaches are their outputs. DP approaches produce an optimal function that is applicable to the entire time horizon and all storage states whereas SP approaches emphasise the current decision and storage stage. The value of this is an overall reduction in the computation time for similar problem types and classes but to consider multiple scenarios, such as for system studies, this benefit erodes.

Chapter 3

NEW ZEALAND SYSTEM MODEL DESIGN

As illustrated through the literature on the development of hydro scheduling methodologies, a persistent goal is to both sufficiently represent the real world system and its dynamics while ensuring the application of the modelling tool is computationally tractable. In general, the vast majority of studies implied the purpose for their modelling tools were for real world applications rather than system studies. The uses are not mutually exclusive, but it does influence what is prioritised when developing the modelling tool and system model. The purpose for the modelling tool and system model in this research is for system studies only.

There are two components to managing the computational tractability: The applied hydro scheduling methodology (or modelling tool) and the system model. Here, the development of the New Zealand system model is presented and will serve as the case study system that the modelling tool will be applied to. The modelling tool is covered in Chapter 4.

For this research, the objective is to develop a modelling tool that can evaluate the impacts of increasing renewable generation and reduction of conventional thermal generation in hydro dominant electricity systems as well as investigate the value of investments into generation, storage and transmission capacity. For the system model to be fit-for-purpose, it needs to represent each of these elements.

The implemented New Zealand model is depicted in Figure 3.1. Geographically, New Zealand consists of two islands (the North and South Islands, left and right respectively), both of which have alternating current (ac) electricity systems connected by a HVdc (High Voltage direct current) transmission line called the HVdc link. Each island has hydro generation with storage, demand and a combination of renewable generation represented as a must run generator. Both islands also have fictitious non-supply generation to emulate demand curtailment. All thermal generators are located in the North Island and are aggregated into a single generator with a range of pricing tranches.

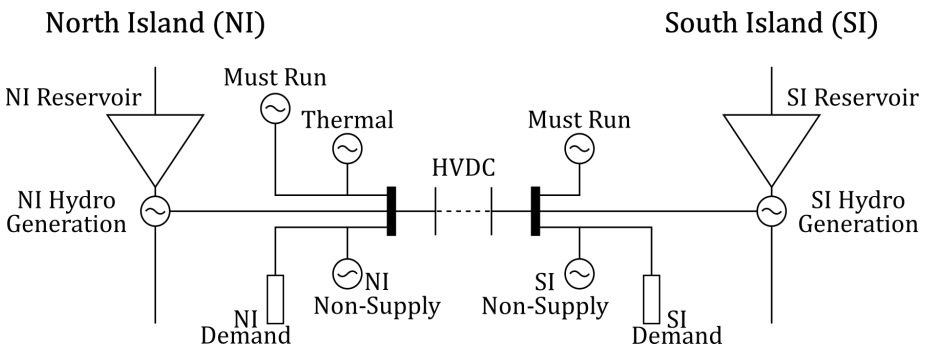

Figure 3.1 New Zealand System Model

Others have implemented similar two-node, two-reservoir models to represent New Zealand's system [Read and Hindsberger 2010, Read 2014] . The key reason for this model is that New Zealand system's operation is dominated by the different hydro inflow patterns in the North and South Islands. The majority of the hydro inflows, generation and storage capacities are in the South Island while the majority of demand is in the North Island. There is a significant constraint in that the HVdc link limits the transfer between the islands. Although this two-node, two-reservoir model is simple as it has a small number of components, it still captures the major system constraints while allowing faster computation times.

Figure 3.2 depicts the distribution of demand, hydro generation, storage and annual inflows between the islands which demonstrates the importance of the HVdc link.

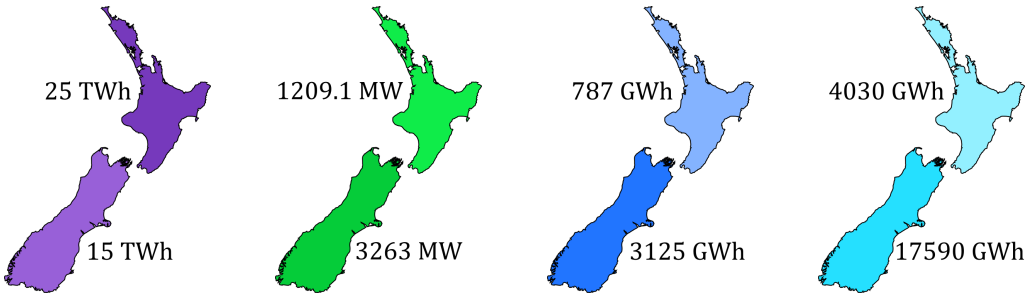

(a) Demand (b) Hydro Capacity (c) Hydro Storage (d) Hydro Inflows

Figure 3.2 Island Distribution: Demand, Hydro Capacity, Hydro Storage and Hydro Inflow (2015)

The HVdc link's capacity influences generation dispatch and by extension the distribution of active storage in the North and South Islands. Another major mismatch in New Zealand's system that is captured by the two-node, two-reservoir model is the difference in inflow seasonality which is discussed in Section 3.1.

Two variants of this basis system model were produced to represent the contemporary system (2015-2020, labelled as 2015) and a future system (2030). The 2015 system

scenario is used to study the modelling tool's sensitivity to parameters such as the time interval and storage discretisation (Chapter 5). It also allows the modelling tool's operation of New Zealand's system to be compared to the New Zealand market's operation. This comparison is only to judge whether the modelling tool is performing appropriately and not to benchmark the tool's or market's performance. The 2030 system scenario considers greater penetration of renewable generation, reduction of thermal generation and allows other system investments to be explored.

A major aspect of future highly renewable systems is the management of variability from demand and intermittent renewable generation. Typically this has been achieved with dispatchable generation such as hydro and thermal, but other flexible energy resources such as demand response and battery storage will need to be deployed given the phase out of thermal generation. Demand response involves consumers varying their electrical load in reaction to high prices, either to avoid expense, as a service facilitated by the electricity market or both. Demand response can either shift or reduce load depending on its provider. The function of battery storage is to shift electrical energy from periods of high production and low demand to those of low production and high demand. Both of these flexible energy resources can assist with managing capacity requirements over short time horizons (intra-day). The focus of this thesis is the development of the hydro scheduling tool, and by extension capturing New Zealand's hydro storage's seasonal storage. As such, incorporating demand response and battery storage was considered out-of-scope and regarded as future work.

Unless otherwise stated, all data for the New Zealand system model were sourced from the Electricity Authority's Electricity Market Information database [Electricity Authority 2021] . The Electricity Authority is the organisation that oversees and regulates New Zealand's electricity market. Note that for all leap year time series data 31st December is removed to ensure the time series between years have the same length.

The remainder of the chapter covers each of the components of the system model and where applicable the specifics on the 2015 and 2030 scenarios, a summary of the 2015 and 2030 system models and a comparison of the modelling tool's operation of the New Zealand system model with the real world operation to demonstrate the tool performance.

3.1 HYDRO SYSTEM MODEL

The hydro system model significantly influences the computational burden borne by the Dynamic Programming based hydro scheduling tool with the number of storage reservoirs and the number of discretised storage vectors. A common practice when

developing hydro system models is aggregating schemes together into a smaller number of representative reservoirs and generators, with the requirement to adequately represent the constraints of the hydro system while reducing its dimensionality as mentioned in Chapter 2.

Among the hydro schemes in New Zealand, there are five which account for the majority of hydro generation and storage capacity. Waikato and Waikaremoana are the schemes in the North Island and Waitaki, Manapouri and Clyde schemes are the South Island schemes. All other smaller hydro schemes were modelled as run-of-river hydro generators (Section 3.4.3) and their details are presented in Appendix A.

In some cases, the hydro system models implemented in Dynamic Programming based tools, such as Stochastic DP and Implicit Stochastic Optimisation with DP, aggregate the hydro system into a small number of reservoirs. This is primarily to minimise the computational burden. This research uses a hydro system model that has two separate reservoirs which allows mismatch between the North Island's demand, the South Island's hydro resource and the energy transfer constraint imposed by the HVdc link to be represented.

Table 3.1 presents the total generation and storage capacity of each scheme and island as well as total annual inflow percentiles.

Table 3.1 New Zealand Hydro Scheme Generation Capacities, Storage Capacities and Annual Inflow Percentiles. The inflow percentiles represent 85 years of inflow sequences (1932-2016)

Island	**Hydro Scheme**	**Total Generation Capacity (MW)**	**Total Storage Capacity (GWh)**	**Total Annual Inflow Percentiles (GWh)**		
				25th	**50th**	**75th**
North Island	Waikato	1071.1	633	4139	4502	4891
	Waikaremoana	138	154			
	Total	**1209.1**	**787**			
South Island	Waitaki	1723	2388	16035	17575	19452
	Clutha	740	299			
	Manapouri	800	438			
	Total	**3263**	**3125**			

The conversion for water volume (storage) and flow rate (inflows) is covered in Section 3.1.2. The South Island's hydro resources (capacity, storage and inflows) are significantly greater than that of the North Island. A potential risk due to the HVdc link

constraint is that energy could be stranded in the South Island while there is insufficient resource in the North Island. This is a possible concern when examining the 2030 scenario in which a portion of North Island's thermal generation is decommissioned.

3.1.1 Hydro System Characteristics

To provide context on New Zealand's hydro system, its inflow seasonality, annual inflow distribution and inflow-storage relationship will be briefly presented. Figure 3.3 presents each island's inflow seasonality over a year as quantile plots of the available 85 years of inflow data (1932-2016). Note that these are quantile series so do not represent actual inflow sequences. The South Island typically has low inflows during winter (June to August) as much of the precipitation in the hydro scheme catchment areas falls as snow rather than rain. Inflows are higher during spring and summer time (September to February) as the snow pack melts and precipitation falls as rain. The North Island is generally warmer than the South Island hence its precipitation is rain during the winter months giving higher inflows while being relatively dry during summer and autumn. Overall, the South Island's inflow seasonality dominates New Zealand's inflow seasonality due to its magnitude.

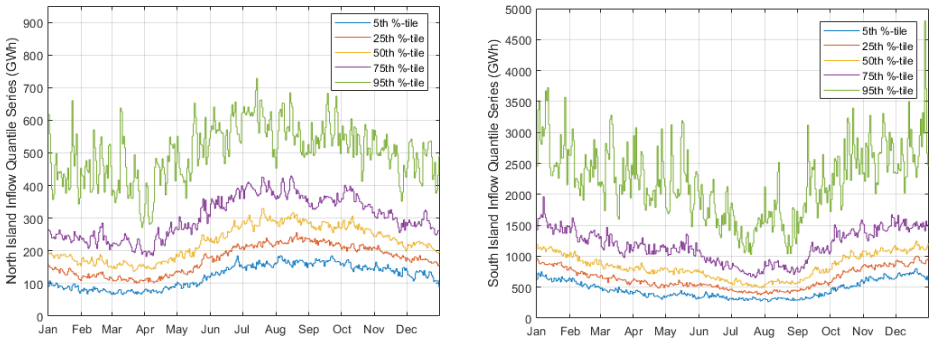

(a) North Island Inflow Quantiles

(b) South Island Inflow Quantiles

Figure 3.3 Inflow Seasonality: Inflow Quantile Time Series for 5th, 25th, 50th (median), 75th and 95th percentiles

Figure 3.4 shows the annual inflow distribution of the North Island, South Island and New Zealand. Although infrequent (1 in 20 years), low inflow (dry) years pose a significant risk to New Zealand's security of supply since hydro generation provides circa 50% of New Zealand's electricity. Managing dry year risk is the major challenge for New Zealand's electricity system. At present thermal generation is the main asset to combat this but as it is decommissioned, there will be greater importance on managing hydro storage in combination with the additional variable and intermittent renewable generation.

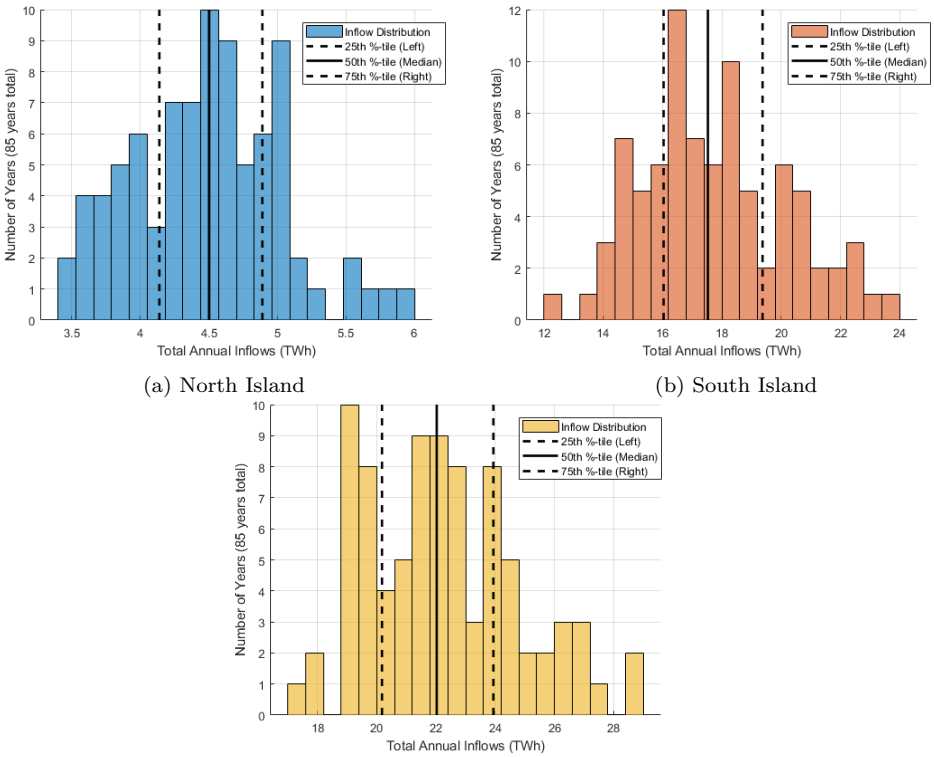

(a) North Island

(b) South Island

(c) New Zealand

Figure 3.4 Annual Inflow Distribution (85 years of inflow sequences; 1932-2016)

New Zealand's reservoirs are relatively small, only storing around 9% of New Zealand's annual demand which equates to approximately 3 to 6 weeks worth depending on the time of year. To illustrate the limit of their storage capacities, Figure 3.5 presents North and South Island inflows (orange) and storage (blue) from 2015 as operated by New Zealand's Electricity Market. As can be seen in both islands, when an inflow event occurs, there is a coincident marked increase in storage. Although this is only a single year of data, it highlights the importance of inflow events in New Zealand contributing to hydro storage, rather than snow melt.

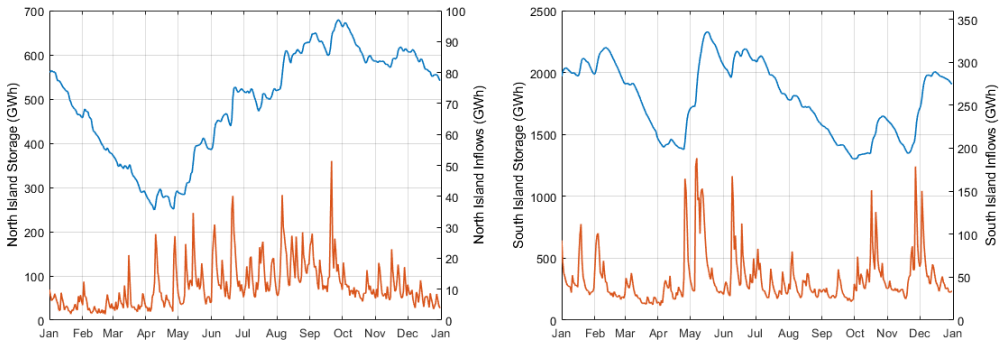

(a) North Island Storage and Inflows

(b) South Island Storage and Inflows

Figure 3.5 Storage and Inflow Relationship of the North Island (left-hand figure) and South Island (right-hand figure) - 2015 Storage (left y-axis) and Inflows (right y-axis)

3.1.2 Hydro Scheme Aggregation

An aggregated hydro scheme model consists of a single reservoir, generator and inflow sequence. Due to the simplicity of this model, other characteristics cannot be explicitly represented and are either neglected or emulated which imposes assumptions on the accuracy of the model. Such characteristics include flow constraints and delay between water leaving a reservoir and arriving at a downstream reservoir.

Figure 3.6 presents the layout of each scheme that needs to be aggregated into a single reservoir model. Each scheme has one or two major reservoirs at the beginning of the scheme with control gates moderating the outflows from the reservoirs. The major reservoirs receive the majority of inflows (in terms of energy) into the scheme while other smaller tributary flows enter along the scheme into reservoirs or waterways. Each reservoir has spillways that transfer water to a downstream reservoir or beyond the generation of the scheme. Manapouri has a control gate that manages flow as per the imposed flow constraints on the scheme. This is accounted for in the inflow data [WSP Opus 2018] and in the system model is treated as a spillway. Note that these structures are not exact representations of the physical water flows.

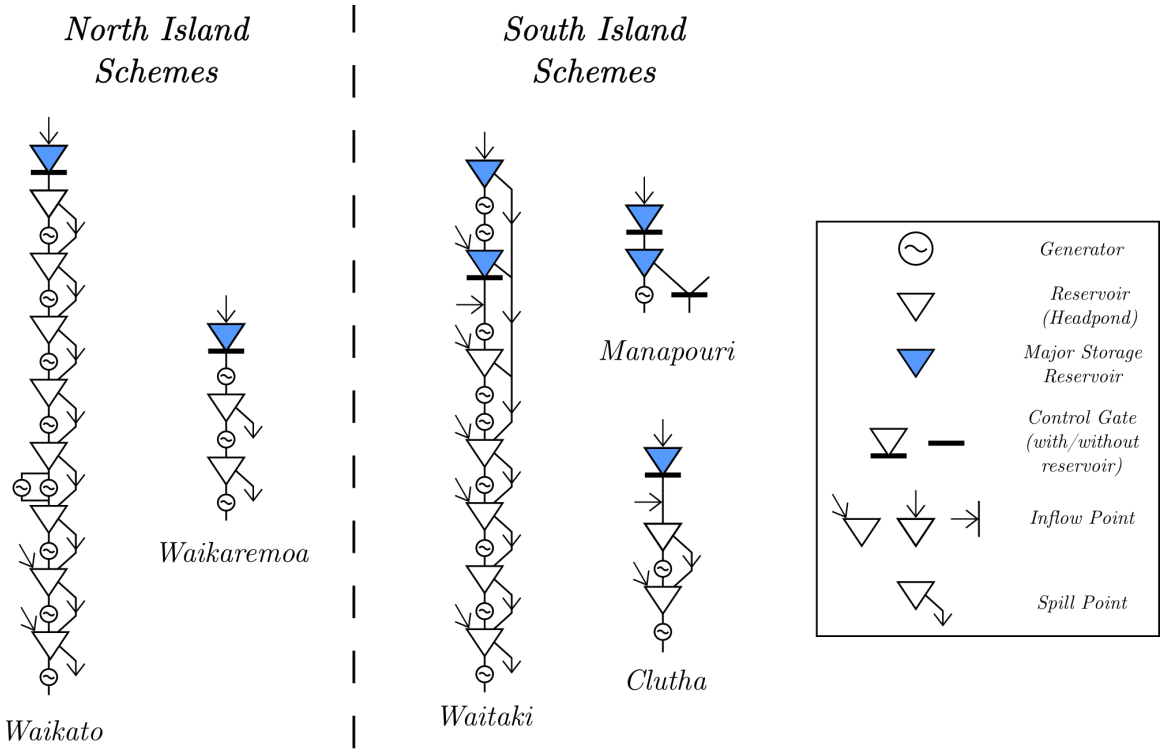

Figure 3.6 New Zealand Hydro Schemes

The aggregation process for a hydro scheme is:

- Convert the scheme's reservoir storage water volumes (Mm^3) into energy (GWh)

and sum these together.

- Convert the scheme's inflow sequences from flow rate (Cumecs, Cubic Metres Per Second) to MWh/h and scale they to the appropriate time interval. These MWh/h inflow sequences are summed together.
- Combine all generation capacities.

For the island level hydro system models, the island's aggregated hydro scheme values (storage, inflow sequences and generation capacities) are summed together. The storage and generation capacities were presented in Table 3.1.

The conversion of the water volume and flow rates to energy based values involves calculating the energy that would be produced when the water passes through all downstream hydro generators. In reality, the water to energy function is dependent on a variety of factors including turbine design and force behind the water flow, which can be represented as a function of the headpond water level. As the headponds and turbines are not explicitly modelled, each hydro generator's average plant factor (Cumecs / MW) are used for the conversion calculation.

Along with the water level storage constraints placed on hydro schemes by local or municipal authorities, minimum and maximum flow constraints are often required for various waterways. New Zealand's hydro schemes flow constraints are available on the Electricity Authority's EMI database. Specific measures of the flows along waterways are not a concern, but they can influence the hydro scheme's generation. Maximum flow constraints if directly upstream of a hydro generator are essentially generation capacity constraints. Of those in New Zealand's hydro schemes, there are no maximum flow constraints that impose any additional capacity limitations.

If minimum flow constraints are directly downstream of a hydro generator and assuming the water flows through the turbine, it can be matched by a minimum generation constraint, through a penalty of not meeting the constraint in the dispatch optimisation, or by splitting the generator into two; a must-run generator representing minimum flows and a dispatchable generator for the above minimum flows. The effect of these would be to ensure there would be sufficient storage ahead of time to meet the constraint. A penalty component was selected as the other two options could lead to the optimisation being infeasible, particularly at empty storage levels in the discretised storage state space.

Note that there are several tributary inflows along the hydro schemes that flow into small reservoirs. By aggregating the hydro scheme, these tributary inflows are modelled

as entering the aggregated reservoir, giving the modelled system more flexibility to manage those inflows, avoiding full reservoirs and spill. There is an implicit assumption that hydro scheme managers will use an optimisation based dispatch process that manages individual reservoir levels in a way that avoids unnecessary spill or restriction of generation capacity. One tributary flow in the Waitaki scheme passes through a hydro generator before reaching a reservoir. Assuming that the water is passed through the turbine rather than spilt, this is simply added to the minimum flow penalty amount.

Many of the spillways direct water to a downstream reservoir hence the energy of the water only decreases by the amount that the bypassed generator(s) would have provided. However in the single reservoir model, spill is treated as exiting the scheme completely hence all energy is lost. The assumption is that the storage of the single reservoir model would be distributed appropriately across all reservoirs in the system. As such, when spill occurs with the single reservoir model, this corresponds to all reservoirs of the hydro scheme being full and spilling.

The aggregation of a hydro scheme assumes no delay when water is exiting one reservoir and entering another whereas in reality the water takes time to flow. For the macro-scale modelling approach of this research, it is assumed that a hydro scheme operator would ensure sufficient available water for all hydro generators along the scheme in headponds and incoming upstream flow to satisfy any prospective generation dispatch, minimising the effect of the delay.

All of the inflow sequences and other hydro scheme data are available in the Electricity Authority's EMI database except for one inflow sequence. With the Clutha scheme, the inflows that enter directly after the major reservoir are outflows of two uncontrolled reservoirs and outflow data is only available for one of them. As such, an appropriate inflow sequence needed to be produced, requiring some assumptions. Refer to Appendix B for these details. Regarding the discretisation of the modelled storage reservoirs, a range of options are evaluated in Chapter 5.

3.2 TRANSMISSION SYSTEM AND DEMAND

New Zealand's transmission system consists of many nodes and transmission branches (lines and transformers) spread across both islands and the two node system representing each island's ac system is simplistic, ignoring all ac transmission constraints. Having a more extensive transmission system model will require some disaggregation of the aggregated hydro schemes.

The aggregation combines all hydro generators and their nodes that are geographically spread throughout the transmission system. Refer to Appendix C for a New Zealand transmission system map. Power flow between nodes within each island is not modelled. Due to the interconnection of nodes within each island, determining appropriate capacity constraints and loss functions for the transmission lines to the remaining nodes is more complex. The two node model still allows investment into the HVdc link capacity to be demonstrated. Note that the losses of the excluded transmission system were accounted for by scaling the demand profile by 3%. This value is based on the aggregate electricity statistics from the Ministry of Business Innovation and Employment [2020] .

In the 2015 model, the HVdc link capacity is 1200 MW although, as shown in Figure 3.7, it rarely carries more than 1000 MW northward and 700 MW southward. Figure 3.7 shows the HVdc Link's power flow from mid-2009 to late 2020. The limitation is due to a combination of stability constraints around the North Island HVdc connection node and security constraints limiting the available capacity to minimise the risk of demand curtailment if an unexpected outage on the transmission line occurred. With the operation of New Zealand's system, the Risk Management Tool (RMT) is run in conjunction with the generation dispatch to account for voltage stability in the North Island and other aspects [Transpower New Zealand 2021] . This effectively imposes a variable HVdc capacity constraint, dependent on the system conditions. Implementing a similar tool as the RMT would scale the computational intensity of the modelling tool so the HVdc link's full capacity is used. For the 2030 model, a hypothetical HVdc capacity increase up to 2400 MW was considered.

The HVdc losses are modelled with a piecewise linear function dependent on power flow due to the use of linear programming to solve the generation dispatch in the modelling tool (refer to Chapter 4 Section 4.4 for the formulation). Figure 3.8 presents the total loss and loss factors over the power flow tranches for the 2015 and 2030 scenarios. The HVdc loss data was sourced from Newham [2008]. They implemented a Stochastic Dual Dynamic Programming hydro scheduling modelling tool focused on expansion planning in New Zealand. For the 2030 scenario, the additional portion of the loss function was extrapolated from the 2015 loss function and the loss factors derived from that.

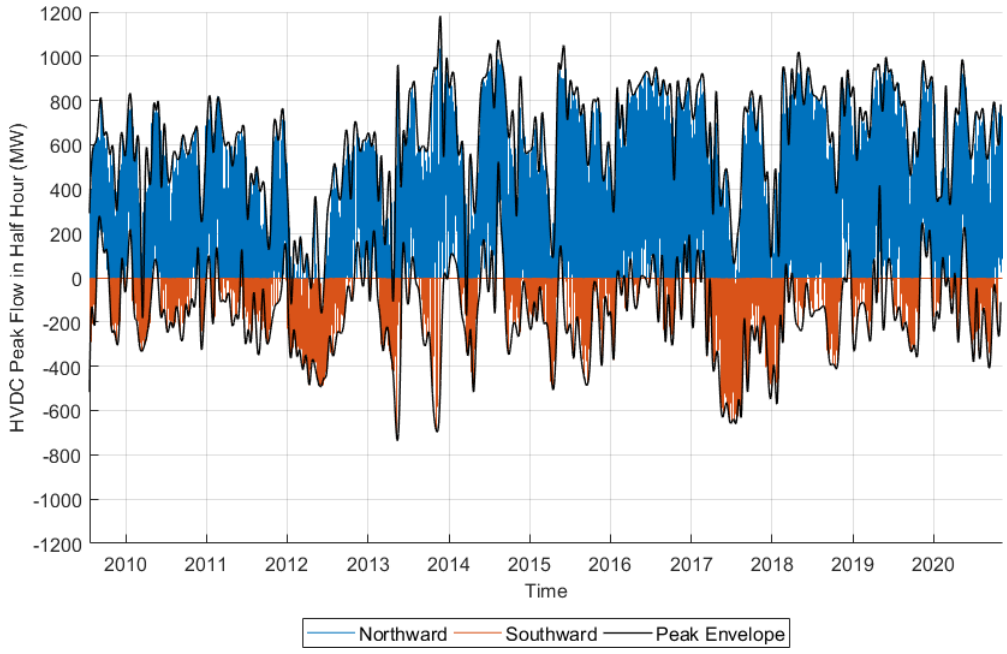

Figure 3.7 Historical HVdc Link Transfer

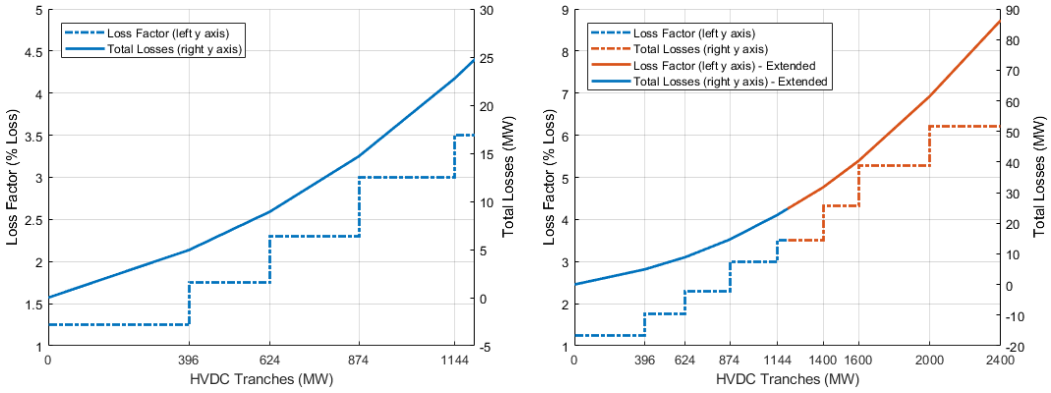

(a) HVDC Losses - 2015 Scenario

(b) HVDC Losses - 2030 Scenario

Figure 3.8 HVdc Transmission Line Losses

With each island being represented by a single node, the demand within each island's nodes are summed together. The 2015 demand profile is used for all simulations in this thesis. Figure 3.9 presents the 2015 demand profiles for the North Island, South Island and for reference, the total New Zealand demand profile. All plots show the half hourly (coloured) and daily demand series (black). The North Island has an evident seasonal variation with high demand during the winter months (June to August). The South Island demand profile is significantly flatter due to irrigation during the drier summer months (December to February). Overall, the North Island's demand seasonality dominates as shown in the total New Zealand demand figure.

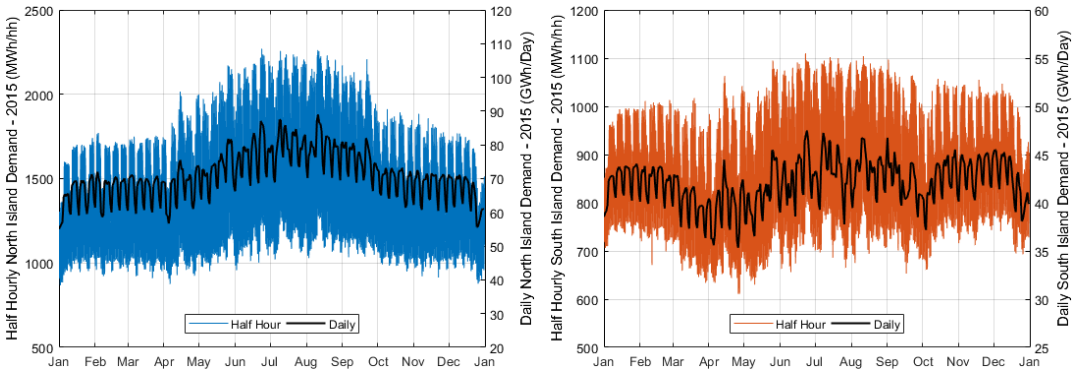

(a) North Island Demand - 2015

(b) South Island Demand - 2015

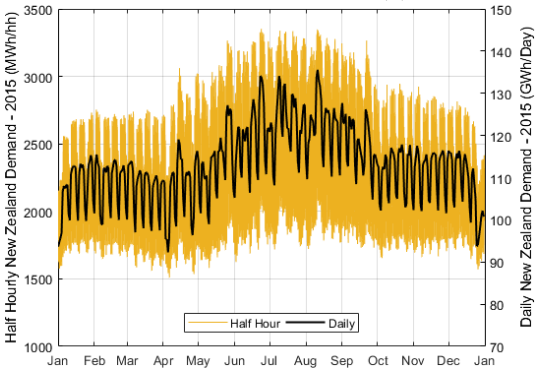

(c) New Zealand Demand - 2015

Figure 3.9 North Island, South Island and total New Zealand Demand - 2015

For the 2030 scenario, the 2015 demand profile is scaled in accordance with Transpower New Zealand's (TPNZ) base future scenario from its Te Mauri Hiko: Energy Futures report [Transpower New Zealand 2018b]. TPNZ is New Zealand's state owned transmission asset owner and system operator. Te Mauri Hiko explores various scenarios for New Zealand's energy and electricity systems accounting for the electrification of the transport fleet and industry, the uptake of renewable generation and the decommissioning of thermal generation. The 2030 demand profile was produced by:

1. Each island's demand profiles were split into low and high frequency components. The low frequency component was the daily moving average while the remaining series was the high frequency component

2. The low frequency components are scaled to the 2030 demand level from Te Mauri Hiko (57 TWh, increase of 14 TWh from 2015). The existing demand ratio between the North and South Island was maintained

3. The scaled low frequency and original high frequency components are added together giving the final series

Figure 3.10 presents the 2030 scenario demand profiles. With the 8832 MW peak demand, the assumption is that 2030's high frequency variation is equivalent to that of 2015. The high frequency component is largely due to residential demand, but may be compensated to some extent by demand side management and battery systems.

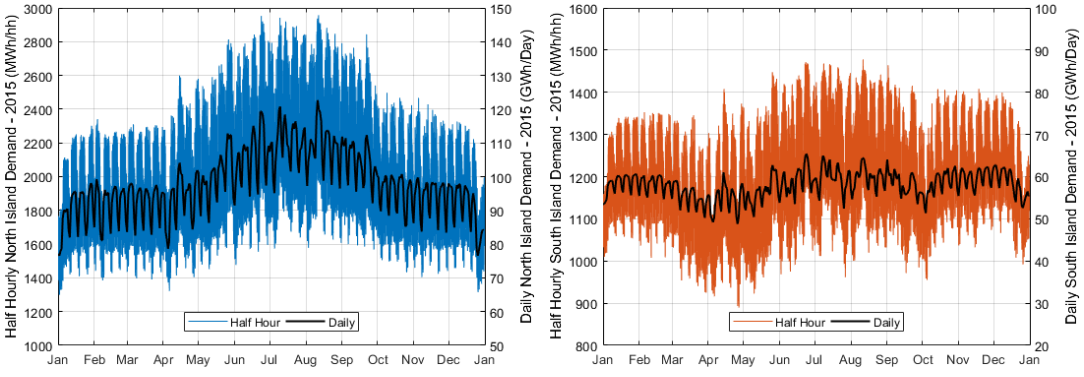

(a) North Island Demand - 2030

(b) South Island Demand - 2030

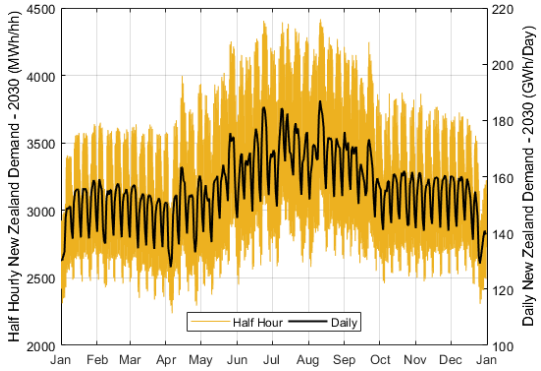

(c) New Zealand Demand - 2030

Figure 3.10 North Island, South Island and total New Zealand Demand - 2030

The reason behind using a daily average to represent the low frequency component is that the TPNZ scenario posits the majority of demand growth is from the electrification of transport fleet and industrial energy use which will predominantly be baseload and gradual changes in demand. It is assumed that the transport fleet's charging can be managed and smoothed over the day.

3.3 THERMAL GENERATION

In New Zealand's system, thermal generation fulfils the role of maintaining adequate hydro storage, supplying peak demand and managing dry year risk. All of the thermal generation is in the North Island due to the proximity of natural gas supply and seaports for coal supply. They are fortunately close to Auckland, New Zealand's largest city responsible for a significant portion of New Zealand's demand.

In the system model, thermal generation is aggregated but has tranches that correspond to the capacities and prices of each thermal generator. The prices for the thermal generator tranches are estimated with available data as the strategy behind how thermal generation is offered into New Zealand's electricity market and the information on the fuel contracts is commercially sensitive.

The thermal generation prices are based on their heat rate (GJ/MWh) and wholesale cost ($/GJ) of their corresponding fuel (coal or natural gas). The heat rates for New Zealand's thermal generation is publicly available from the Electricity Authority's EMI database [Electricity Authority 2021] or the manufacturers specifications[1]. The price of coal was taken from a 2015 projected price relative to 2013 [Covec 2014] and natural gas price was from Concept Consulting Group Limited [2013] which considered pricing scenarios dependent on the future of New Zealand's gas supply. The price used assumes that the natural gas supply in New Zealand remains consistent over 2012 to 2027. Due to the fuel prices being out of date, they were verified by comparing to thermal generation offer data which is presented in Appendix D. The capacities, heat rates and prices are presented in Table D.1. The thermal generation price curve is presented in Figure 3.11.

By 2030, it is expected that some of New Zealand's thermal generation will be decommissioned. Te Mauri Hiko indicates that New Zealand's only coal generator at the Huntly power plant (500 MW) is likely to be decommissioned as well as at least one natural gas generator. For the 2030 scenario, the 500 MW Huntly Coal and 385 MW Taranaki Combined Cycle (TCC) natural gas generators were removed from New Zealand's system model. The TCC generator seemed the most suitable as it is the oldest combined cycle generator and its operation suits baseload or slow variations which will be displaced by new renewable generation.

Table 3.2 Thermal Generation Capacities and Prices. McKee's and TCC's heat rates were from the manufacturer's specifications

Thermal Generator	**Capacity (MW)**	**Heat Rate (GJ/MWh)**	**Fuel Type**	**Price ($/GJ)**	**Price ($/MWh)**
Huntly Coal	500	10.3	Coal	5.72	58
Huntly e3p	400	7.2	Gas	7	50
Huntly p40	48	9.8	Gas	7	68.6
McKee	100	9.127	Gas	7	63.9
Stratford Peaker	200	8.362	Gas	7	58.5
TCC	385	7.6	Gas	7	53.2

[1]The make and model of the thermal units were also available from EA's EMI database

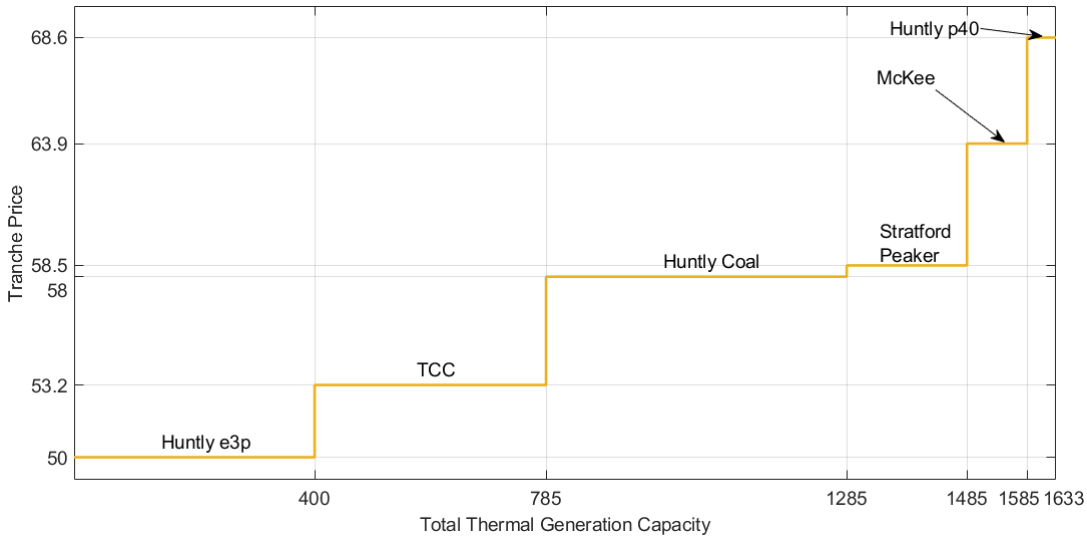

Figure 3.11 Thermal Generation Price Tranches, based on fuel costs

Note the Whirinaki diesel thermal generator is excluded from the model. Whirinaki is exclusively a peaking plant, only operating during extreme high nodal price periods. This mode of operation cannot be imposed in the modelling tool which could dispatch Whirinaki as a baseload generator if conditions were appropriate.

3.4 MUST-RUN GENERATION

Generation types that are inflexible or not dispatchable are must-run generators and include wind, solar, run-of-river (RoR) hydro and geothermal generation. Wind, solar and RoR hydro generation are driven by variable and intermittent sources and are dispatched with no or little control aside from curtailing the production. Geothermal generation is inflexible due to the degradation that would occur if its output was varied often.

Must-run generators are offered into New Zealand's electricity system at $0 or $0.01 such that it is dispatched ahead of all other generation. In the model, they are priced at $0 and to ensure that storage hydro generation is not dispatched at the same priority, the minimum hydro generation price is set to $0.01. The remainder of the section covers each of the must run generation members and their implementation in the model. In all cases, the 2015 data was used and for the 2030 scenario, these data are scaled where appropriate. The representation of must-run generation in the 2030 scenario is covered in Section 3.5.

3.4.1 Wind Generation

Wind farms consists of multiple wind turbines that are spun by wind flow pushing the turbine blades. The wind generation data was produced by McQueen [2016]. McQueen studied the benefit of constructing wind generation in a spatially diverse manner. A major component of this research was developing a wind power model that took low spatial resolution wind speed time series and converted it to a wind power series that could be used to represent specific wind farm sites in New Zealand. A contribution of their work was the development of a Wavelet Multi-resolution Analysis model that transformed the wind speed time series to embody the temporal and spatial characteristics of wind specific locations. Several wind generation investment scenarios were produced, of which the Business-As-Usual distribution was used in this research. For the 2030 scenario, the 2015 wind generation profile was scaled. The magnitude of scaling is covered in Section 3.5. The 2015 wind generation half hourly and daily time series are presented in Figure 3.12.

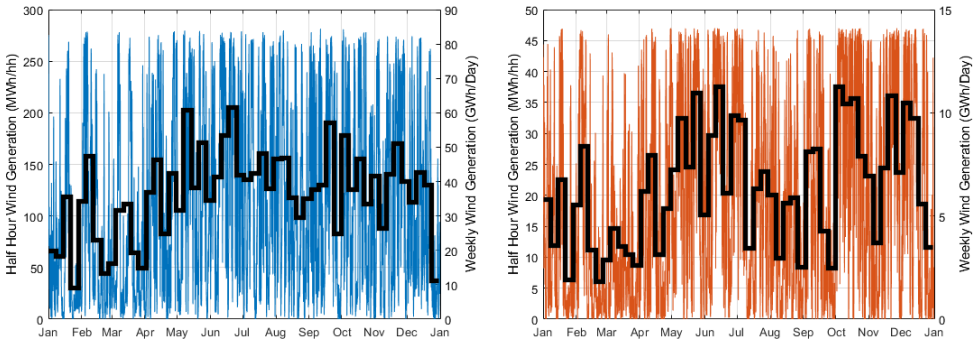

(a) North Island Wind - 2015 (b) South Island Wind - 2015

Figure 3.12 New Zealand Wind - 2015

Unlike the use of multiple inflow sequences, no variation in the modelled wind generation profile was explored in order to limit the number of simulations to conduct. Implicit with this, any correlation between hydro inflow sequences and wind generation is ignored. Figure 3.13 presents the quantile series of the 37 years of wind generation data for both islands on a four weekly time interval. The South Island does not exhibit any strong seasonal variation and in the North Island, there is marginally more wind generation later in the year.

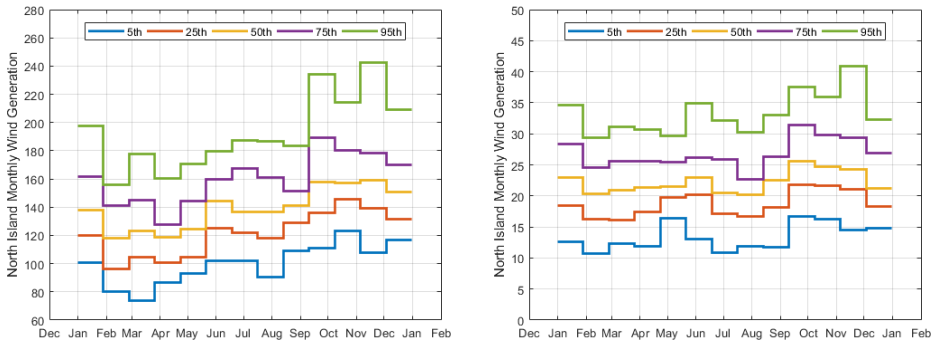

(a) North Island Wind Seasonality (b) South Island Wind Seasonality

Figure 3.13 New Zealand Wind Seasonality - 4 Weekly Quantile Time Series Plots

3.4.2 Solar Generation

Photovoltaic (PV) solar generation produces dc electricity from solar irradiance through PV panels. This is then converted to ac with inverters allowing the system to be connected to the ac power system. As with the wind generation data, an alternative source for solar generation data was used. Santos-Martin and Lemon [2015] produced a PV generation model called SoL. It consists of 9 sub-models which collectively account for the trajectory of the irradiance to the site of the PV solar panels from the Sun, the influence of the Earth's atmosphere, the orientation of the panels and hardware of the PV generator (panels and inverter). This model was applied to New Zealand on a regional basis, providing PV generation data down to a 10 minute temporal resolution.

From the regional data, solar generation sequences from each island were produced. Each region was allocated a proportion of total solar generation capacity based on the number of regional connection versus the total number of connections in New Zealand using June 2020 data from the Electrcity Authority's EMI database. Figure 3.14 presents this distribution. The distribution is correlated with the population density and the capacity factor of solar generation in the region.

Figure 3.15 presents the solar generation sequences used in the simulations. There is a high frequency variation due to the weather along with a strong seasonal variation due to changing sunlight hours and the intensity of received solar irradiance through the year. Both Figure 3.16 and Figure 3.17 show the relative consistency of solar generation year-to-year. Both plots show quantile series of the 16 years of solar generation data (2000 to 2015) on weekly and four weekly time intervals.

Figure 3.14 Distribution of Solar Capacity for 2030 Scenario

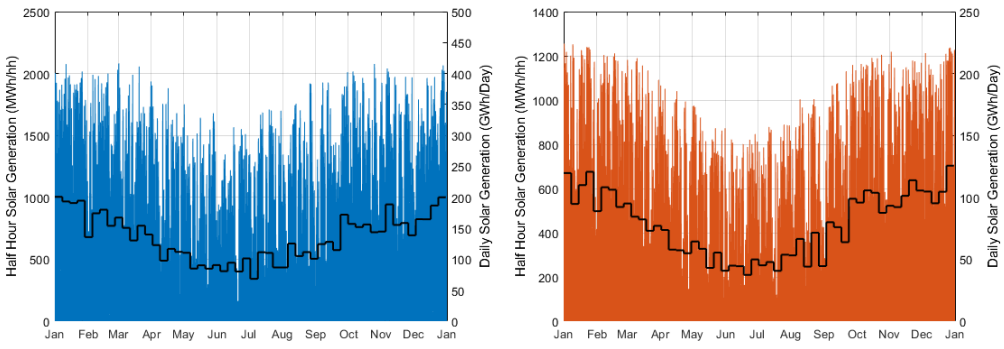

(a) North Island Solar Generation (b) South Island Solar Generation

Figure 3.15 New Zealand Solar Generation. Used for 2030 Scenario

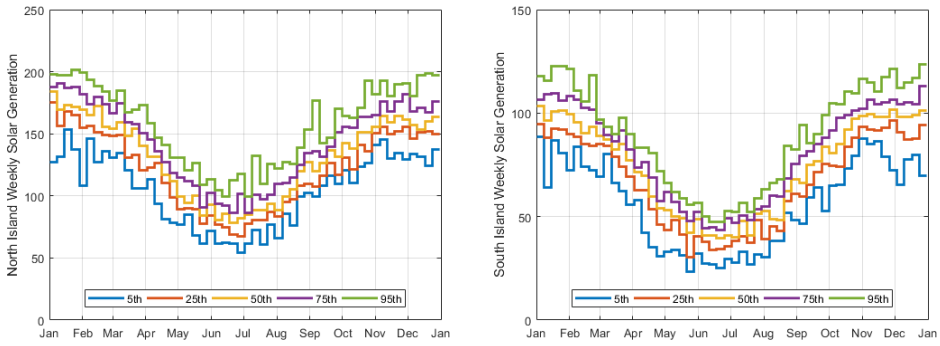

(a) North Island Solar Generation Seasonality (b) South Island Solar Generation Seasonality

Figure 3.16 New Zealand Solar Generation Seasonality - Weekly Quantile Time Series Plots

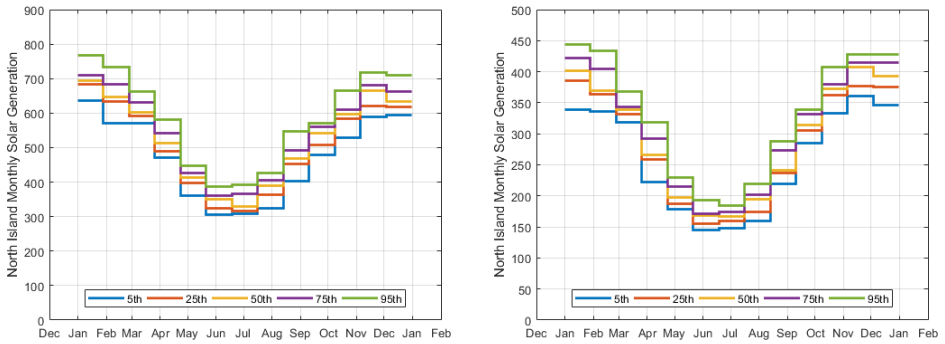

(a) North Island Solar Generation Seasonality (b) South Island Solar Generation Seasonality

Figure 3.17 New Zealand Solar Generation Seasonality - 4 Weekly Quantile Time Series Plots

Solar generation is excluded from the 2015 model as it was a very minor component (0.08% of total annual generation [Ministry of Business Innovation and Employment 2020]). For the 2030 scenario, the base case of Te Mauri Hiko posited a significant uptake in solar generation, both distributed on roof tops and grid connected systems. The particular scaling is covered in Section 3.5.

3.4.3 Run-of-River Generation

Run-of-river (RoR) hydro generation is a hydro scheme that does not have a storage reservoir capable of holding water for multiple days, weeks or months. Without such a reservoir, there is less flexibility to delay the release of water, hence its dispatch is closely tied to its inflows. RoR schemes do have headponds to maintain water pressure and, although limited in size, can offer intra-day flexibility. Figure 3.18 presents the 2015 RoR generation sequence used in the simulations.

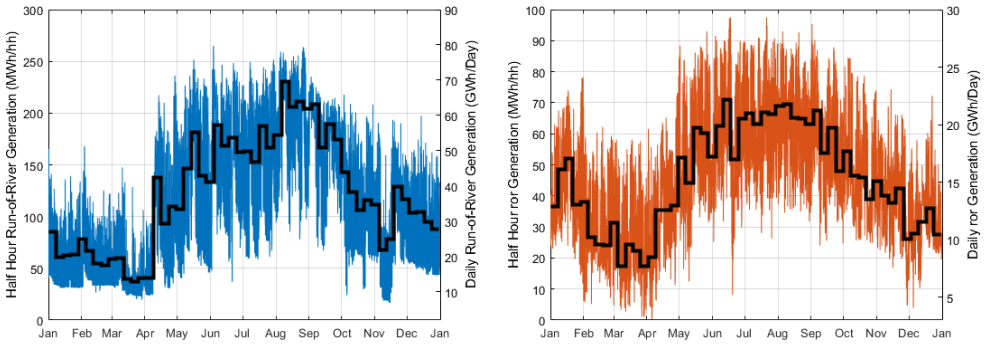

(a) North Island Run-of-River Generation (b) South Island Run-of-River Generation

Figure 3.18 New Zealand Run-of-River Generation

3.4.4 Geothermal Generation

Geothermal generation is powered by high pressure, high temperature geothermal fluid in underground reservoirs heated by the activity in the Earth's mantle. The geothermal fluid is drawn up through boreholes, passed through the turbine and reinjected into the reservoir. As mentioned, geothermal generation is dispatched at a relatively constant level with some minor seasonal variation. Large changes in total generation production is generally due to planned outages for plant maintenance (this is not modelled). The modelled geothermal generation is dispatched at a constant level which reflects the existing geothermal plant operating regimes. For the simulations, geothermal generation is dispatched at a constant rate relative to the average capacity factor from 2009 to 2016 which is 88.41%.

3.5 MODEL SUMMARIES

Table 3.3 and Table 3.4 present the model parameters of the 2015 and 2030 scenarios. Note that each island's peak demand values may not occur at the same time hence their sum do not equal the New Zealand peak demand value. Also, the total energy demand values include the 3% increase that represents transmission losses.

The 2030 scenario is based on the 2015 scenario with increased demand and reduced thermal generation capacity, and additional renewable must-run generation (marked by ">" in Table 3.4) will be added to the model to cover the energy deficit. The proportion in which they are increased by is guided by Te Mauri Hiko [Transpower New Zealand 2018b]. The report outlines the sources of new electricity for the 2030 scenario which consist of 11 TWh of solar generation, 6 TWh of wind generation and 4 TWh of geothermal generation. These exact values were not implemented but a range of added renewable generation was investigated with this ratio maintained. Hydro generation

capacity and storage, and the HVdc Link capacity were explored as investment options also.

Table 3.3 2015 Scenario: Generation Capacities and Energy produced, Storage Capacity, HVdc Link Capacity, Demand Peak and Annual Demand Energy. "Geo." refers to Geothermal

	North Island		**South Island**		**New Zealand**	
	Capacity (MW)	**Energy (GWh)**	**Capacity (MW)**	**Energy (GWh)**	**Capacity (MW)**	**Energy (GWh)**
Hydro	1209.1	-	3263	-	4472.1	-
Thermal	1633	-	0		1633	-
Wind	568	1902.1	94	331.2	662	2233.2
Solar	-	-	-	-	-	-
RoR	528.7	2072	172	882	700.7	2954
Geo.	985	7628	0	0	985	7628
Storage	-	787.4	-	3125.5	-	3912.8
HVdc	1200	-	1200	-	-	-
Demand	4540	25968	2220	15356	6704	41324

Table 3.4 2030 Scenario: Generation Capacities and Energy produced, Storage Capacity, HVdc Link Capacity, Demand Peak and Annual Demand Energy. The "+" represents elements whose capacities will be varied in the 2030 scenario simulations while ">" indicates the renewable generation types that will be increased by some degree.

	North Island		**South Island**		**New Zealand**	
	Capacity (MW)	**Energy (GWh)**	**Capacity (MW)**	**Energy (GWh)**	**Capacity (MW)**	**Energy (GWh)**
Hydro	1209.1+	-	3263+	-	4472.1+	-
Thermal	748	-	0		748	-
Wind	>568	>1902.1	>94	>331.2	>662	>2233.2
Solar	-	-	-	-	-	-
RoR	528.7	2072	172	882	700.7	2954
Geo.	>985	>7628	0	0	>985	>7628
Storage	-	787.4+	-	3125.5+	-	3912.8+
HVdc	1200+	-	1200+	-	-	-
Demand	5914	36894	2956	21816	8832	58710

3.6 OPERATION OF NEW ZEALAND MODEL

A brief example of the deterministic dynamic programming tool's application to the New Zealand system model is presented here. The example simulation uses the 2015 data as presented above as well as the New Zealand electricity market's (NZEM) operation. The inclusion of the NZEM operation is not for comparison given that:

- The modelling tool is deterministic, while the market's operation managed various uncertainties, including inflows
- The New Zealand power system model does not capture the detail of the real system
- The modelling tool performs a single system-wide optimisation while the NZEM operation consists of several parties and stages

There are also some discrepancies between the data used in the modelling tool and NZEM operation data, as such only the macro-scale dynamics of the storage trajectories, hydro generation, thermal generation and HVdc transfer can be compared while specific values cannot be. Appendix G covers the discrepancies.

Figure 3.19, Figure 3.20 and Figure 3.21 present the storage trajectories, thermal generation and HVdc transfer, and hydro generation series for the NZEM operation (top row) and simulated operation (bottom row). Note that the NZEM South Island storage trajectory (Figure 3.19b) has two steps at April and October due to Lake Tekapo having seasonal based conditions on the minimum storage level (i.e. maximum storage capacity). The overall minimum storage capacity is used in the system model.

Comparing the South Island's storage trajectories, the simulated operation results in a larger dynamic storage range (storage range between the minimum and maximum storage levels) than the NZEM operation, probably due to the perfect foresight on inflows. However, the overall pattern between them is similar.

The simulated operation of the system is quite different to the NZEM operation with regards to the North Island storage trajectory, North Island hydro generation, thermal generation and HVdc power flow. The major contributing factor to this is that in the New Zealand system model, the thermal generation price curve is constant over the time horizon, both in terms of tranche sizes and prices. In the NZEM, thermal generation offers vary depending on the operator's contracted demand and other market factors (refer to Appendix D) resulting in a far more variable dispatch. Having a significant baseload supply results in the simulated North Island hydro generation profile being high during winter and low during summer, spanning the full capacity range whereas in the NZEM, the North Island hydro generation is relatively bounded and aligns with the inflow sequence and demand profile patterns. From the HVdc transfer profile, it is apparent from the dominant northward flow that the South Island hydro generation is consistently being dispatched to cover the South Island's demand and supply a portion of the North Island.

(a) North Island - NZEM

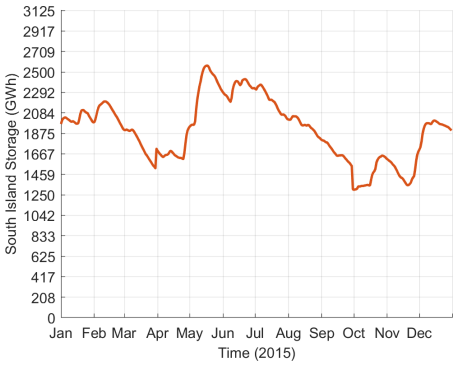

(b) South Island - NZEM

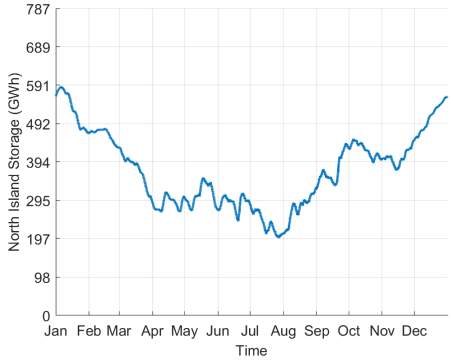

(c) North Island - Simulated Operation

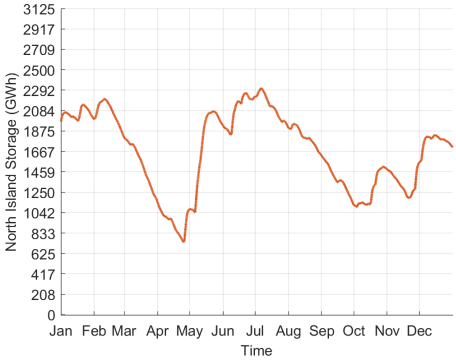

(d) South Island - Simulated Operation

Figure 3.19 Comparison of 2015 Operation: Storage Trajectory

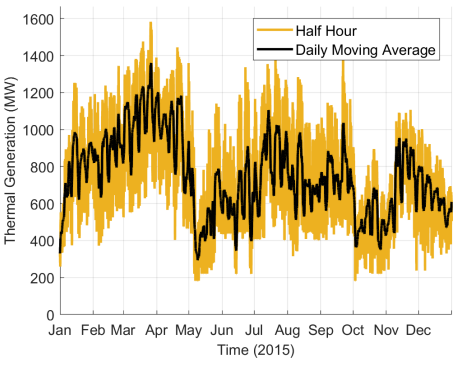

(a) Thermal Generation - NZEM

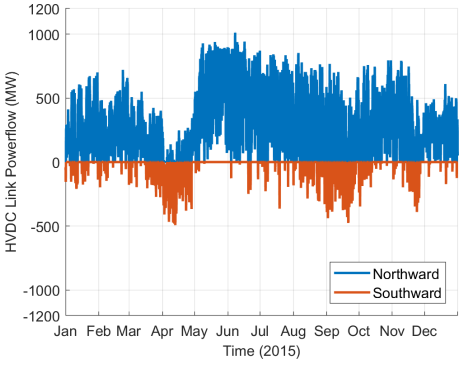

(b) HVdc Power Flows - NZEM

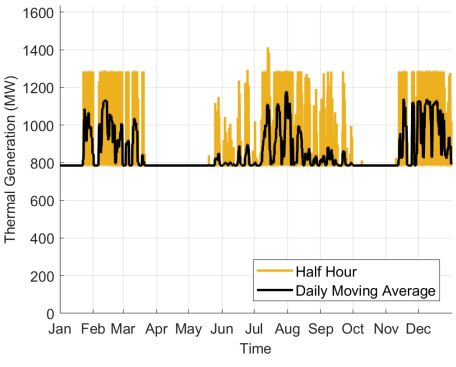

(c) Thermal Generation - Simulated Operation

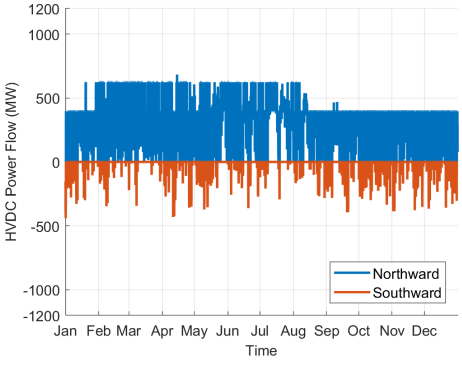

(d) HVdc Power Flows - Simulated Operation

Figure 3.20 Comparison of 2015 Operation: Thermal Generation and HVdc Flows

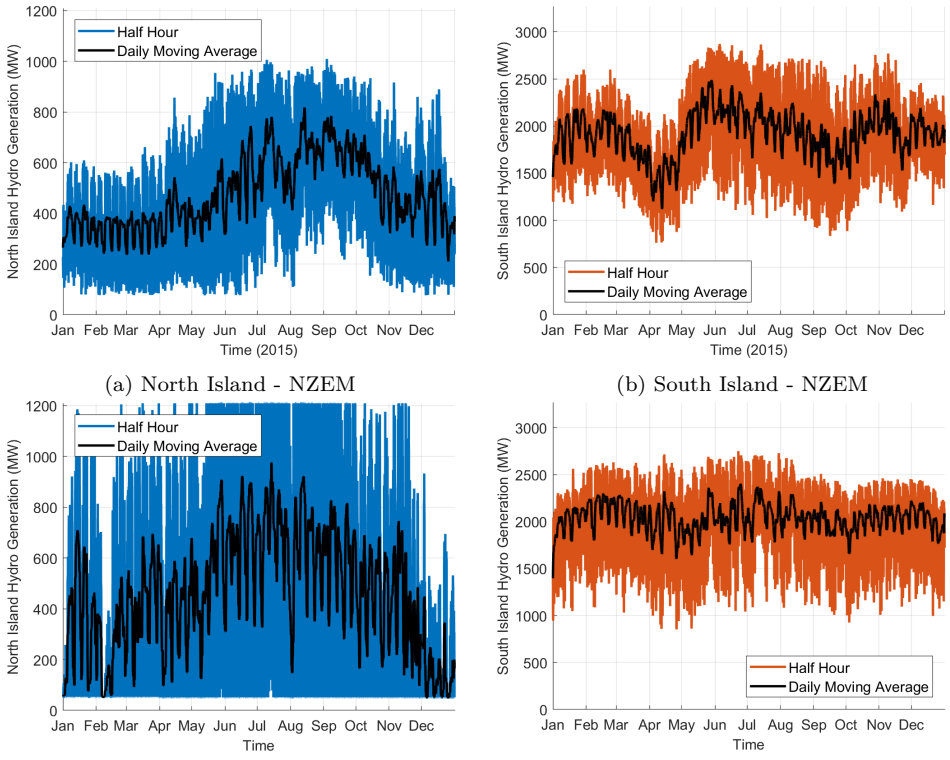

(a) North Island - NZEM

(b) South Island - NZEM

(c) North Island - Simulated Operation

(d) South Island - Simulated Operation

Figure 3.21 Comparison of 2015 Operation: Hydro Generation

Chapter 4

HYDRO SCHEDULING TOOL

Before discussing the hydro scheduling tool, a brief overview of the market operation of New Zealand's electricity system is given. The majority of hydro schemes and other generation are managed by for-profit generator-retailer companies, although not all electricity retailers own and operate generation. Generator-retailer companies both operate their generation portfolios and provide electricity to their customers, an arrangement typically agreed upon through contracts. Each half hour, they provide generation offers to the spot market, operated by the state owned enterprise Transpower New Zealand (TPNZ). These offers specify tranches of capacity and their associated price that the company is willing to provide. With these offers, TPNZ conducts a least cost optimisation with the Scheduling, Pricing and Dispatch tool (SPD) [Transpower New Zealand 2018a] which incorporates system constraints such as transmission and generation capacities, security and contingency event aspects and the forecasts of demand and renewable generation. TPNZ then signals the required generation dispatch levels to the appropriate generators who enact them[1]. From their profit maximising perspective, generator-retailer companies aim to offer such that their generation is dispatched at their forecast contracted demand and beyond this level, offer their generation at a premium price as it would be sold to their competitors. Other factors also contribute to their offering behaviour such as the hydro storage conditions and efficiencies.

From a modelling perspective this operational structure can be viewed as a set of local optimisations performed by the generation-retailer companies for profit maximisation. The collective output of these are the generation offers from which the least cost generation dispatch is determined. In contrast, the hydro scheduling tool developed performs a global optimisation that determines the management of the hydro system and operation of the electricity system assuming direct control of the modelled hydro system for the least cost dispatch. Given this, the goal with the hydro scheduling tool is not to approximate the market operation of New Zealand's system but allow conclusions to be drawn from the simulated performance which can provide an estimate of the

[1]Note that this description is simplistic as the real time dynamics are not covered

impact of increased renewable generation and decommissioned thermal generation, and can approximate the value of different system investments.

The hydro scheduling tool consists of two sub-tools: Price Discovery and System Operation Simulation. The Price Discovery is a deterministic Dynamic Programming based approach that constructs the water value functions for each hydro system for the planning horizon. The System Operation Simulation, given initial storage levels, uses these water value functions to serve as hydro generation price functions, used to simulate the operation of the system and produce storage trajectories and other time series. Figure 4.1 presents the structures of the Price Discovery (Figure 4.1a) and System Operation Simulation (Figure 4.1b).

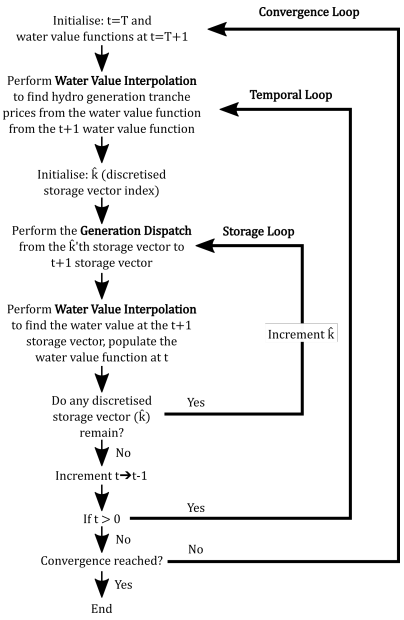

(a) Price Discovery

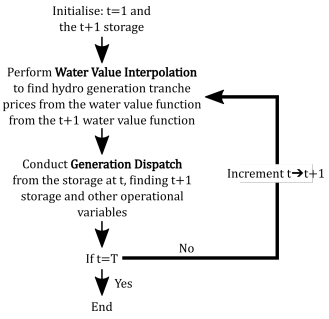

(b) System Operation Simulation

Figure 4.1 Hydro Scheduling Tool Structures

A major deviation with this modelling tool from conventional modern day hydro scheduling tools is that the Price Discovery is deterministic, hence does not account for the uncertainty of inflows. Generally, inflow uncertainty is accounted for by considering a collection of historical or synthetically generated inflow data and in short- and medium-term tools, inflow forecasts are also incorporated. With New Zealand's small hydro storage capacity of 9-10% of annual demand covering 4 to 6 weeks, there is no significant inter-year hydro storage management. As such there is greater emphasis on managing reservoirs on short to medium term horizons. With a two to three week time horizon and accurate forecasting of inflows over this period, the management of New Zealand's hydro system tends toward deterministic operation. This is not to say inflow uncertainty

within this horizon does not impose risks, simply that a deterministic tool on this horizon is acceptable specifically for system studies (not for operation). In other words, if a dry year occurs, the lake levels at the start of the year do not strongly impact the system operation. An important purpose of the developed tool is to investigate the importance of some key parameters of the Price Discovery process, such as the time interval and storage discretisation. The Price Discovery can be easily extended to a stochastic representation of inflows if required. Also, given that temporal decomposition of the hydro scheduling problem was such an early and now established practice, high temporal resolution, medium term modelling tools are atypical and assumably rare.

Although the Price Discovery is deterministic, the primary value is to provide an absolute upper bound to the effectiveness of real world market operation. It would not be possible for the market to operate the system in this way but the modelling tool output is useful, as if issues such as significant spill or demand curtailment are present, it indicates that these are almost certain to occur in practice.

It may be considered unnecessary to develop a hydro scheduling tool to study future systems given its complexity. An alternative approach would be to model the system on long time intervals and make assumptions on the use of hydro storage. However, New Zealand's hydro storage plays a pivotal role in providing seasonal storage (intra-year) but is not adequately sized to provide inter-year storage. The importance of its seasonal storage capability will only increase with the transition from thermal generation and its fossil fuel storage to intermittent renewable generation with no inherent storage. For this reason, considering systems like New Zealand without a hydro scheduling tool would be overly optimistic.

In Figure 4.1, the Price Discovery's temporal and storage loops construct the water value functions ($\hat{v}^*_{t+1}$) over the discretised storage state space ($\hat{\sigma}_{\hat{k}}$) and convergence is checked after each temporal loop completion. The System Operation Simulation simply has a single temporal path, which upon completion produces time series of operational variables such as storage and generation dispatch. The details of what these involve are discussed in Section 4.2 and Section 4.3.

Note that both the Price Discovery and System Operation Simulation utilise the Water Value Interpolation and Generation Dispatch processes. The Water Value Interpolation involves finding the water value of a particular storage vector and is used to produce the hydro generation tranche prices. The Generation Dispatch consists of a linear programming problem that determines the least cost generation dispatch. Both of these components are discussed in Section 4.5 and Section 4.4, and were written in MATLAB

[2019].

4.1 NOTATION

Before explaining the hydro scheduling tool components, the notation is outlined. Note that the notation for this chapter differs from that in Chapter 2. t is the decision stage index and where $t = 1$ and $t = t_{end}$ are the decision stages at the beginning and end of the year respectively. The span from $t = 1$ to t_{end} is called the planning or time horizon:

$$t = 1, ..., t_{end} \tag{4.1}$$

The modelled system has N_s hydro reservoirs and i indexes them. s_t^i is the amount of stored water in the i'th reservoir at time t and is bounded by the maximum and minimum storage levels:

$$\underline{s}_t^i <= s_t^i <= \overline{s}_t^i \tag{4.2}$$

where $\overline{s}_t^i$ and $\underline{s}_t^i$ are the maximum and minimum storage of the i'th reservoir. Typically $\underline{s}_t^i$ is zero. As covered in Chapter 3, all hydro system variables are converted from water volume and flow rate to energy equivalent values. The storage reservoir receives water as inflows from upstream waterways (f_t^i) and water is released through a hydro generator to produce electricity:

$$s_{t+1}^i = s_t^i + f_t^i - g_{h,t}^i \tag{4.3}$$

where f_t^i are inflows into the i'th reservoir and $g_{h,t}^i$ is the hydro generation below the reservoir. If the stored water is above the maximum storage capacity, the excess amount is spilt. Spill is not explicitly represented in Equation (4.3).

As required by Dynamic Programming, the storage state space is discretised. Each storage reservoir is discretised into K^i levels:

$$\widetilde{S}^i := \left\{\sigma_{k^i}^i; k^i \in 1, 2, \ldots, K^i\right\}; \quad i = 1, 2, ..., N_s \tag{4.4}$$

where:

- k^i indexes the i'th reservoir's discrete storage levels,
- $\sigma_{k^i}^i$ is the k^i'th discrete storage level of the i'th hydro reservoir, and
- $\tilde{S}^i$ is the set of discrete storage levels for the i'th hydro reservoir.

σ^i is selected to distinctly represent discrete storage levels whereas s_t^i represents the continuous storage variable. The collection of all combinations of $\sigma_{k^i}^i$ creates the set of discretised storage vectors:

$$\widetilde{S}^{\forall i} := \left\{ \hat{\sigma}_{\hat{k}} = \begin{bmatrix} \sigma_{k_1}^1 & \cdots & \sigma_{k^i}^i & \cdots & \sigma_{k^{N_s}}^{N_s} \end{bmatrix}^T \right\} \forall\, k^i \in 1, 2, ..., K^i$$
$$\hat{k} = \begin{bmatrix} k^1 & \cdots & k^i & \cdots & k^{N_s} \end{bmatrix} \tag{4.5}$$

where:

- $\hat{k}$ is the vector of k^i indices,
- $\hat{\sigma}_{\hat{k}}$ is the discrete storage vector, and
- $\widetilde{S}^{\forall i}$ is the set of all discrete storage vectors.

Figure 4.2 depicts a two reservoir storage state space with each reservoir being discretised into three levels. The x and y axes correspond to the storage in the two reservoirs, each marked with their respective discretised levels ($\sigma_{k^i}^i$ from Equation (4.4)). Each dot represents a discrete storage vector ($\hat{\sigma}_{\hat{k}}$ from Equation (4.5)). An example notation of the highlighted vector is presented in Equation (4.6).

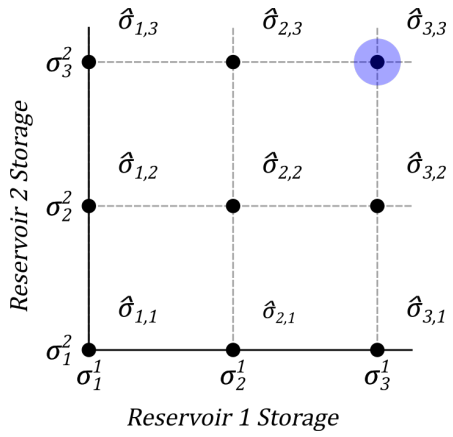

Figure 4.2 Discretised Storage State Space - Two Reservoir

$$\hat{\sigma}_{3,3} = \begin{bmatrix} \sigma_3^1 \\ \sigma_3^2 \end{bmatrix}; \qquad \hat{k} = \begin{bmatrix} k^1 \\ k^2 \end{bmatrix} = \begin{bmatrix} 3 \\ 3 \end{bmatrix} \tag{4.6}$$

A water value function is produced for each reservoir. A reservoir's water value function, $v_t^i(\hat{\sigma}_{\hat{k}})$, consists of a water value at each discrete storage vector and time. Figure 4.3 presents the specific water value function notation relative to the discretised storage vector at time t.

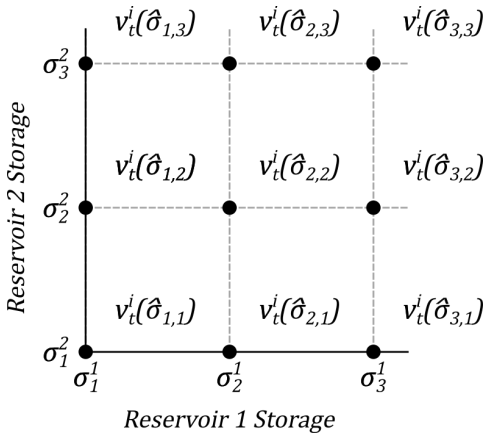

Figure 4.3 Water Value Function on the discretised storage state space - Two Reservoir

The electricity system model has four base variables:

- Demand: $d_{<node>,<Time\ Index\ t>}$
- Generation: $g_{<Type>,<Time\ Index\ t>}$
  - Types: h - Hydro, $thrml$ - Thermal, mr - Must-Run, ns - Non-supply
- Transmission Power Flow: $p_{<sending\ node,\ receiving\ node>,<Time\ Index\ t>}$
- Transmission Losses: $l_{<sending\ node,\ receiving\ node>,<Time\ Index\ t>}$

The variables have a number of sub- and super-scripts denoting their spatial, temporal and other properties. Other notation is explained when presented.

4.2 PRICE DISCOVERY

The price discovery produces the water value functions for the planning horizon for each reservoir. The core process is repeatedly projecting the $t+1$ water value functions $(v_{t+1}^i(\hat{\sigma}_{\hat{k}})\ \forall\ i, \hat{k})$ backward to t. The planning horizon is one year and the time interval between t and $t+1$ can be a minimum of a half hour (17520 intervals in a year). The basis of the projection is from the water value equivalent of Bellman's Equation (detailed in Chapter 2 Section 2.4):

$$v_t^i(\hat{\sigma}_{\hat{k}}) = v_{t+1}^i(\hat{s}_{t+1}^*) \tag{4.7}$$

where $*$ denotes s_{t+1} resulting from an optimal dispatch from $\hat{\sigma}_{\hat{k}}$ at time t. The link between $v_t^i(\hat{\sigma}_{\hat{k}})$ and $v_{t+1}^i(\hat{s}_{t+1})$ is the storage trajectory from the discrete storage vector $\hat{\sigma}_{\hat{k}}$ to $\hat{s}_{t+1}$ which is found with the water balance equation:

$$\hat{s}_{t+1}^* = \hat{\sigma}_{\hat{k}} + \hat{f}_t - \hat{g}_{h,t}^* \tag{4.8}$$

The " ˆ " denotes a variable vector where each i'th element corresponds to the i'th reservoir and $\hat{g}_t^*$ is the optimal hydro generation vector at time t determined by the generation dispatch optimisation (Section 4.4). The potential range of s_{t+1} for a single reservoir is depicted in Figure 4.4a and Figure 4.4b and shows the s_{t+1} range as dispatched from σ_3. The water value $v_t^i(\hat{\sigma}_{\hat{k}})$ could become one of those in the s_{t+1} range. $\hat{s}_{t+1}$ is on a continuous storage space whereas the water value function is defined on a discrete storage state space. In order to find $v_{t+1}^i(\hat{s}_{t+1}*)$, the value is interpolated from the water value function on the discrete storage state space ($v_{t+1}^i(\hat{\sigma}^{\hat{k}})\ \forall\ \hat{k}$. The interpolation is discussed in Section 4.5.

The backward projection begins at $t = t_{end}$, so $t_{end}+1$ water value functions ($v_{t_{end}+1}^i\ \forall\ i$) are needed. Appropriate $v_{t_{end}+1}^i\ \forall\ i$ are determined by creating an arbitrarily defined water value function and conducting the backward projection over the planning horizon (one year) multiple times. Each repeated year is called a cycle, indexed by ψ. Each cycle uses the same data for each year (inflows, demand and renewable generation) and the beginning of year water value function from cycle ψ ($v_{1,\psi}^i\ \forall i$) is used as the $t_{end}+1$ water value function of the next cycle ($\psi+1$):

$$v_{t_{end},\psi+1}^i(\hat{\sigma}_{\hat{k}}) = v_{1,\psi}^i(\hat{\sigma}_{\hat{k}})\ \forall\ i, \hat{k} \tag{4.9}$$

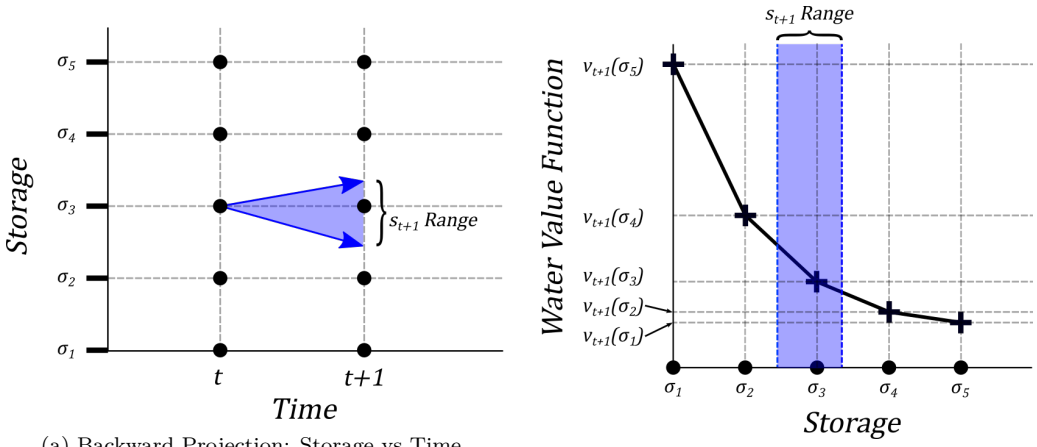

(a) Backward Projection: Storage vs Time

(b) Water Value Function at $t+1$

Figure 4.4

The purpose of cyclically repeating the price discovery is to produce a steady state water value function conditioned to the particular inflow sequence used. To determine whether a steady state as been achieved, a separate convergence process is conducted. This involves applying the System Operation Simulation using the latest cycle's water value function producing a storage trajectory for each hydro reservoir specific to that cycle ψ ($\hat{s}_{T+1,\psi}$). The System Operation Simulation requires an initial storage vector which is either an arbitrarily defined storage vector if $\psi = 1$ or the end of planning

horizon storage vector of the previous cycle ($\hat{s}_{T+1,\psi-1}$). Next, the water values of each hydro reservoir that correspond to its end of planning horizon storage are interpolated ($\hat{v}_{T+1,\psi}(\hat{s}_{T+1,\psi})$). Convergence is reached when subsequent cycles' end of planning period storage vectors and associated water values result in a Gauss-Seidel error of less than 0.5%. The Gauss-Seidel error ($\epsilon_{\psi-1,\psi}$) is:

$$\epsilon_{\psi-1,\psi} = \left| \frac{(a_\psi - a_{\psi-1})}{a_\psi} \right| \tag{4.10}$$

where a_ψ is a placeholder variable for the end of planning period storage or water value at cycle ψ.

An example of the Gauss-Seidel error over 4 cycles is presented in Figure 4.5. The first row of plots are the end-of-year storage error of the North (left) and South (right) Island reservoirs and the second row shown their water value error. As can be seen, the price discovery converges within 3 to 4 cycles.

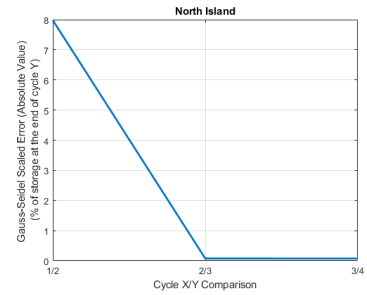

(a) North Island Storage Gauss Seidel Error

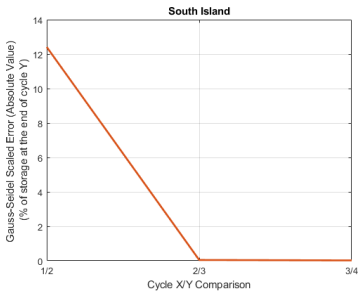

(b) South Island Storage Gauss Seidel Error

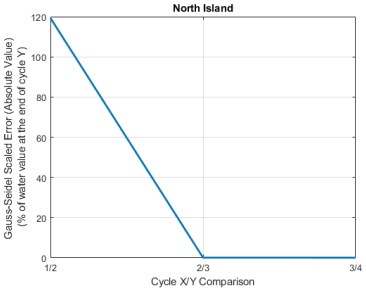

(c) North Island Water Value Gauss Seidel Error

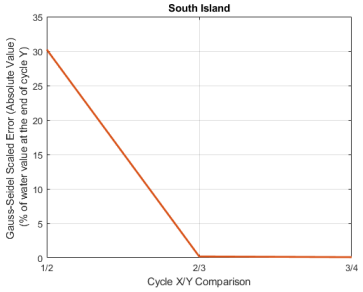

(d) South Island Water Value Gauss Seidel Error

Figure 4.5 Price Discovery Convergence - 1998 Inflow Year

This convergence condition is strictly based on the periodic nature of the Price Discovery's procedure. In Figure 4.6, there are several plots comparing the inter-year behaviour of the water value function and hydro generation between 8 subsequent yearly cycles and it illustrates why a convergence condition comparing the water value function of the full span of the time horizon is inappropriate. The first row of plots compare the optimal hydro generation values from the Price Discovery's generation dispatch at each

$\hat{\sigma}_{\hat{k}}$. The plots show the difference between hydro generation a time t of cycles ψ and $\psi - 1$ as quantile series. The quantiles are formed from the values at all storage vectors in the discretised state space ($\hat{\sigma}_{\hat{k}}$). The bottom row plots show the difference in hydro generation between cycles produced by System Operation Simulation that is run at the end of each cycle.

As seen in Figure 4.6a and Figure 4.6b, from the Year 4 to Year 8 cycle there is a periodic error in the maximum quantile capped around the hydro generation tranche capacity (250 MW). This indicates that the subsequent cycle varies by a single hydro tranche for both hydro generators. Similarly, there are intermittent differences in the hydro generation (Figure 4.6c and Figure 4.6d).

These oscillatory patterns are due to the generation dispatch alternating between dispatching a hydro generation tranche and a thermal generation tranche from cycle to cycle. This is due to the hydro tranche prices containing an available thermal generator tranche price and the slight change in the water value function in subsequent cycles changes the merit order dispatch curve. This is only evident when considering short term variations whereas the medium to long-term effect is minimal. With the convergence criteria being based on comparing the start and end storage and water values, the convergence is insensitive to this short term variability.

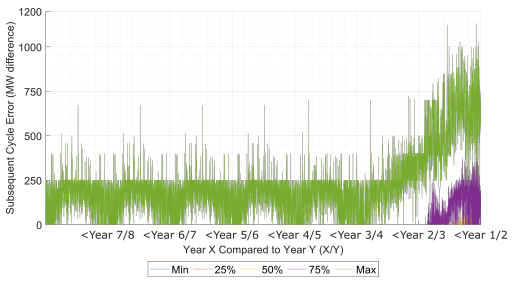

(a) Price Discovery Quantile Plot: System Operation
North Island Hydro Generation

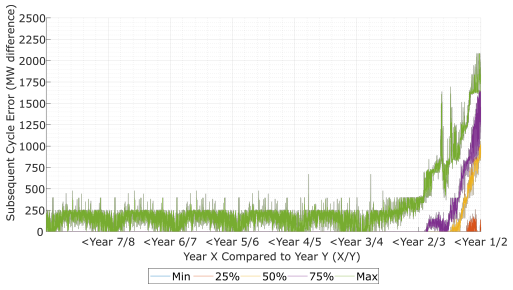

(b) Price Discovery Quantile Plot: System Operation
South Island Hydro Generation

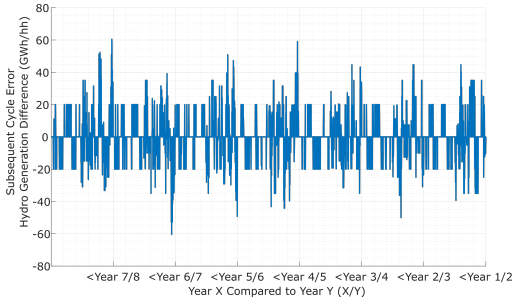

(c) System Operation:
North Island Hydro Generation

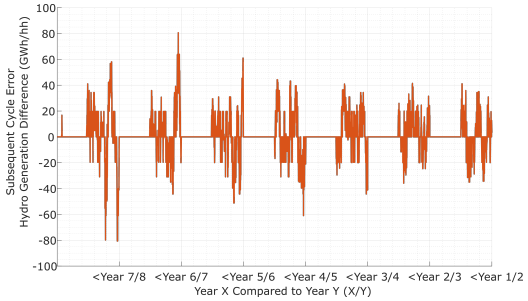

(d) System Operation:
South Island Hydro Generation

Figure 4.6 Inter-cycle difference - Top Row: Price Discovery Hydro Generation; Middle Row: Price Discovery Water Value Function; Bottom Row: System Operation Hydro Generation

4.2.1 Water Value Function - Form, Dynamics and Boundary Values

The general form of a water value function is high values at empty storage and low (almost zero) at full storage, as depicted in Figure 4.7. At full storage, there is a risk of the water level exceeding the maximum level requiring the excess to be spilt. Spilt water is effectively wasted fuel so reservoirs are operated such that they can absorb inflow events hence the low values. At empty storage, a hydro generator's capacity is limited to the inflow which imposes the risk of curtailing demand. Curtailing demand incurs a high cost hence the water value at low storage levels should be significantly higher than the most expensive thermal generator. This ensures that the thermal generation is dispatched ahead of hydro generation sufficiently early to conserve water in the reservoir.

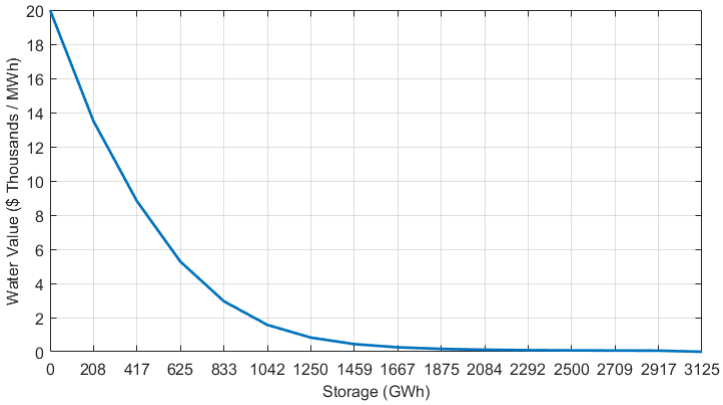

Figure 4.7 Water Value Function Example

Given this monotonic non-increasing form of the water value function, the manner in which the price discovery projects the water value function at the same discretised storage level (σ_k) from $t+1$ to t can be examined. Note for the following discussion, a single reservoir system is considered for simplicity and as such, k^i is replaced with k. The range of projection outcomes are listed below and depicted in Figure 4.8:

- Outcome 1: If optimal dispatch results in $s_{t+1} > \sigma_k$ then $v_t(\sigma_k)$ is less than or equal to $v_{t+1}(\sigma_k)$
- Outcome 2: If optimal dispatch results in $s_{t+1} < \sigma_k$ then $v_t(\sigma_k)$ is greater than or equal to $v_{t+1}(\sigma_k)$
- Outcome 3: If optimal dispatch results in $s_{t+1} = \sigma_k$ then $v_t(\sigma_k)$ is equal to $v_{t+1}(\sigma_k)$

Thus water storage values incrementally change as the price discovery process progresses back in time.

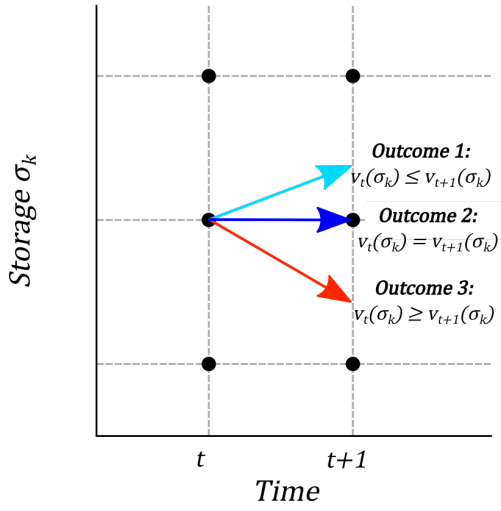

Figure 4.8 Water Value Function changes

These water value changes are only applicable with internal discrete storage points, that is σ_k at $k = 2, 3, ..., K-1$ (K is the number of discrete storage levels of the reservoir). At the boundary storage points (σ_k at $k = 1, K$), s_{t+1} cannot be outside the storage minimum or maximum as shown in Figure 4.9. As such, at maximum storage, the water value can only remain constant or increase and at minimum storage, the water value can only remain constant or decrease.

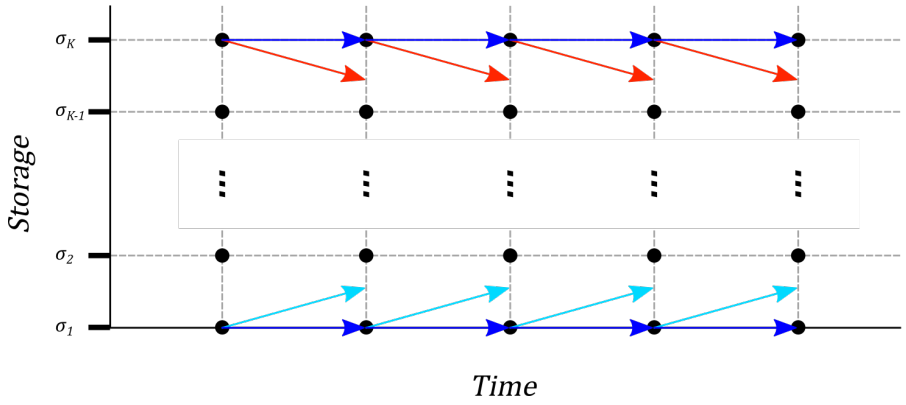

Figure 4.9 Water Value Function Projection at the Boundary

Over the course of the price discovery process, the water values at the maximum and minimum storage levels will decrease and increase, respectively. The net result of this is demonstrated by the boundary water value plots in Figure 4.10. The plots were produced with the New Zealand system model which has two reservoirs, the North and the South Island. Each reservoir has its own water value function, which are presented on the left and right hand sides respectively. The boundary water value plots are water value functions produced with a dry year's (1976) and a wet year's (1998) inflow

sequences.

With New Zealand's system, at a reservoir full storage level (e.g. $\sigma^1_{K^1}$), there are K^2 storage vectors, $\hat{\sigma}_{[K^1,k^2]}\ \forall\ k^2$. Note that the $\square^2$ is the index i value and not to the power of 2. Similarly for the other boundary storage levels which are all depicted in Figure 4.11. The shaded areas represent the range of water values for each boundary storage level ($\sigma^1_1, \sigma^1_{K^1}, \sigma^2_1$ and $\sigma^2_{K^2}$).

The plots in Figure 4.10 all show the North and South Island's boundary water values, and by extension all water values tend to a single value. Note that the water value is projected backwards, hence the progression is from right to left. The value converged to is related to the inflow sequence. The 1976 dry inflow year water value functions settles to a water value greater than the price of all thermal generation (leading to all thermal generation being baseloaded). The 1998 wet inflow year converges to values in between the thermal generation prices. Obviously, a constant water value over the entire year means the reservoir storage is not being operated according to the immediate conditions, risking spill, demand curtailment or both.

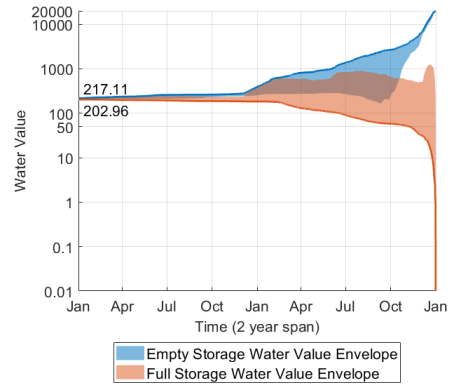

(a) 1976 - North Island

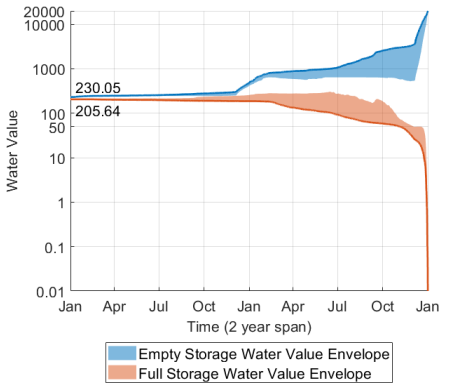

(b) 1976 - South Island

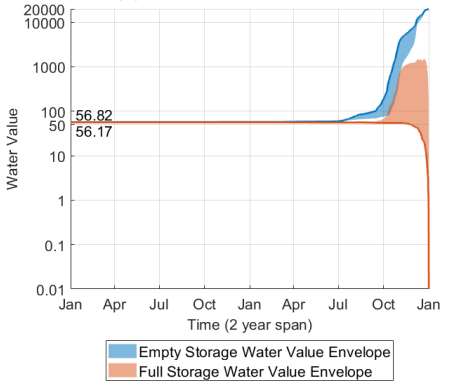

(c) 1998 - North Island

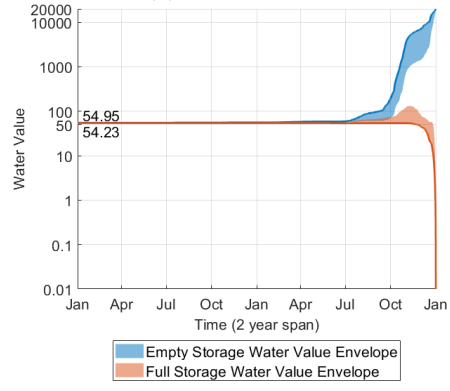

(d) 1998 - South Island

Figure 4.10 Collapse of Boundary Water Values

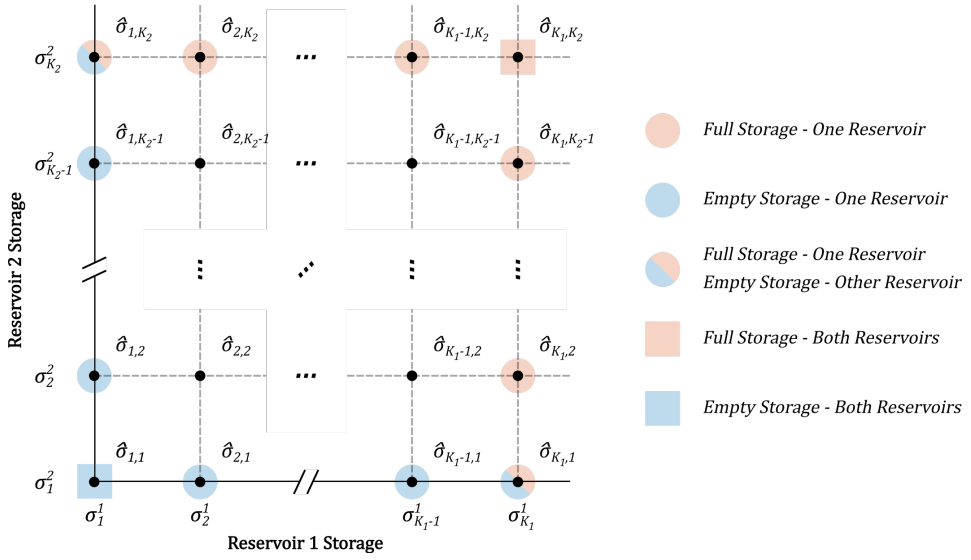

Figure 4.11 Boundary Storage Vectors and Water Values

Stage and Larsson [1961] and Lindqvist [1962] both implement a conditional approach to boundary water values. These are:

- At full storage, if spill occurs, the water value is set to zero
- At empty storage, if demand is curtailed, the water value is set to an extremely high price (value of lost load)

An issue with this conditional approach is that the occurrence of demand curtailment and spill occurring depends on the span of the time interval used. In particular, demand curtailment would be most apparent during peak demand periods which are only evident in short time intervals (e.g. half hourly). With longer time intervals (e.g. six hourly and longer), demand variation is averaged out effectively removing the demand peak. Lindqvist [1962] mentions this, stating that demand curtailment would be rarely apparent with the monthly time interval they used. If demand curtailment never occurs, the convergence of the maximum and minimum storage boundary water values to each other will still occur.

To demonstrate this, Figure 4.12 presents the water value quantile series of the North Island's empty storage vectors ($\hat{\sigma}_{[1,k^2]}$) from conducting the price discovery with 2 and 6 hour time intervals. The 1947 inflow sequence was used. These plots are similar to the boundary water value ranges (Figure 4.10) but the quantiles show the distribution of water values. The maximum series (green) corresponds to $\sigma_{[\hat{1},1]}$ (both reservoirs empty) and similarly the minimum series (blue) corresponds to $\sigma_{[1,\hat{K^2}]}$ (North Island reservoir is empty while the South Island reservoir is full). The key difference between the 2 and

6 hour empty storage water values is the water value spike in late May with the 2 hour time interval which influences the entire year's empty storage water value series and by extension the whole water value function. This is due to the 2 hour time interval capturing a demand period where the North Island hydro generation capacity is needed. In contrast, the 6 hour time interval, quantile series show over 50% of the empty storage water values are in proximity to the thermal generation prices ($50 to $70). This would indicate that the water values at non-empty North Island storage vectors would be low as well.

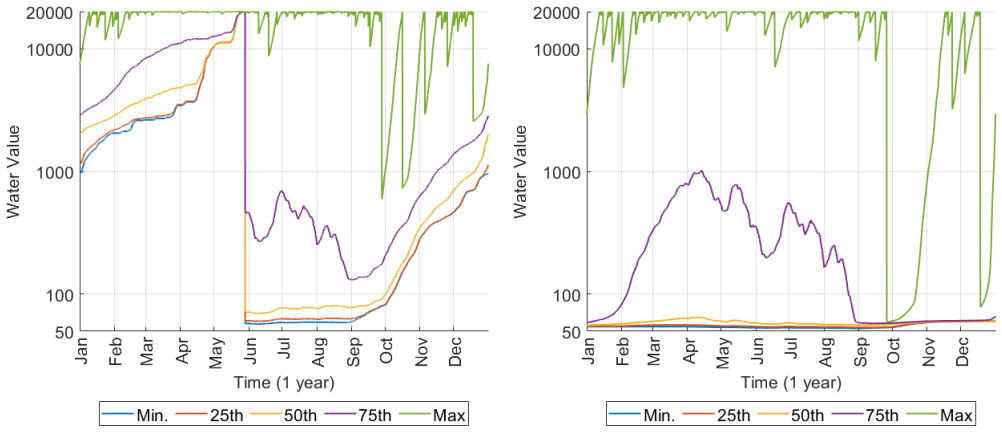

(a) 2 Hour Time Interval (b) 6 Hour Time Interval

Figure 4.12 North Island Boundary Water Value Range - Comparing the effect of different time intervals on conditional boundary water values

Figure 4.13 presents the effect of the time interval and the consequential water value function on the operation of the North Island's reservoir. The 2 hour time interval water value function holds water in the reservoir throughout the year whereas the 6 hour time interval water value function results in the North Island's reservoir being drained to empty. This draining would occur if the water value is lower than all thermal generators' prices and the South Island hydro generator's water value.

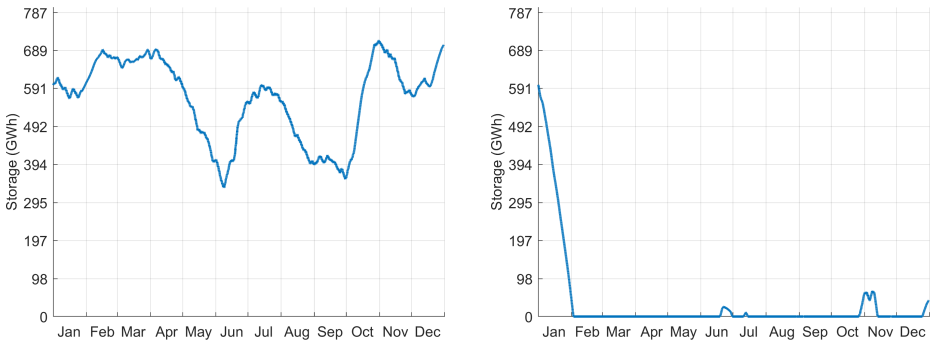

(a) 2 Hour Time Interval (b) 6 Hour Time Interval

Figure 4.13 North Island Storage - Comparing the effect of different time intervals on conditional boundary water values

Even with the risky operation of the North Island hydro reservoir, the system operation

leads to minimal demand curtailment (>0.01 GWh over the year). However, the hydro scheduling tool does not account for other aspects which would invalidate this operation. These include:

- Security constraints. The modelling tool assumes 100% reliability of generation and transmission assets
- Uncertainty of demand and renewable generation variations within the time interval. New Zealand's electricity system's dispatch is updated every 5 minutes with reserve procurement, system inertia and other facilities managing the variation within the 5 minute interval.
- The hydro generator owners (Generation-Retail companies) having their own committed demand to supply. As such, draining a reservoir to empty compromises this objective.

The conditional boundary water value approach is presumably still implemented in modern Stochastic Dynamic Programming (SDP) tools, as Wolfgang et al. [2009] cites both Stage and Larsson [1961] and Lindqvist [1962] for the methodology. As described in Chapter 2, the hydro scheduling problem is often decomposed into long, medium and short-term tools. Generally SDP is used for the long and medium-term role and the short-term tools account for the high temporal resolution features such as peak demand.

Given that only a single hydro scheduling tool is being developed, it is out-of-scope for this research to produce multiple tools that temporally decomposed the hydro scheduling problem, hence an alternative boundary water value condition approach is needed. Two options were investigated:

- System-Wide Boundary Condition (BC) depicted in Figure 4.14a: At the discrete storage vector where all reservoirs are full, the water value is set to the minimum hydro generation price ($0.01). At the discrete storage vector where all reservoirs are empty, the water value is set to the value of lost load ($20000).
- Reservoir Centric Boundary Condition (Figure 4.14b): At the discrete storage vectors where the i'th reservoir is full, the i'th reservoir water value is set to the minimum hydro generation price. At the discrete storage vectors where the i'th reservoir is empty, the i'th reservoir water value is set to the value of lost load.

The reservoir centric BC aims to maintain adequate storage in each reservoir, regardless of the storage condition in others, and this implicitly assumes that the inter-node transmission system often constrains system operation which imposes significant risk. In contrast, the system-wide BC is concerned with storage across the entire system,

rather than specific reservoirs and as such is the inverse case of the reservoir centric BC with regards to inter-node transmission system constraints and risk.

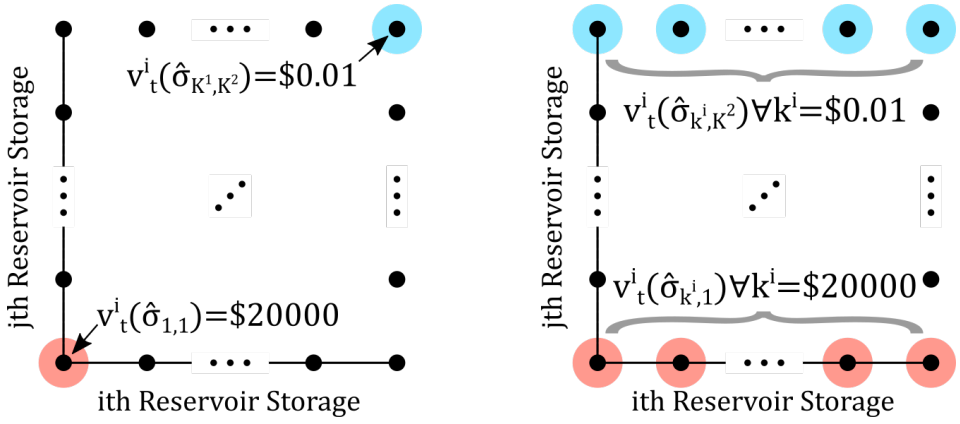

(a) System Wide (b) Reservoir Centric

Figure 4.14 Boundary Water Value Conditions

Figure 4.15 and Figure 4.16 present the storage series from simulations with the System Wide (top row) and Reservoir Centric (bottom row) Boundary Condition and Table 4.1 shows the annual total thermal generation and spill of the year. Two inflow sequences were used, 1976 (a dry year) and 1998 (a wet year).

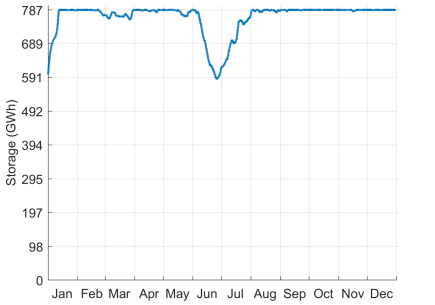

(a) North Island Storage - System Wide - 1976

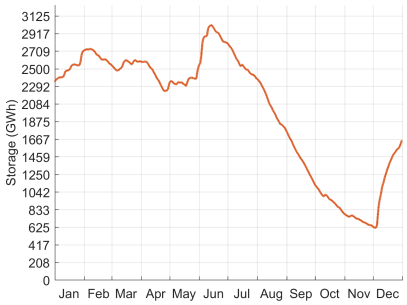

(b) South Island Storage - System Wide - 1976

(c) North Island Water Value - Reservoir Centric - 1976

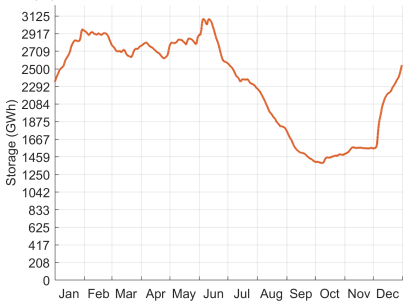

(d) South Island Water Value - Reservoir Centric - 1976

Figure 4.15 Comparison between Boundary Conditions (System Wide and Reservoir Centric) - Storage Series - 1976 Inflow)

Both boundary water value options operate the South Island reservoir similarly, although in 1998 where the system-wide BC produces more spill. The major concern is in the operation of the North Island reservoir with the System-Wide BC. In the 1976 dry inflow year, the North Island reservoir is kept at maximum capacity for a large proportion of the year resulting in spill whereas in the 1998 wet inflow year, storage is driven to empty. No demand curtailment occurs but, as listed above for the conditional boundary water values, it is untenable. In both inflow years, the System-Wide BC results in more thermal generation and spill than the Reservoir-Centric results, shown in Table 4.1.

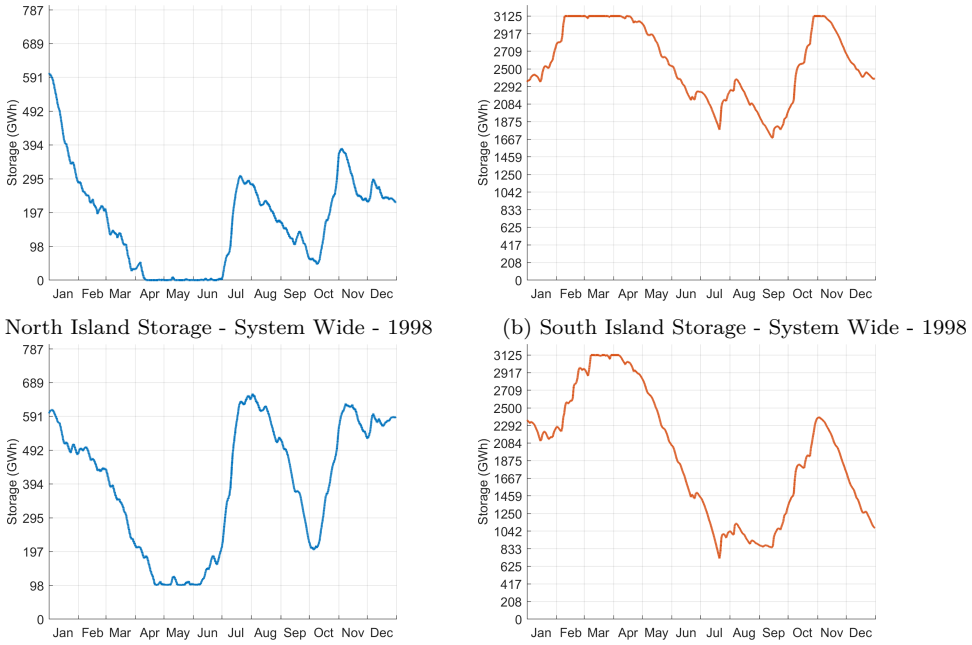

(a) North Island Storage - System Wide - 1998

(b) South Island Storage - System Wide - 1998

(c) North Island Water Value - Reservoir Centric - 1998

(d) South Island Water Value - Reservoir Centric - 1998

Figure 4.16 Comparison between Boundary Conditions (System Wide and Reservoir Centric) - Storage Series - 1998 Inflow

This operation with the System-Wide BC water value function is due to the weak influence that the boundary water values have on the water value function as a whole, leading to a similar behaviour as the conditional boundary water values discussed prior. Figure 4.17 presents the North Island's boundary water value series of the System-Wide BC water values over the time horizon for 1976 and 1998 inflow years. Although the System-Wide boundary water values do not converge as the conditional boundary water values do, in 1976 the water values are such that all thermal generators are effectively baseloaded and in 1998 hydro generation is dispatched ahead of thermal generation for the vast majority of storage levels. Given these results on the boundary water value conditions, the Reservoir Centric boundary condition is used in the modelling tool.

Table 4.1 Annual Thermal Generation and Spill of System-Wide and Reservoir-Centric for 1976 and 1998 Inflow Year

	Thermal Generation (GWh)		Spill (GWh)	
	System-Wide	**Reservoir-Centric**	**System-Wide**	**Reservoir-Centric**
1976	13925	12701	1928	0
1998	3884	1866	2095	894

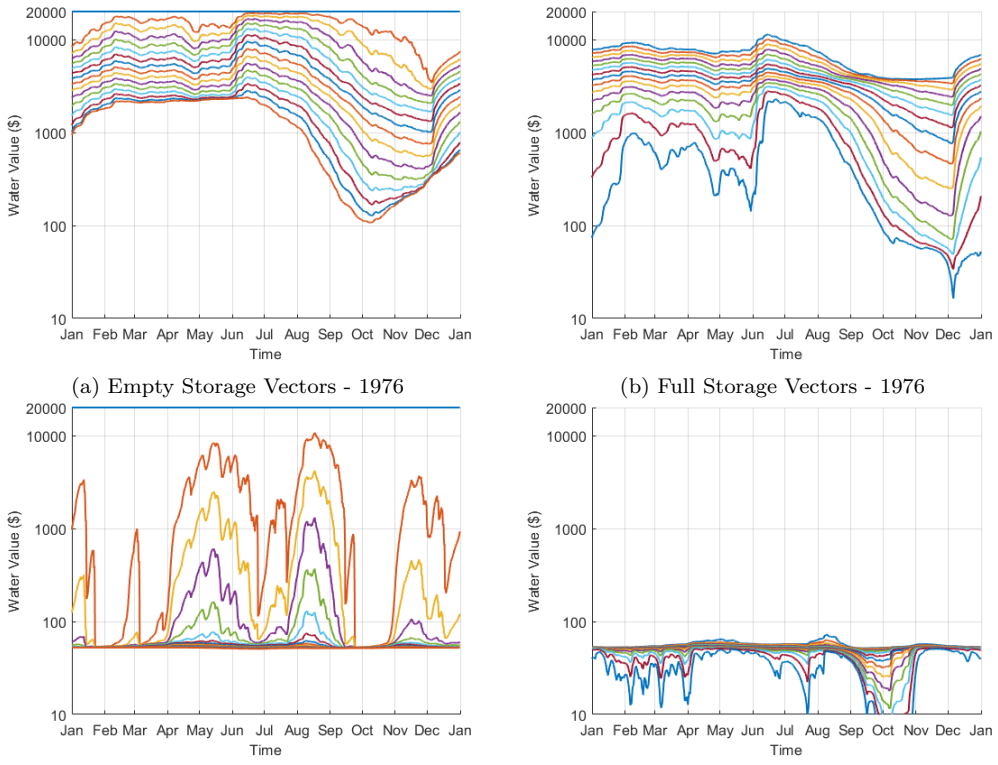

(a) Empty Storage Vectors - 1976

(b) Full Storage Vectors - 1976

(c) Empty Storage Vectors - 1998

(d) Full Storage Vectors - 1998

Figure 4.17 North Island Boundary Water Values from System Wide Condition (1976 Inflow). Note that the water value series at $\hat{\sigma}_{\hat{k}}; \hat{k} = [1, 1]^T$ is at \$0.01 across the year. This is beyond the minimum y-axis y value

4.3 SYSTEM OPERATION SIMULATION

The System Operation Simulation provides the generation, storage and other time series that are used to judge the performance of the modelling tool and provide the data from which aggregate measures are calculated. These measures include the annual renewable generation percentage, annual spill and demand curtailment.

The algorithm of the system operation simulation is presented in Figure 4.1b. The system operation simulation applies the same generation dispatch optimisation and hydro generation price determination as the price discovery. Typically the initial storage vector is an average of historical starting storage levels unless otherwise specified.

4.4 GENERATION DISPATCH OPTIMISATION

The generation dispatch optimisation (GDO) determines the least cost generation dispatch given the system model and system conditions (e.g. demand and renewable generation). In the Price Discovery, the GDO is applied at each discrete storage vector ($\hat{\sigma}_{\hat{k}}$), providing the optimal storage trajectory ($\hat{s}^*_{t+1}$) which is used to determine the water value that populates the water value function at time t ($v^i_t(\hat{\sigma}_{\hat{k}})$). With the System Operation Simulation, the GDO is applied at each time step. This incrementally builds the storage trajectory and the other time series data. Note, the storage trajectory is not pinned to the discretised storage levels $\hat{\sigma}_{\hat{k}}$.

The generation dispatch optimisation is formulated as a linear programming (LP) problem and solved with IBM's CPLEX Optimiser [IBM 2018]. Although linear programming is computationally efficient, the system must be modelled with linear equations, requiring any non-linear relationships to be approximated. This approximation will be discussed when necessary.

The general form of a linear programming minimisation formulation is shown in (Equation (4.11)) for reference [Chong and Zak 2013]:

$$\begin{aligned} &min \quad \hat{c}^T\hat{x} \\ A_{eq}\hat{x} = \hat{b}_{eq} \quad &A_{ineq}\hat{x} \leq \hat{b}_{ineq} \\ &\underline{\hat{x}} \leq \hat{x} \leq \overline{\hat{x}} \end{aligned} \tag{4.11}$$

where $\hat{x}$ is the vector of decision variables and $\hat{c}$ is the vector of per-unit costs associated with the decision variables. A_{eq} and A_{ineq} are the equality and inequality constraint matrices with $\hat{b}_{eq}$ and $\hat{b}_{ineq}$ being their counterpart vectors, and $\underline{x}$ and $\overline{x}$ are the lower and upper bounds of the decision variables. The remainder of this section presents the specific GDO formulation consisting of the cost function and the nodal energy balance, water (energy) balance, transmission losses and minimum hydro generation constraints.

Cost Function

The cost function (Equation (4.12)) consists of the total cost of the dispatched generation (C_{gen}) and the penalty cost for not satisfying the minimum hydro generation requirement (P_{minh}). This penalty cost is described when presenting the minimum hydro generation

constraints.

$$\begin{gathered} \min C_{gen} + P_{minh} \\ C_{gen} = C_{hydro} + C_{thrml} + C_{non-supply} + C_{mustrun} \\ C_{thrml} = \hat{c}_{thrml} \cdot \hat{g}_{thrml} \\ C_{non-supply} = \hat{c}_{non-supply} \cdot \hat{g}_{non-supply} \\ C_{mustrun} = 0 \end{gathered} \tag{4.12}$$

The system model consists of four generation types: Hydro, thermal, non-supply and must-run (non-dispatchable renewable generation), each of which have a cost associated with them. Determining the hydro generation cost function involves an interpolation process on the water value function and is covered separately in Section 4.5.1. C_{thrml} is the total thermal generation cost with each element of $\hat{c}_{thrml}$ containing a thermal generator's price. For the specific prices, refer to Table D.1 in Chapter 3.

To represent demand curtailment, fictitious non-supply generation ($\hat{g}_{non-supply}$) is modelled at each node. Their price ($\hat{c}_{non-supply}$) is set to the extremely high value of lost load and is only dispatched as a last resort. $C_{mustrun}$ is the must-run generation cost. In New Zealand's electricity market, must-run generation is set at a price that essentially guarantees their dispatch, hence its price is zero.

Nodal Energy Balance

At each node, generation injects electric power into the system which flows through the transmission system and supplies demand, as depicted in Figure 4.18. To ensure that adequate generation is dispatched, the nodal energy balance constraint requires the energy injected by generation, used by demand and entering or exiting the node through transmission lines sum to zero. The constraint's formulation is:

$$\begin{gathered} d_\alpha + \sum_{\beta \in B_\alpha} \left(\frac{l_{\alpha,\beta}(p_{\alpha,\beta})}{2} \right) = \sum_{\omega \in \Omega_\alpha} \left(g_\omega \right) + \sum_{\beta \in B_\alpha} \left(p_{\beta,\alpha} \right) \quad \alpha = 1, ..., N_{nd} \\ 0 \leq \hat{g} \leq \hat{\bar{g}} \qquad \hat{\underline{p}} \leq \hat{p} \leq \hat{\bar{p}} \qquad p_{\beta,\alpha} = -p_{\alpha,\beta} \end{gathered} \tag{4.13}$$

where α is the subject node's index, N_{nd} is the number of nodes in the system and $\beta \in B_\alpha$ indexes the nodes connected to node α. Ω_α is the set of generator indices that are connected to node α. The terms in Equation (4.13) are:

- d_α is the subject node's demand

- g_ω is the ω'th generator attached to the node, limited by its capacity, $\overline{g}_\omega$
- $p_{\beta,\alpha}$ is the power flow from node β to node α and limited by their forward and backward capacities, $\underline{\hat{p}}$ and $\overline{\hat{p}}$
- $l_{\alpha,\beta}$ is the transmission losses due to power flows between node α and node β ($p_{\alpha,\beta}$) which are distributed evenly between the receiving and transmitting nodes

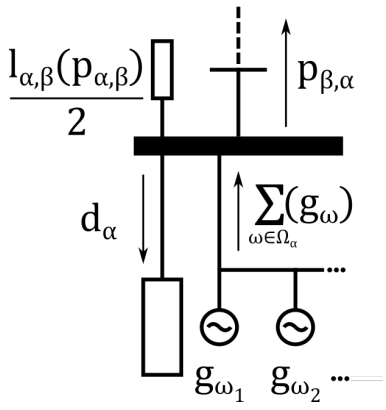

Figure 4.18 Nodal Energy Flow

A feature excluded from nodal energy balance were the impedances of the transmission branches which determine how power flow is distributed over these branches. This reduces the computational requirement of the generation dispatch optimisation at the cost of limiting the transmission system model to node-to-node and branching structures, without mesh structures.

Transmission Losses

The losses in a transmission branch are a non-linear function of its power flow. For this reason, the losses are approximated with a piecewise linear function. The variable used in the piecewise function is the absolute value of the power flow ($|p_{\alpha,\beta}|$) as transmission losses occur regardless of the direction of power flow. Equation (4.14) presents the equations to produce $|p_{\alpha,\beta}|$ with the above notation.

$$\begin{aligned} |p_{\alpha,\beta}| &= p^+_{\alpha,\beta} - p^-_{\alpha,\beta} \qquad & p_{\alpha,\beta} &= p^+_{\alpha,\beta} + p^-_{\alpha,\beta} \\ 0 &\leq p^+_{\alpha,\beta} \leq \overline{p}_{\alpha,\beta} \qquad & \underline{p}_{\alpha,\beta} &\leq p^-_{\alpha,\beta} \leq 0 \end{aligned} \tag{4.14}$$

where $p_{\alpha,\beta}$ is the power flow from node α to node β, $p^+_{\alpha,\beta}$ and $p^-_{\alpha,\beta}$ are the positive and negative components of $p_{\alpha,\beta}$ and $|p_{\alpha,\beta}|$ is the absolute value of $p_{\alpha,\beta}$. $\overline{p}_{\alpha,\beta}$ and $\underline{p}_{\alpha,\beta}$ are the capacity limits on $p_{\alpha,\beta}$. The piecewise function for transmission loss of the branch

is:

$$|p_{\alpha,\beta}| = \sum_{\tau=1}^{N_{l,\alpha,\beta}} \left(p^{\tau}_{\alpha,\beta}\right) \qquad l_{\alpha,\beta}(p_{\alpha,\beta}) = \sum_{\tau=1}^{N_{l,\alpha,\beta}} \iota^{\tau}_{\alpha,\beta} \cdot p^{\tau}_{\alpha,\beta}$$
$$\iota^{\tau}_{\alpha,\beta} < \iota^{\tau-1}_{\alpha,\beta} \qquad 0 \le p^{\tau}_{\alpha,\beta} \le \overline{p}^{\tau}_{\alpha,\beta} \tag{4.15}$$

$l_{\alpha,\beta}$ are the losses that result from $p_{\alpha,\beta}$, $\overline{p}^{\tau}_{\alpha,\beta}$ is the τ'th loss tranche of $|p_{\alpha,\beta}|$ and $p^{\tau}_{\alpha,\beta}$ is power flow associated with that tranche. The number of tranches is $N_{l,\alpha,\beta}$. $\iota^{\tau}_{\alpha,\beta}$ is the τ'th tranche's loss factor (MWh Loss / MWh Power Flow). Figure 4.19 presents examples of loss factor and total transmission loss relationships.

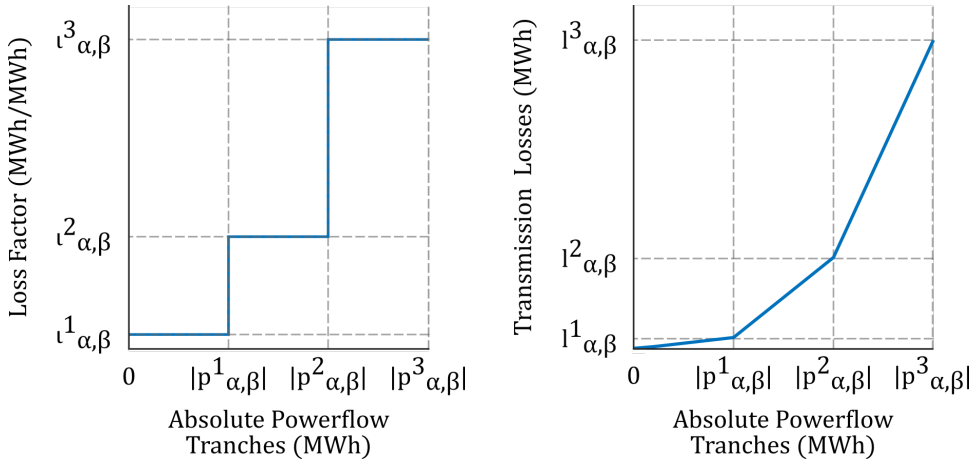

(a) Loss Tranches (b) Total Losses

Figure 4.19 New Zealand System Model's HVdc Link Losses

To ensure that the absolute value and piecewise linear functions are treated correctly, the LP problem is solved with a simplex method rather than an interior point method. The power flow absolute value constraints have an infinite number of solutions which correspond to points within the valid constraint space of the problem which interior point methods could deem optimal. Simplex methods only examine solutions at the vertices of the constraint space which gives the correct absolute power flow values.

Water (Energy) Balance

The water balance constraint accounts for the inflows, outflows (hydro generation) and change in storage over time. The constraint is:

$$\hat{s}_{t+1} = \hat{s}_t + \hat{f}_t - \hat{g}_{h,t}$$
$$\hat{s}_{t+1} \ge 0 \tag{4.16}$$

where $\hat{s}_{t+1}$ and $\hat{s}_t$ are the future and current storage vectors, $\hat{f}_t$ is the inflow vector and

$\hat{g}_{h,t}$ is the dispatched hydro generation. Note that in the Price Discovery, $\hat{s}_t$ is a storage vector from the discretised state space ($\hat{\sigma}_{\hat{k}}$). Only the minimum storage constraint is imposed. In both the Price Discovery and System Operation Simulation, if a reservoir's $t+1$ storage level is greater than its maximum, the excess is recorded as spill and s^i_{t+1} is set to the storage capacity.

Minimum Hydro Generation

Minimum flow constraints and unstorable inflows impose a mininmum hydro generation requirement, as discussed in Chapter 3 Section 3.1. Minimum flow constraints are set by municipal bodies for environmental and societal reasons and unstorable inflows refer to inflows that pass through hydro generation before entering a reservoir. It is assumed that these flows pass through the generator producing electricity rather than being spilt, hence they can be emulated as a minimum hydro generation requirement. When undergoing the conversion from water to energy based values for the hydro system model, the minimum flow and unstorable inflows are summed producing a minimum generation series for each hydro generator.

Implementing the minimum hydro generation requirement as a constraint would result in generation dispatch being infeasible when insufficient water is available. Insufficient water could occur in the Price Discovery when low inflows are coincident with solving the generation dispatch at $\hat{\sigma}_{\hat{k}}$ with an empty storage level.

To incentivise the minimum hydro generation, a penalty price is placed on the difference between the minimum hydro generation requirement ($g^{i,hmin}_{h,t}$) and the hydro generation dispatch $g^i_{h,t}$. The penalty is only applied if the hydro generation dispatch is below the minimum requirement. The penalty price chosen was the non-supply price. Equation (4.17) presents the associated constraints:

$$\begin{aligned} C_{minh} &= \textstyle\sum_{i=1}^{N_s} c_{non-supply} \cdot (g^{i,hmin}_{h,t} - g^{i,blw}_{h,t}) \\ g^i_{h,t} &= g^{i,abv}_{h,t} + g^{i,blw}_{h,t} \\ 0 \leq g^{i,blw}_{h,t} &\leq g^{i,hmin}_{h,t} \\ 0 \leq g^{i,abv}_{h} &\leq \overline{g}^i_h - g^{i,hmin}_{h,t} \end{aligned} \tag{4.17}$$

where $g^{i,hmin}_{h,t}$ is the required minimum hydro generation for the i'th hydro generator at time t. Each hydro generator is split into two components: below ($g^{i,blw}_h$) and above ($g^{i,abv}_h$) the minimum generation threshold.

4.5 WATER VALUE FUNCTION INTERPOLATION

As the water value functions are defined on a discretised storage state space, water values in between these need to be interpolated. This is done for the hydro generation prices before conducting the generation dispatch optimisation as well as in the Price Discovery to populate the water value function and when determining convergence.

As per the New Zealand model consisting of two reservoirs, the interpolation procedure is described for a two-reservoir system and is depicted in Figure 4.20. This can be extended to a system with more reservoirs. Consider interpolating the water value at storage $\hat{s}_p = [s_p^i, s_p^j]^T$ as shown in Figure 4.20a. The procedure applies two steps for each storage dimension. The steps are:

1. Function Representation Step: Produce a set of piecewise functions that represent the water value function along one storage dimension (e.g. s^i)
2. Water Value Evaluation Step: With each piecewise function, determine the water value at s_p^i

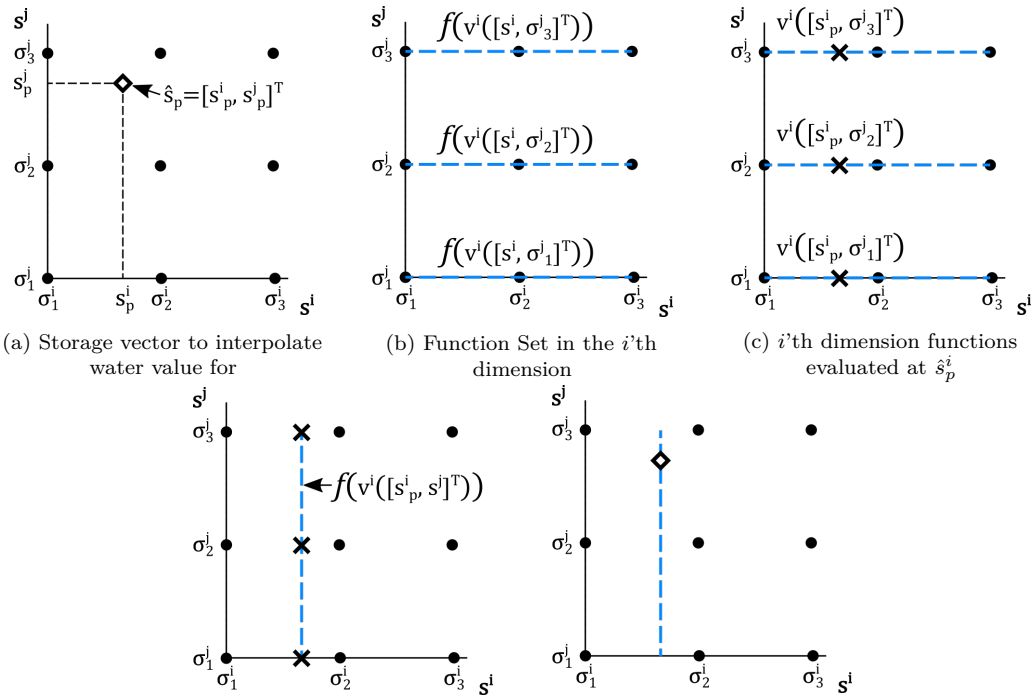

Figure 4.20 Water Value Function Interpolation - The time interval (t) denotation has been excluded for clarity

The first step is to produce piecewise functions representing the water values at σ_{kj}^j

along the i''th dimension (Figure 4.20b):

For each $j \in 1, 2, ..., K^J$

$$\text{With } v^i(\hat{\sigma}_{\hat{k}});\ \hat{k} = \begin{bmatrix} k^i \\ k^j \end{bmatrix}; k^i = 1, 2, ..., K^i \longrightarrow \mathcal{F}(v^i\left(\begin{bmatrix} s^i \\ \sigma^j_{k^j} \end{bmatrix} \right)); \quad \sigma^i_1 \leq s^i \leq \sigma^i_{K^i} \tag{4.18}$$

where $\mathcal{F}(v^i\left(\begin{bmatrix} s^i \\ \sigma^j_{k^j} \end{bmatrix} \right))$ represents the piecewise function that interpolates along s^i at $\sigma^j_{k^j}$. A linear piecewise function is used although other candidates such as cubic spline are possible. The second step is evaluating the water values at s^i_p with each of these piecewise functions producing a set at each $\sigma^j_{k^j}$ (Figure 4.20d). The Function Representation Step is repeated with these water values:

$$\text{With } v^i\left(\begin{bmatrix} s^i_p \\ \sigma^j_{k^j} \end{bmatrix} \right); k^i = 1, 2, ..., K^i \longrightarrow \mathcal{F}(v^i\left(\begin{bmatrix} s^i_p \\ s^j \end{bmatrix} \right)); \quad \sigma^j_1 \leq s^j \leq \sigma^j_{K^j} \tag{4.19}$$

$\mathcal{F}(v^i\left(\begin{bmatrix} s^i_p \\ s^j \end{bmatrix} \right))$ is then evaluated at $s^j = s^j_p$ producing the desired water value, $v^i(\hat{s}_p)$. If the $\hat{s}_p$ is outside of the storage bounds, the appropriate boundary water value is used.

The interpolation procedure repetitively applies a one dimensional interpolation rather than a single multi-dimensional interpolation. The reason behind this was to allow for a flexible number of reservoirs in the system model while using the native interpolation functions of MATLAB.

4.5.1 Hydro Generation Pricing

The above interpolation procedure is appropriate when dealing with a single storage vector such as when populating the water value function or finding the water value that corresponds to the end-of-horizon storage for the Price Discovery convergence. However in the generation dispatch optimisation, the $t + 1$ storage has the potential to be a range of values. As such an appropriate portion of the water value function needs to be represented in the dispatch's linear programming formulation. This subsection describes how this is done.

Consider solving the generation dispatch at time t and storage $\hat{s}_t$ (Figure 4.21). Note that two instances of time are being represented (t and $t + 1$) on the figure. The

potential $\hat{s}_{t+1}$ range of the generation dispatch is found with the water balance equation (Equation (4.20)), resulting in (Equation (4.21)).

$$\hat{s}_{t+1} = \hat{s}_t + \hat{f}_t - \hat{g}_{h,t} \tag{4.20}$$

$$\begin{aligned} s_t^i + f_t^i - \bar{\bar{g}}_{h,t}^i \leq s_{t+1}^i \leq s_t^i + f_t^i \\ s_t^j + f_t^j - \bar{\bar{g}}_{h,t}^j \leq s_{t+1}^j \leq s_t^j + f_t^j \\ \hat{\bar{\bar{g}}}_{h,t}) = min(\hat{\bar{g}}_h, \hat{s}_t + \hat{f}_t, \hat{d}^{acs}) \end{aligned} \tag{4.21}$$

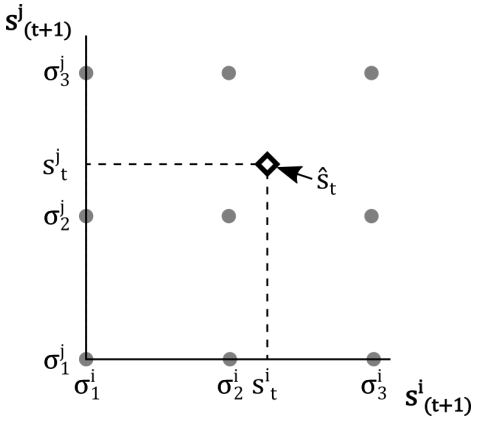

Figure 4.21 Generation Dispatch Optimisation Situation

where $\bar{\bar{g}}_{h,t}^i$ and $\bar{\bar{g}}_{h,t}^j$ are the maximum hydro generation which is the minimum of the hydro generation capacity ($\hat{\bar{g}}_h$), the available water ($\hat{s}_t + \hat{f}_t$) and the accessible demand ($\hat{d}^{acs}$). Accessible demand accounts for transmission capacity constraints. The $\hat{s}_{t+1}$ range is depicted by the blue and orange lines in Figure 4.22.

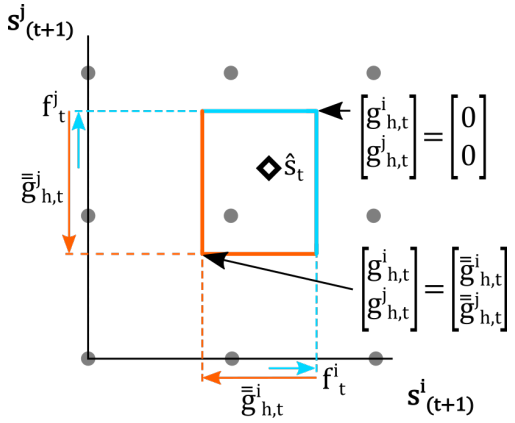

Figure 4.22 i'th hydro generation tranche ranges

Note that this region is not necessarily rectangular given that the maximum hydro

generation boundary (orange lines) may include or be replaced by a sloped line. This would occur if the total demand was less than the total hydro generation capacity. The water value function of the i'th hydro generator ($v^i_{t+1}(\hat{s}_{t+1})$) in this range serves as its price function, hence its contribution to the total cost of the generation dispatch is:

$$\begin{aligned} C^i_h &= \int_0^{g^i_{h,t}} v^i_{t+1}(\hat{s}_{t+1}) \cdot u^i_t d(u^i_t) \\ &= \int_0^{g^i_{h,t}} c^i_h(u^i_t) d(u^i_t) \end{aligned} \tag{4.22}$$

where $c^i_h(g^i_{h,t})$ is the instance of cost at $g^i_{h,t}$. Substituting the water balance equation (Equation (4.20)) into $c^i_h(g^i_{h,t})$ gives:

$$c^i_h(g^i_{h,t}) = v^i_{t+1}(\hat{s}_{t+1}) \cdot g^i_t = v^i_{t+1}(\hat{s}_t + \hat{f}_t - \hat{g}_{h,t}) \cdot g^i_t \tag{4.23}$$

Further, when solving the generation dispatch, both the storage and inflows of each reservoir are known ($\hat{s}_t$ and $\hat{f}_t$) hence Equation (4.23) can be simplified to be in terms of hydro generation only:

$$\begin{aligned} v^i_{t+1}(\hat{s}_t + \hat{f}_t - \hat{g}_{h,t}) \cdot g^i_t = & \quad v^i_{t+1}(\hat{g}_{h,t}) \cdot g^i_t \\ = & \quad v^i_{t+1}\left(\begin{bmatrix} g^i_{h,t} \\ g^j_{h,t} \end{bmatrix} \right) \cdot g^i_t \end{aligned} \tag{4.24}$$

Equation (4.24) shows the two non-linear components of the hydro generation instance, and by extension the total hydro generation cost: $\left(g^i_{h,t}\right)^2$ and $g^j_{h,t} \cdot g^i_{h,t}$ due to the multiplication of the water value function and i'th hydro generation dispatch. This non-linearity means the water value function interpolation cannot be integrated into the generation dispatch optimisation directly since the dispatch is solved with linear programming. For this reason, an approximate linearised representation of the water value function is used. This comprises of separating the i'th hydro generator's capacity into distinct tranches and allocating different water values as prices for each tranche (Figure 4.23):

$$\begin{gathered} C^i_{hydro} = \int_0^{g^i_{h,t}} v^i_{t+1}(\hat{s}_{t+1}) \cdot u^i_t d(u^i_t) \\ \approx \sum_{\tau=1}^{N^i_h} \rho^i_\tau \cdot \gamma^i_\tau \\ g^i_h = \sum_{\tau=1}^{N^i_h} \gamma^i_{h,\tau} \quad \overline{g}^i_h = \sum_{\tau=1}^{N^i_h} \overline{\gamma}^i_\tau \\ 0 \leq \gamma^i_\tau \leq \overline{\gamma}^i_\tau; \tau = 1, \ldots, N^i_h \end{gathered} \tag{4.25}$$

where $\overline{g}^i_h$ is the i'th hydro generator's capacity, $\overline{\gamma}^i_\tau$ is the τ'th tranche's with γ^i_τ being the portion of the tranche that is dispatched and ρ^i_τ is the τ'th tranche's allocated price. N^i_h is the number of tranches for the i'th hydro generator.

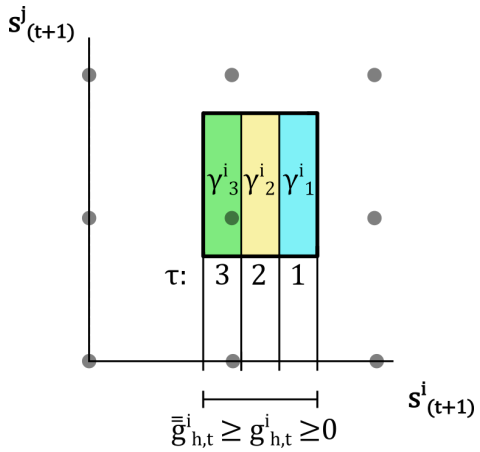

Figure 4.23 i'th hydro generation tranche ranges

The tranche prices (ρ_τ^i) are found by interpolating a water value function in the appropriate tranche's storage range, which is:

$$s_t^i + f_t^i - \sum_{\phi=0}^{\tau-1}\left(\overline{\gamma}_{h,t}^i\right) \leq s_{t+1}^i \leq s_t^i + f_t^i - \sum_{\phi=0}^{\tau}\left(\overline{\gamma}_{h,t}^i\right) \tag{4.26}$$

Only a single water value from the water values in the generation tranche's storage range can be used due to the linear function constraint. To determine the sensitivity to the position, the hydro scheduling tool was implemented with 9 tranche price positions as depicted in Figure 4.24. This was conducted with the 1976 and 1998 inflow sequences and the storage series are shown in Figure 4.25 which are colour coded with the positions in Figure 4.24. The difference between all of the storage series is minimal. The position selected was the central tranche value (yellow).

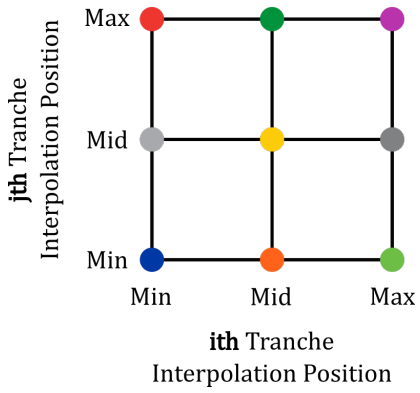

Figure 4.24 Water Value Interpolation Locations - Associated Colours

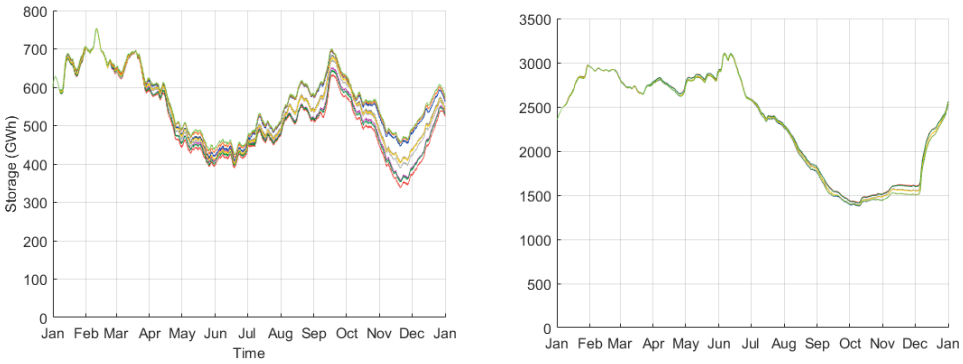

(a) North Island Storage - 1976

(b) South Island Storage - 1976

(c) North Island Storage - 1988

(d) South Island Storage - 1998

Figure 4.25 Storage Trajectories for different Water Value Interpolation Locations

Chapter 5

SENSITIVITY STUDIES

Throughout the development of the hydro scheduling tool and system model, a multitude of decisions on the structure and parameters of the Price Discovery, System Operation Simulation and New Zealand system model have been made based on balancing the representation of the real world system while minimising computational intensity. For example representing New Zealand's system as a two-node, two-reservoir system captures important features of the system while not imposing a significant computational requirement.

There is no apparent best option for two aspects: the Price Discovery's time interval for which the water value functions are constructed, and the resolution of the discretised storage state space. Typically with hydro scheduling tools that produce water value functions or operating rules, the temporal resolution is in the order of weeks to months, whereas for this research, time intervals between a half hour to 24 hours are considered. This is due to the relatively short planning horizon due to New Zealand's limited storage capacity and to determine whether generation and transmission capacity constraints in the system have any major bearing on the water value function hence system operation.

For this sensitivity study, a limited selection of the 85 years (1932-2016) of inflow data is used to represent the range of conditions. They are selected by applying the hydro scheduling tool with all inflow sequences, examining the distribution of the total renewable generation percentage and selecting 8 years to represent poor to good inflow volumes and patterns. These years in order from poor to good are 1976, 1947, 1963, 2008, 1986, 1955, 1933 and 1998. A simulation based approach was taken to account for the timing of inflows through the year, as well as the annual inflow magnitudes. For details on the selection, refer to Appendix E.

5.1 TIME INTERVAL

The Price Discovery time intervals investigated were 0.5, 1, 2, 6, 12 and 24 hours and are represented by Δt. Note that regardless of the Price Discovery time interval, the System Operation Simulation in all cases uses a half hour time interval. Henceforth, whenever a time interval is discussed, it refers to that belonging to the Price Discovery only.

For short intervals (half hour), the intra-daily variation of demand and renewable generation is captured, in particular peak demand. For longer intervals, the emphasis is energy demand and the capacity constraints are rarely active. The computational time required for the Price Discovery is longer with short intervals (17520 half hours in a year) than with long intervals (365 days in a year).

This investigation compares:

- how the time interval affects the water value function produced by the Price Discovery given the same system model and conditions (inflows, demand), and
- how the system operation is influenced.

The Price Discovery was implemented with each time interval and the 8 representative inflow years, producing a water value function vector for each:

$$v_t^{i,\Delta t,yr} = v_t^{i,\Delta t,yr}\ (\hat{\sigma}_{\hat{k}})\ \forall\ i, \hat{k}, yr \tag{5.1}$$

where i is the reservoir index, Δt indicates the time interval and yr is the inflow year. The discretised storage vector is omitted for clarity given the additional notation. The time variant parameters and data of the system model (e.g. capacities, inflows, demand and renewable generation) are transformed to suit the time interval.

To allow the direct comparison between time interval's $v_t^{i,\Delta t,yr}$ in time, they are all interpolated to a half hour resolution. This was done by repeating each element of $\hat{v}_t^{\Delta t,yr}$ by the number of half hours within the Δt (a "previous" neighbour approach). Henceforth, when discussing water value function of $\Delta t \neq 0.5$, the interpolated version is being referred to.

With each $v_t^{i,\Delta t,yr}\,\forall\, i, t$, the System Operation Simulation is performed, producing the system operation series and the storage trajectories of both reservoirs. The starting

storage for these simulations were the average beginning-of-year storage from 2009 to 2016 (unless otherwise specified):

$$\hat{s}_t = \begin{bmatrix} \text{North Island: } 600GWh \text{ (76.2\% of capacity)} \\ \text{South Island: } 2350GWh \text{ (75.2\% of capacity)} \end{bmatrix} \tag{5.2}$$

5.1.1 Storage Trajectory Comparison

Figure 5.1 presents example storage trajectories of the North (left) and South (right) Island reservoirs for each time interval corresponding to the 1976 (dry year) inflow sequence. Note the y-axes do not begin at zero to emphasise the differences between the time intervals. Upon initial inspection, the trajectories are relatively similar, with the South Island storage trajectory exhibiting a trend of lower storage levels with longer time intervals.

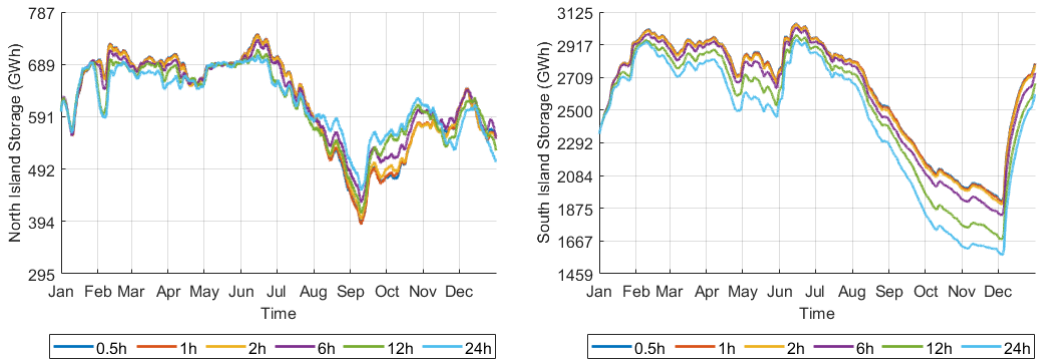

(a) North island (b) South Island

Figure 5.1 1976 Storage Trajectory for all Price Discovery Time Intervals - 1/2, 1, 2, 6, 12 and 24 hour. Historical starting storage

Figure 5.1 only depicts the trajectories for a single year so to concisely compare the storage trajectories of multiple time interval lengths for each inflow year, statistical measures were calculated. Firstly, the similarity between the storage trajectories were determined with an RMS based measure.

For each inflow year, the average storage trajectory for all time intervals ($\tilde{s}_t^{i,\forall\Delta t,yr}$) was calculated. Next the difference between each time interval's storage trajectory ($s_t^{i,\Delta t,yr}$) and its inflow year's average is found, and the root mean square of this difference (or root mean square difference, RMSD) is calculated:

$$RMSD^{\Delta t,yr} = \sqrt{\frac{1}{T}\sum_{t=1}^{T}\left(\tilde{s}_t^{i,\forall\Delta t,yr} - s_t^{i,\Delta t,yr}\right)^2} \tag{5.3}$$

This produces a root mean square difference for each inflow year and time interval which were normalised by dividing by the i'th reservoir's storage capacity. The range of normalised RMSD values over the time intervals are plotted by inflow year in Figure 5.2. As the storage trajectory is highly dependent on the starting storage vector, to verify the comparison a second set of plots (Figure 5.3) are presented which are based on storage trajectories from a 50% starting storage.

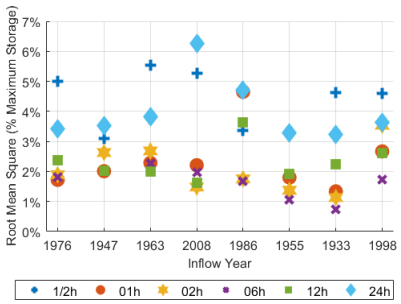

(a) North island (787 GWh Capacity)

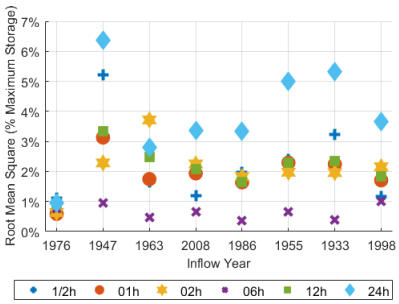

(b) South Island (3125 GWh Capacity)

Figure 5.2 RMSD values comparing each time interval's storage series to the average storage series across all intervals. Price Discovery Time Intervals were 1/2, 1, 2, 6, 12 and 24 hour. Historical starting storage

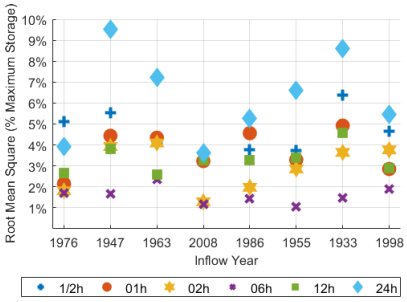

(a) North island (787 GWh Capacity)

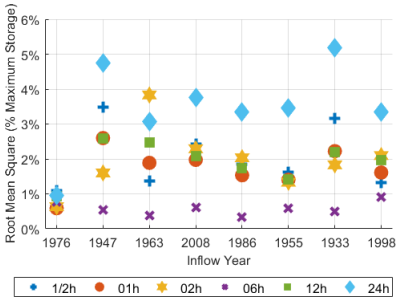

(b) South Island (3125 GWh Capacity)

Figure 5.3 RMSD values comparing each time interval's storage series to the average storage series across all intervals. Price Discovery Time Intervals were 1/2, 1, 2, 6, 12 and 24 hour. 50% storage capacity starting storage

Broadly speaking for both starting storages, the storage trajectories across all time intervals are similar, with the majority being under 4%. The peak RMSD values across all instances are 9.5% and 6.5% for the North and South Island reservoirs respectively. To show the minor magnitude difference of the outlier cases, their storage trajectories are shown in Figure 5.4 along with the average storage series ($\tilde{s}_t^{i,\forall\Delta t,yr}$). As can be seen, the difference is predominantly during the year, with similar end of year storage levels. Overall, the storage trajectories across all time intervals are highly similar.

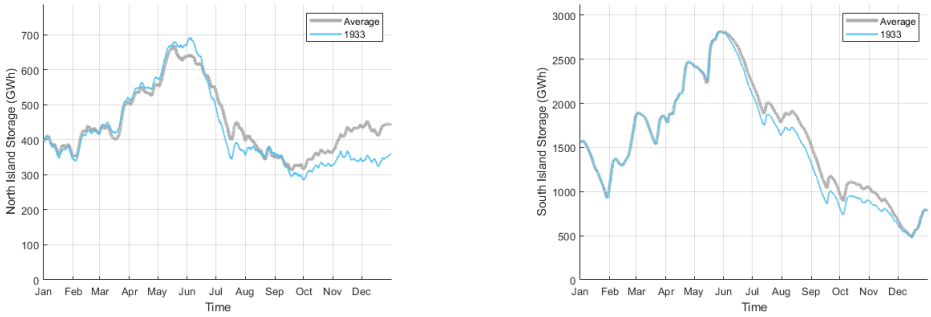

(a) North island - 1933

(b) South Island - 1933

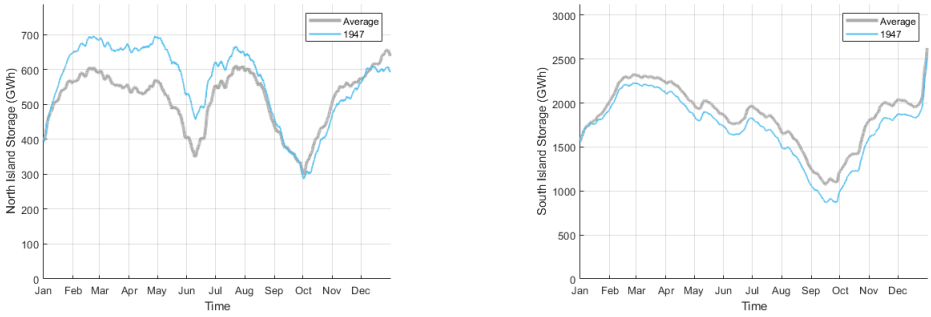

(c) North island - 1947

(d) South Island - 1947

Figure 5.4 1933 and 1947 Storage Series compared to the Average Storage Series (over all time intervals)

As seen in Figure 5.1b, there is a trend in how the water value function with increasing time intervals leads to lower operating storage. To quantify this trend, a measure that compares the storage trajectories of different time interval's water value functions was produced to condense the dimensionality. The calculation procedure is:

1. Normalise the storage series:

   (a) Calculate the average storage series for each inflow year over all Price Discovery time intervals:

   $$\widetilde{s}_t^{i,\forall\Delta t,yr} = \frac{1}{\#\Delta t}\sum_{\forall\Delta t} s_t^{i,\Delta t,yr} \tag{5.4}$$

   (b) For each year, calculate the difference between each storage series and its corresponding average storage series, producing deviation-from-average storage series (henceforth called deviation series):

   $$\underset{\sim}{s_t}^{i,\Delta t} = s_t^{i,\Delta t,yr} - \widetilde{s}_t^{i,\forall\Delta t,yr} \tag{5.5}$$

2. Calculate the average of each deviation storage series. This produces a table of average deviations with columns corresponding to time intervals and rows corresponding to inflow years. Table 5.1 presents the table for the South Island storage.

3. For each time interval (along each column), determine the minimum, average and maximum of the average deviations. Figure 5.5 presents the average of the average deviations over the time intervals as the bold purple line, with the shaded purple area spanning between the minimum and maximum average deviations.

4. Steps 2 and 3 are repeated to find the minimum and maximum deviations (instead of average deviation) and subsequent average and range over all inflow years presented in Figure 5.5 as the blue (minimum) and green (maximum) lines and shaded areas.

Figure 5.5 and Figure 5.6 present the range of the maximum, minimum and average deviations in the North Island and South Island reservoirs as well as the combined New Zealand storage. As can be seen in Figure 5.5b and Figure 5.6, the larger the time interval, the lower the storage reservoirs are operated. Lower storage indicates less thermal generation hence longer time intervals value water less than shorter time intervals.

Table 5.1 Average Deviation for each Time Interval and Inflow Year - South Island (GWh)

Inflow	**Time Intervals**					
Year	**0.5**	**1**	**2**	**6**	**12**	**24**
1976	67	64	55	17	-62	-140
1947	129	87	54	-3	-90	-178
1963	30	52	56	20	-53	-105
2008	91	61	54	9	-65	-150
1986	-28	42	84	-11	-46	-42
1955	-7	39	49	13	-38	-56
1933	41	28	39	-3	-35	-69
1998	18	6	9	-17	-10	-5

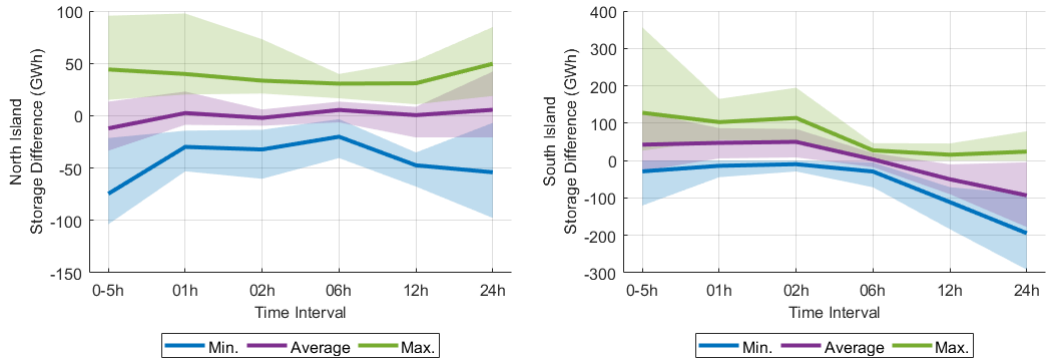

(a) North island (787 GWh)

(b) South Island (3125 GWh)

Figure 5.5 Difference in Storage Operation for each Price Discovery Time Interval - 1/2, 1, 2, 6, 12 and 24 hour. Historical starting storage. North and South Island

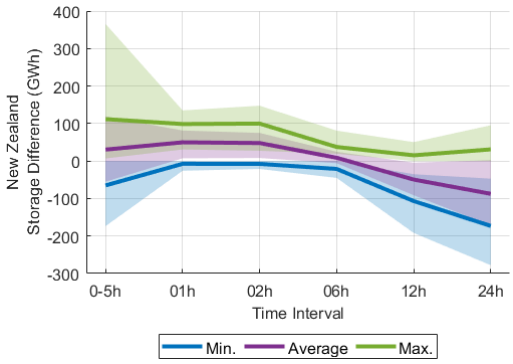

Figure 5.6 Difference in Storage Operation for each Price Discovery Time Interval - 1/2, 1, 2, 6, 12 and 24 hour. Historical starting storage. New Zealand

5.1.2 Water Value Function Comparison

The role of a water value function is to provide hydro generation prices which are used in the least cost generation dispatch optimisation and as such it is not an explicit output of the hydro scheduling tool. In saying this, it is still worthwhile examining how it changes with different time intervals.

Given that a reservoir's water value function is four dimensional (water value, time step and discretised storage level in both reservoirs), it is difficult to depict. A common approach is to use water value surfaces and contours. A water value surface presents the i'th storage over the j'th storage's discretised levels and time that corresponds to a specific water value. Finding the water value surfaces that coincide with thermal generation prices is useful as they then indicate at which storage vectors ($\hat{s}_{t+1}$, not $\hat{\sigma}_{\hat{k}}$) and point in time that the thermal generator would be dispatched ahead of the hydro generator given the least cost generation dispatch optimisation. Note that only viewing the water value surfaces is not sufficient as the system constraints are not accounted for.

Figure 5.7 shows the \$50 water value surface of the South Island's water value function produced with the 1998 inflow year (wet year) and a half hour time interval. \$50 is the price of the cheapest thermal generator. A water value surface is found by interpolating the i'th storage values over time ($t = 1, 2, ..., T$) and at each j'th storage level ($\sigma^j_{k^j} \forall k^j$) that correspond to a specific water value.

The black lines on Figure 5.7 are cross-sections of the \$50 water value surface along specific j'th discretised storage levels and are called water value contours. Plotting the water value contours of a range of thermal generation prices (\$50 to \$68.60) shows the i'th storage ranges when particular thermal generators would be dispatched at a $\sigma^j_{k^j}$ (Figure 5.8). Note that the \$50 contour (orange) corresponds to the bold black line in the water value surface plot (Figure 5.7).

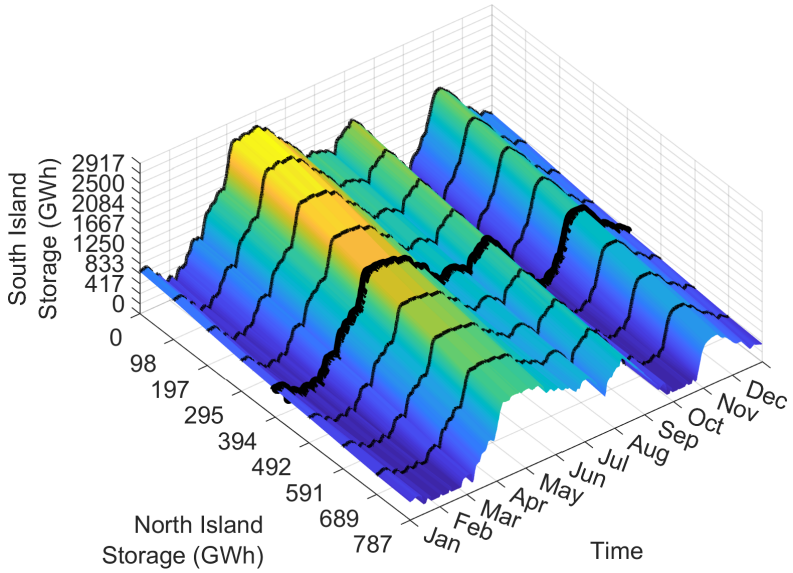

Figure 5.7 South Island $50 Water Value Surface - 1998 Inflow Year; Half Hour Time Interval

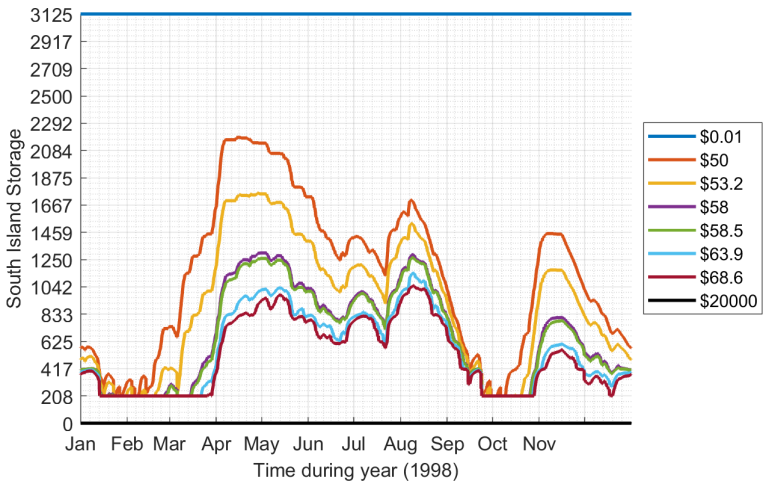

Figure 5.8 South Island Water Value Contours of all thermal generation prices - 1998 Inflow Year; Half Hour Time Interval

To compare the effect of the time interval on the water value functions, the water value surface corresponding to the $50 and $68.60 thermal generation prices are used. Together they represent the storage range which determines the thermal generation dispatch, serving as three dimensional proxies for thermal generation price surfaces. To determine the similarity of the water value function for different time intervals, RMSD values of the $50 and $68.60 water value surfaces were calculated. These values are presented in Figure 5.9.

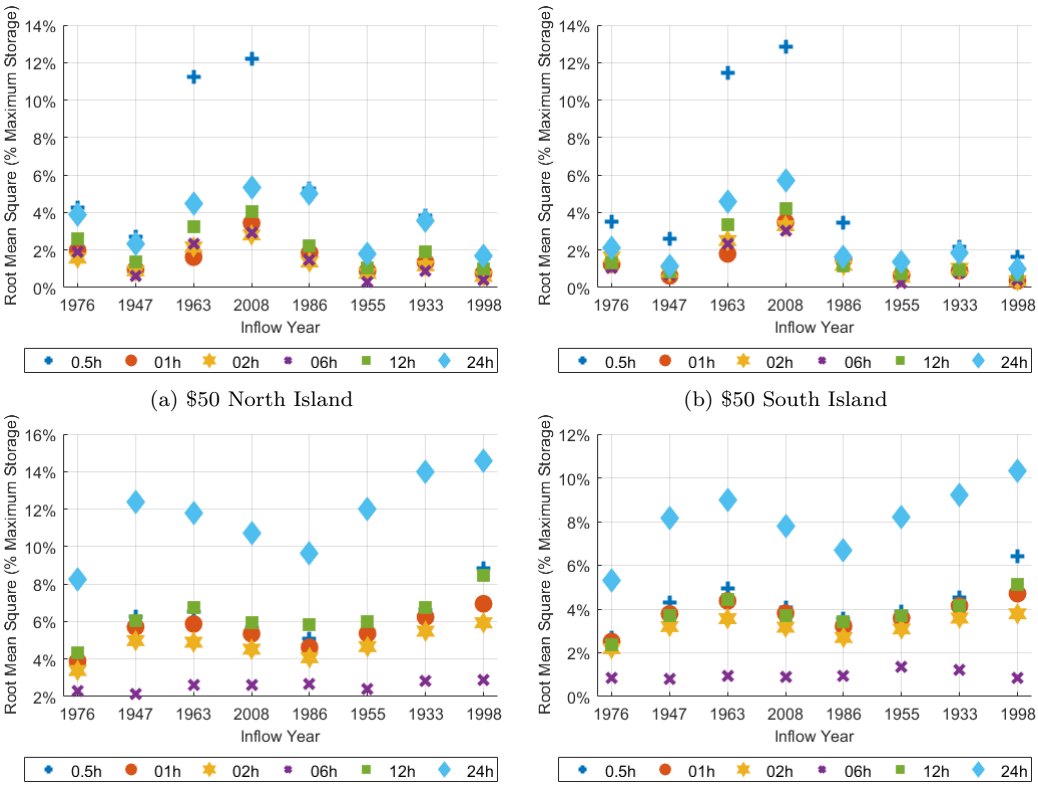

(a) $50 North Island

(b) $50 South Island

(c) $68.60 North Island

(d) $68.60 South Island

Figure 5.9 $50 and $68.60 Water Value Contour Comparison between Price Discovery Time Intervals - 1/2, 1, 2, 6, 12 and 24 hour

For each inflow year, the $50 water value surfaces across all time intervals and reservoirs are similar with RMS differences of less than 6%. There are two outliers, the half hour time interval water value surfaces for the 1963 and 2008 inflow sequences which are close to 12%. With the $68.60 water value surfaces, the differences are overall greater than with the $50 surface but the majority are under 8%. The evident feature is that the 24 hour $68.60 surfaces are further away from the average for intervals. Broadly speaking, these RMSD plots indicate that all time intervals lead to similar operation of low priced thermal generation but differ with higher priced thermal generation.

To explore this difference, a measure is calculated to compare the time interval's water value surfaces. The measure was calculated for water value surfaces corresponding to each thermal generation price water value surface ($50, $53.20, $58, $58.50, $63.90 and $68.60) and is similar to the storage trajectory's deviation-from-average measure. The procedure is:

1. With each inflow year's water value surfaces, determine the difference between the water value surface of each time interval and the half hour water value surface. This produces deviation-from-half-hour surfaces (deviation surface)

2. For each time interval and inflow year, determine the minimum, average and maximum deviation across all time steps and discretised storage vectors. This produces a table for each measure giving the minimum, average or maximum deviation for each inflow year and time interval.

3. For each time interval and deviation measure (minimum, average and maximum), determine the minimum, average and maximum from all the inflow years

Figure 5.10, Figure 5.11 and Figure 5.12 present the South Island's minimum, average and maximum deviation ranges for the water value surfaces that correspond to thermal generation prices. The North Island surfaces, which are not shown, exhibit a similar relationship.

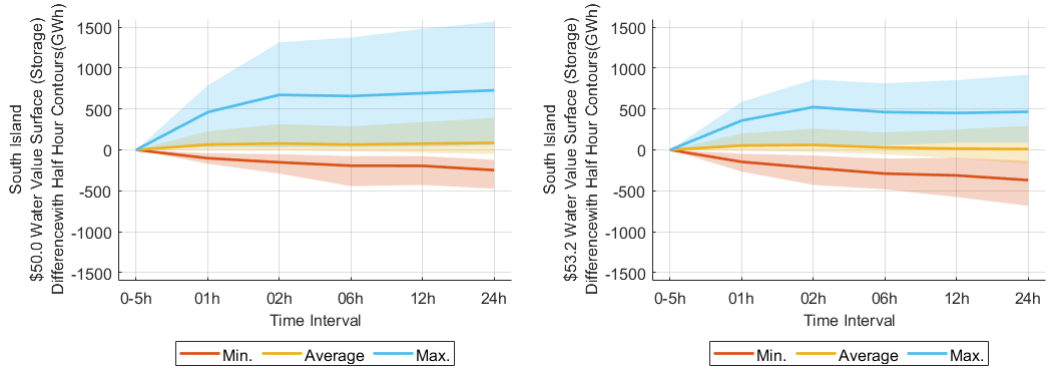

(a) $50 (b) $53.20

Figure 5.10 South Island Water Value Surface Comparison between Price Discovery Time Intervals - 1/2, 1, 2, 6, 12 and 24 hour. $50 and $53.20 Thermal Generators

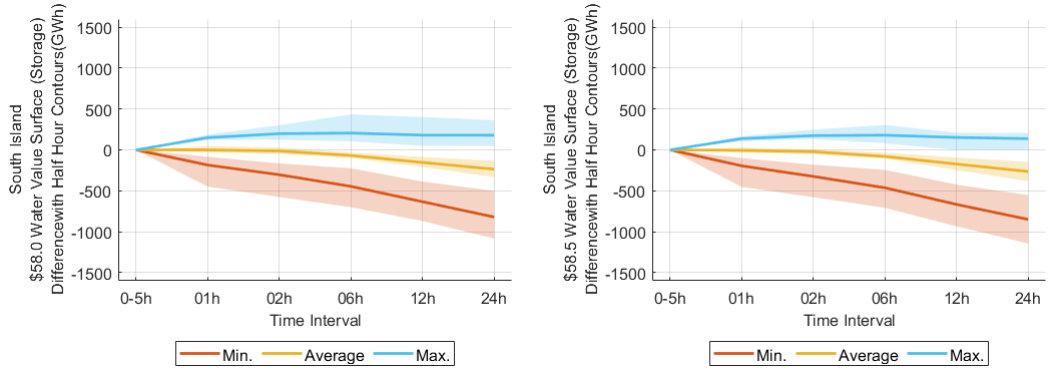

(a) $58 (b) $58.50

Figure 5.11 South Island Water Value Surface Comparison between Price Discovery Time Intervals - 1/2, 1, 2, 6, 12 and 24 hour. $58 and $58.50 Thermal Generators

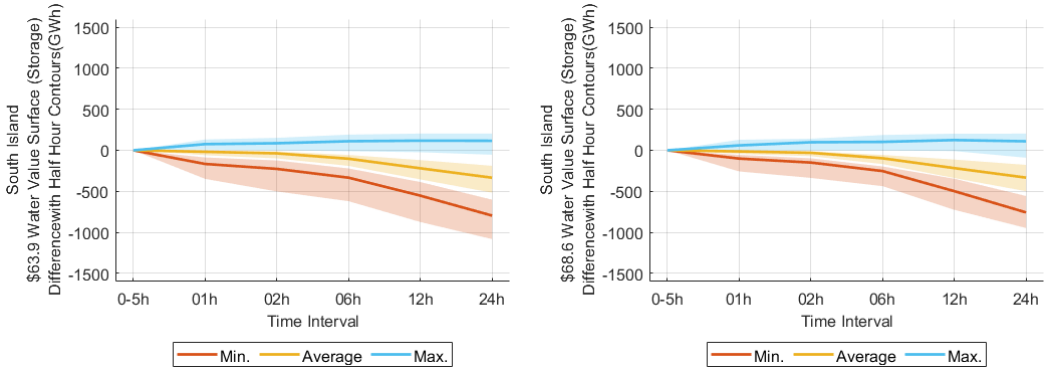

(a) $63.90 (b) $68.60

Figure 5.12 South Island Water Value Surface Comparison between Price Discovery Time Intervals - 1/2, 1, 2, 6, 12 and 24 hour. $63.90 and $68.60 Thermal Generators

The deviation ranges indicate whether a time interval's thermal price water value surfaces are above (positive) or below (negative) that of the corresponding half hour water value surface. With increasing thermal price, all deviation measures trend toward negative differences. On average, longer time intervals lead to lower priced thermal generation being dispatched at higher storage levels than with shorter time intervals. Similarly, shorter intervals dispatch higher priced thermal generation at higher storage levels than with longer intervals.

Both of these features are captured by Figure 5.13 which shows the 1955 South Island water value contours corresponding to a 50% full North Island reservoir for the half hour and 24 hour time intervals. With the 24 hour time interval, the $50 and $53.20 contours are higher than those of the half hour time interval and the $58 and above contours in the half hour interval are higher than their 24 hour counterparts.

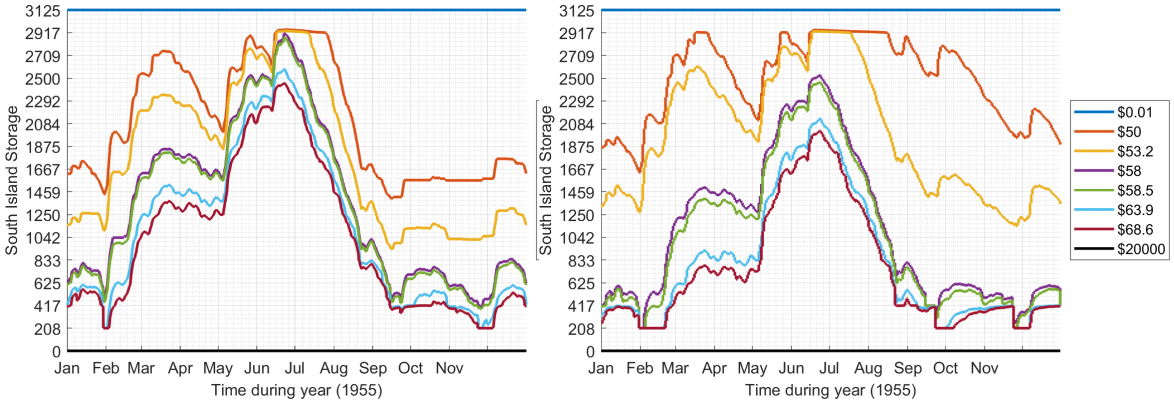

(a) Half Hour (b) 24 Hour

Figure 5.13 South Island Water Value Contours of all thermal generation prices - 1955 Inflow Year

In general, the shorter time intervals value the water stored in reservoirs higher than longer time intervals, aside from at high storage levels. This is shown by the water value surface deviation ranges showing that a shorter time interval tends to have the high priced thermal generation water value surfaces at higher storage levels than those of a longer time interval. Affirming this observation is the fact that shorter time intervals lead to reservoirs being operated at higher storage levels as shown in Figure 5.5.

The trend of shorter time intervals valuing water stored in reservoirs higher than longer intervals is in part due to the influence of capacity constraints (generation or transmission). Capacity constraints are typically active during peak demand periods hence are only captured on short time intervals and when active, they force the generation dispatch optimisation to dispatch more expensive generation. In the Price Discovery, if this results in a hydro generator being dispatched, its reservoir's water value is higher than it otherwise would be if the constraint was not active. A common case from the New Zealand system model is when the HVdc link limits the South Island hydro generation from supplying the North Island's demand, requiring the North Island hydro generation to supply it when the thermal generation is already dispatched or priced above the North Island hydro generation. This either creates or adds to a deviation between the North and South Island's water value functions. In subsequent Price Discovery backwards time steps $(t-1, t-2, ...)$ when the capacity constraints are not active, the effect of the deviation is that, in this example, the South Island's hydro generation would be dispatched more so to reduce and remove this deviation, in turn increasing its water value.

The final result to examine is the convergence rate (number of year long cycles to convergence) and computation time per cycle. Table 5.2 presents the number of cycles for the Price Discovery to converge for each time interval and inflow year. For the majority of cases, the convergence rate was 3-4 cycles aside from 1976 and 2008 with the 24 hour time interval requiring 5 and 8 cycles respectively.

Regardless of the time interval, the computation time of each time step in the Price Discovery was relatively consistent. As such, the computation time versus time interval (Figure 5.14) is a linear relationship (note the spacing of the time intervals are not distributed in this manner). Given this relationship, the value of using a short time interval needs to outweigh the computational cost. The simulations were implemented on a range of computers of the same model and their specifications are in Appendix F.

Table 5.2 Number of Yearly Cycles for the Price Discovery to convergence for Time Interval range - 1/2, 1, 2, 6, 12 and 24 hour

Year	Time Intervals					
	Half Hour	**1 Hour**	**2 Hour**	**6 Hour**	**12 Hour**	**24 Hour**
1933	4	3	4	4	4	4
1947	3	3	3	3	3	3
1955	4	3	3	3	3	4
1963	4	3	3	4	3	4
1976	4	4	4	3	3	5
1986	3	3	3	4	3	3
1998	3	4	4	4	4	4
2008	3	3	3	3	3	8

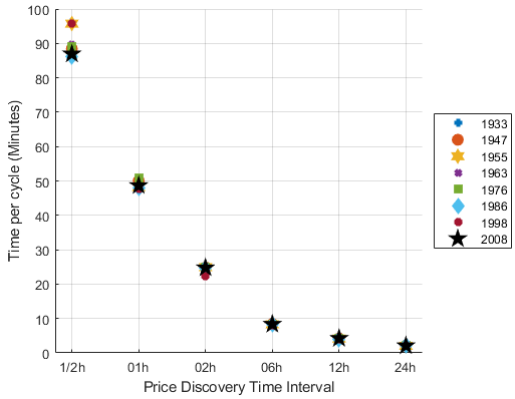

Figure 5.14 Time Per Cycle

Although the relationship with shorter time intervals valuing stored water higher than with longer intervals is apparent, the root mean square differences of both the storage trajectories and water value surfaces show no significant differences in operation. Given the long computation times of shorter time intervals (0.5, 1 and 2 hours), they are less desirable as implementing many scenarios is important. Also accounting for demand and renewable generation variation would be appropriate given that an objective of the model is to investigate renewable generation integration of a future New Zealand system. As a compromise between computation time and capturing temporal variation in demand and renewable generation, a 6 hour time interval is selected.

5.2 STORAGE DISCRETISATION RESOLUTION

As the hydro scheduling tool is Dynamic Programming based, the storage state space is discretised for the creation of the water value function. An investigation into the storage discretisation resolution is conducted to determine how the water value function and

consequential system operation are effected. The three resolutions considered were 6x12, 9x16 and 12x21 with the values referring to the number of levels of the North Island and South Island storage reservoirs respectively. These are depicted in Figure 5.15. The low resolution leads to relatively quick computation times due to the smaller number of backward projections that need to be performed at each time interval, whereas the high resolution option is a closer representation of the continuous storage state space representation and reduces the inaccuracy of using linear interpolation.

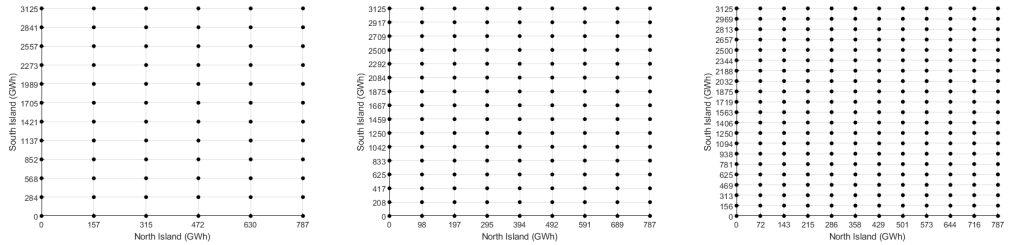

(a) 6x12 (b) 9x16 (c) 12x21

Figure 5.15 Storage Discretisation Resolutions

In a similar fashion to the time interval investigation, the Price Discovery is implemented for the three resolutions and the 8 inflow years, then the resultant water value functions are used in the System Operation Simulation to produce the system operation series. In order to directly compare the water value functions, the 6x12 and 12x21 versions are interpolated to the 9x16 storage discretisation. Before presenting the results of the investigation, the role of the water value function and how it changes over the course of the planning horizon is discussed to provide context for the results.

In the hydro scheduling tool, the hydro generation prices are interpolated from the water value function which is conditioned to a specific inflow sequence and demand profile. Over the course of the year-long planning period, the water value function changes with time. Two examples are presented in Figure 5.16a and Figure 5.16c. They show two water value surfaces from the South Island water value function constructed with the 1976 inflow year at 12:00am on 15th June and 12th November (top and bottom rows respectively) with the 9x16 resolution. Figure 5.16b and Figure 5.16d show side views of the water value surface which emphasise the slope of the water value surfaces. The dotted line is a cross section showing the average South Island water value for all the North Island storage levels.

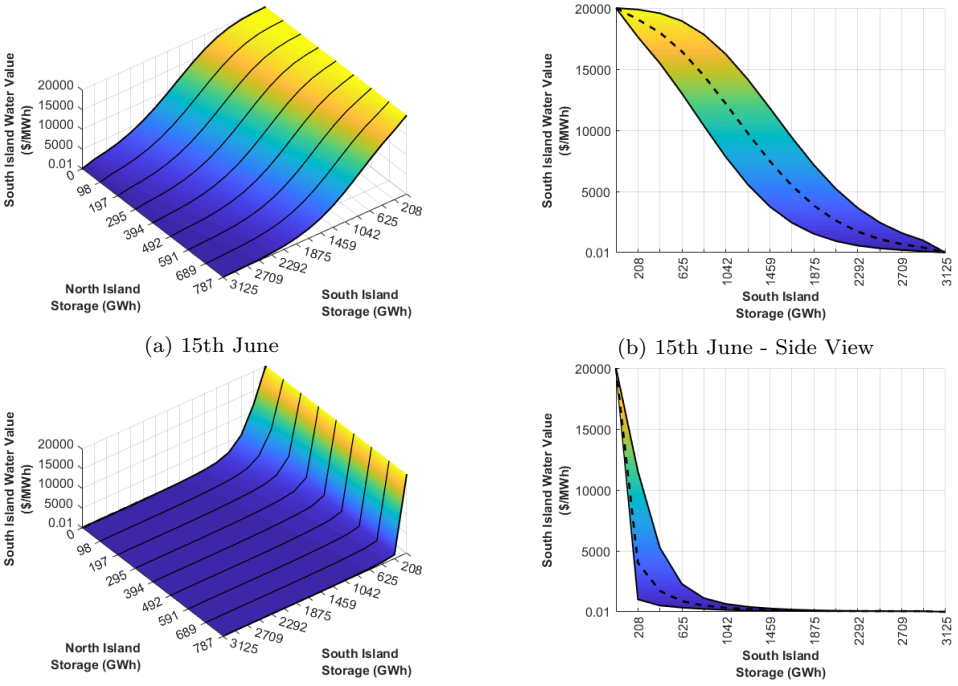

(a) 15th June

(b) 15th June - Side View

(c) 12th November

(d) 12th November - Side View

Figure 5.16 Time Interval specific South Island Water Value Functions Examples. Colour corresponds to the water value and the dotted line is the average South Island water value for all North Island storage levels. 1976 inflow year

Both examples present typical shapes of the water value surfaces. During winter, there are low inflows and high demand and the water value surface is high for all but the highest lake levels. During spring, the high inflows and low demand lead to water value surfaces like the 12th November example. Figure 5.17 presents the average water value shape (dotted line in Figure 5.16b and Figure 5.16d) over time which shows how this shape changes with the changing inflow and demand conditions during the year.

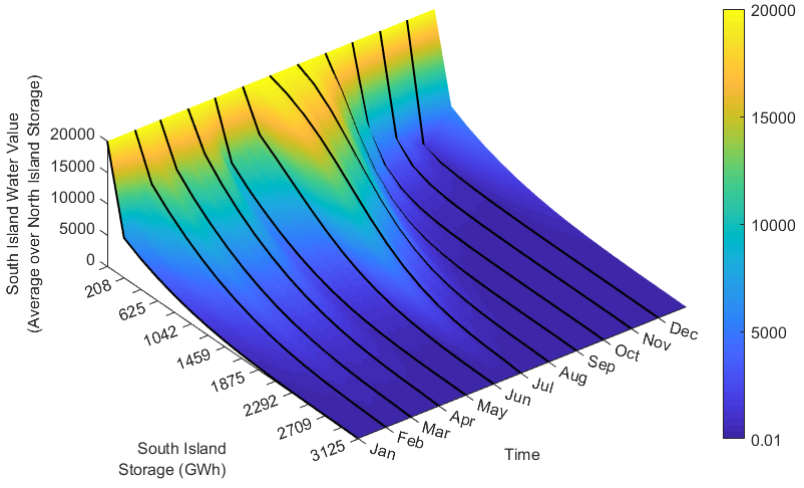

Figure 5.17 South Island Water Value Shape over time - 1976 inflow year

When interpolating to calculate hydro generation prices, if the storage vector ($\hat{s}_t$) is at a high water value on the surface, the hydro generation prices will be high, prompting the system to dispatch thermal generation ahead of hydro generation to conserve stored water and inflows for $t \rightarrow t+1$. From the perspective of the water value surface, the forward step encourages the storage trajectory towards the storage levels with lower water values or down the slope.

For different resolutions, the shape of water value surfaces are similar but the specific water values at particular storage vectors differ. Figure 5.18 presents the average water value shapes for each of the resolution options at 15th June and 12th November. Note that the storage levels marked on the x-axis are the 9x16 resolution South Island levels. As can be seen, with increasing resolution, the water value at a specific storage level is lower. With monotonic non-increasing functions, such as the water value function, linear interpolation will over-estimate the underlying function. Through the backward projection, the error from a stage is carried through to the other stages, eventually reaching a steady state along with the water value functions. This over-estimation decreases with increasing storage discretisation resolution.

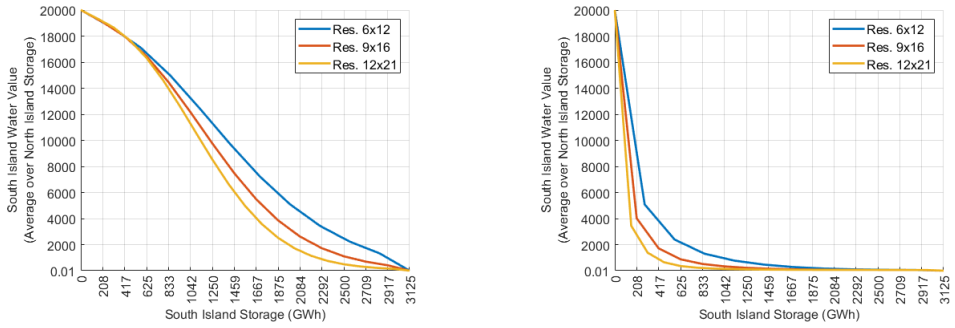

(a) 15th June

(b) 12th November

Figure 5.18 Example of Water Value Shapes for each storage discretisation resolution - 1976 inflow year

This observation is consistent across all time steps and in both reservoirs, as shown in Figure 5.19. Figure 5.19a and Figure 5.19c show the distribution of differences between the 6x12 and 9x16 average water value shapes over time for each inflow year and Figure 5.19b and Figure 5.19d show the distribution of differences between 12x21 and 9x16. As can be seen, the 6x12 water value function is on average above the 9x16 water value function and the 12x21 function is below the 9x16 resolution function.

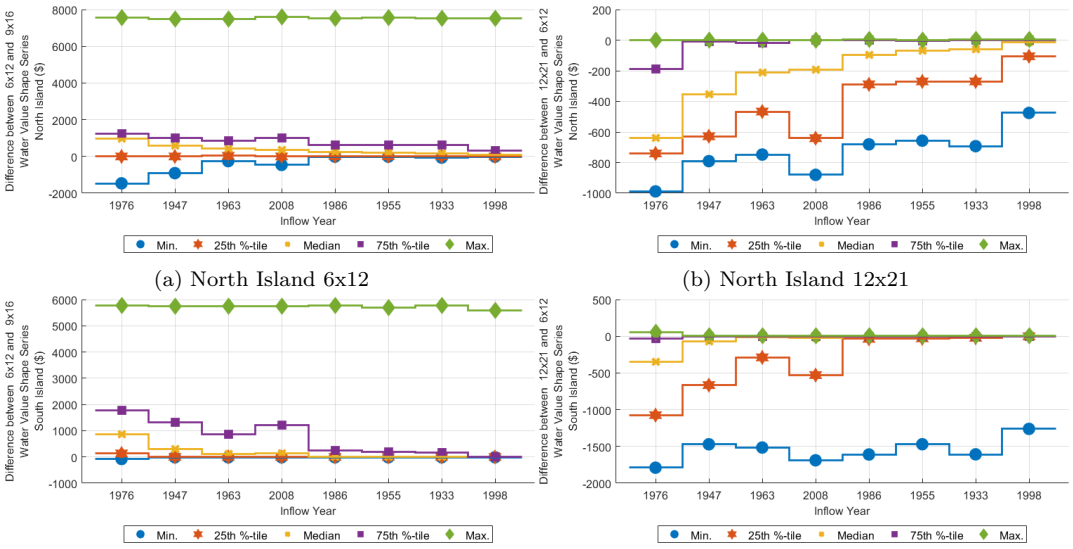

(a) North Island 6x12

(b) North Island 12x21

(c) South Island 6x12

(d) South Island 12x21

Figure 5.19 Difference between Water Value Shapes: Resolution of Storage Levels - 6x12 and 12x21 compared against 9x16 (<North Island Levels>x<South Island Levels>)

Operationally this water value relationship leads to the coarser storage discretisation resolution using more hydro generation and less thermal generation than the higher resolution. Figure 5.20 presents the difference in annual thermal generation between each storage level resolution and the 9x16 resolution for each inflow year, showing this operational difference. Thermal generation is indicative of the hydro storage operation as spill is consistent across all years (Table 5.3), except for in 1976 where the 6x12 resolution leads to 4 GWh of spill.

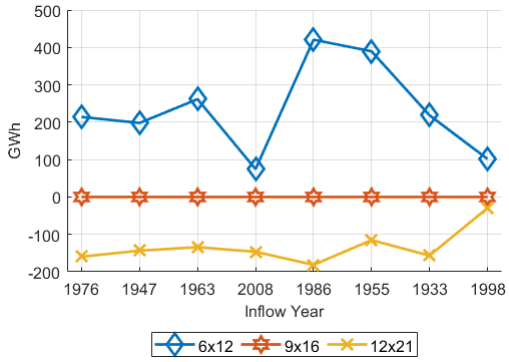

Figure 5.20 Annual Thermal Generation difference between each storage resolution and the 9x16 resolution

The coarser resolution leads to water being valued more highly hence it operates storage at higher level than the higher resolutions. This leads to the 6x12 resolution spilling in the driest year (1976).

Table 5.3 Spill in relevant inflow years for each storage discretisation resolution

Inflow Year	Spill (GWh)		
	6x12	9x16	12x21
1933	303		
1976	4	0	
1998	887		

The main deterrent for using high storage discretisation resolution is the high computation time required. Figure 5.21 shows the time per cycle for each of the resolutions, with 6x12 completing a cycle on average in 4 minutes, 9x16 just above 8 minutes and 12x21 above 12 minutes. As shown in Table 5.4, the 12x21 resolution converges faster than the 9x16 resolution in 1933, 1976 and 1986 inflow years but this is negated by the computation time difference.

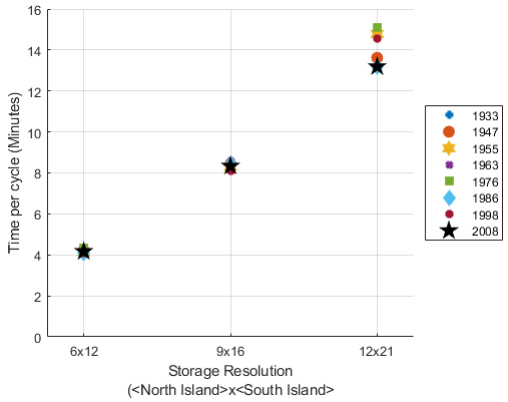

Figure 5.21 Time Per Cycle for each storage resolution

Table 5.4 Number of cycles for the Price Discovery to converge for each inflow year and storage discretisation resolution: 6x12, 9x16 and 12x21

Inflow Year		1933	1947	1955	1963	1976	1986	1998	2008
Storage	**6x12**	4	3	3	4	5	4	4	3
Discretisation	**9x16**	5	3	3	3	5	3	4	3
Resolution	**12x21**	4	3	3	4	3	4	4	3

Given the potential for the 6x12 resolution to over compensate for a dry year inflow sequence (resulting in spill for the 1976 year) and the the computational requirement of the 12x21 resolution, the 9x16 resolution was implemented for the hydro scheduling tool.

Chapter 6

EVALUATING SYSTEM INVESTMENTS

A component of combating climate change is transitioning from fossil fuel thermal generation to low-to-zero emission renewable generation such as wind, solar and geothermal. This transition will involve investing in renewable generation as well as hydro generation, storage and transmission capacity. General consequences of committing to this transition in New Zealand are broadly understood but in order to make informed investment decisions, the benefits and costs of the investments need to be quantified. The costs include economic, environmental, societal and operational components while benefits are related to maintaining security of supply, improving the efficiencies of the electrical power system and reduction of greenhouse gas emissions. Some of the consequences are:

- Building renewable generation to cover low inflow years will result in significant spill in high inflow years. This is commonly referred to as over-building renewable generation.
- Intermittent renewable generation cannot be relied on to provide capacity when needed, particularly during peak demand periods
- In a highly renewable system, thermal generation will tend to operate as peaking plants

The hydro scheduling tool was developed to quantify the impact on hydro dependent electrical power systems as they transition from fossil fuel thermal generation to more must-run intermittent renewable generation. To demonstrate the capability of the tool, a simple case study on a hypothetical 2030 New Zealand system is presented. The impact concerned with here is its ability to improve reliability. This study is not intended to be a robust investigation into potential pathways for New Zealand to transition toward a highly renewable electricity system. To develop these, it would be necessary to account for the costs of the investments, in particular the relative costs, which is the function of system expansion planning tools. Developing such a tool is out-of-scope for this thesis

but the Price Discovery and System Operation Simulation could be integrated into such a tool to provide feedback on the system's viability.

The 2030 system model is detailed in Chapter 3 and Table 6.1 presents an overview of the 2030 system's generation, transmission and storage capacities, annual energy demand and peak demand. The key differences from the 2015 system model are:

- Thermal generation capacity is reduced from 1633 MW to 748 MW which equates to a loss of 885 MW in capacity and 7752.6 GWh of potential energy
- An annual demand increase of 14436 GWh to 58710 TWh (includes the scaling to account for transmission loss) and a peak demand increase of 2128 MW to 8832 MW

Together these mean the system without any extra generation has a maximum energy deficit of 22188.6 GWh and a difference of 2741.1 MW between peak demand and the installed hydro, remaining thermal and the effective geothermal generation capacity (refer to Chapter 3 Section 3.4.4). Note that the maximum energy deficit would only be apparent in dry inflow years.

Table 6.1 2030 Scenario: Generation Capacities and Energy produced, Storage Capacity, HVdc Link Capacity, Demand Peak and Annual Demand Energy. The "+" represents elements whose capacities will be varied in the 2030 scenario simulations while ">" indicates the renewable generation types that will be increased by some degree.

	North Island		**South Island**		**New Zealand**	
	Capacity (MW)	**Energy (GWh)**	**Capacity (MW)**	**Energy (GWh)**	**Capacity (MW)**	**Energy (GWh)**
Hydro	1209.1+	-	3263+	-	4472.1+	-
Thermal	748	-	0		748	-
Wind	>568	>1902.1	>94	>331.2	>662	>2233.2
Solar	-	-	-	-	-	-
RoR	528.7	2072	172	882	700.7	2954
Geo.	>985	>7628	0	0	>985	>7628
Storage	-	787.4+	-	3125.5+	-	3912.8+
HVdc	1200+	-	1200+	-	-	-
Demand	5914	36894	2956	21816	8832	58710

This case study will seek to answer the following questions for the 2030 system model:

1. Determine the amount of additional must run renewable generation required to avoid demand curtailment, focusing on dry inflow years

2. Determine the capability of New Zealand's existing hydro storage capacity to manage the additional intermittent renewable generation and the benefits of increasing its capacity

The study has two steps. The first step is to apply the Price Discovery to the 2030 system with the selection of inflow years used in Chapter 5 and a range of added must-run renewable generation, producing water value functions for each combination. With these water value functions, the System Operation Simulation is conducted using the historical average starting storage, producing system operation series allowing their relationship with the amount of added renewable generation to be examined. The range of added renewable generation is from 15.5 TWh to 26 TWh in 0.75 TWh increments.

The second step is to emulate the proposed Lake Onslow project [Ryan and Bardsey 2020] in the South Island. The proposal is for a pumped hydro storage facility in the lower South Island with a storage capacity up to 4 TWh which would effectively double New Zealand's hydro storage capacity to 7.9 TWh and add around 1 GW of generation capacity, increasing it to 4.263 GW. This project serves as the basis for investigating the effect of increasing hydro storage and generation capacity. Only the additional storage and generation capacities are considered as the hydro scheduling tool does not have the capability to model the pumping component of this project (although this can be easily added) and the inflow sequence into Lake Onslow is negligible. This is modelled by adding 1 GW of capacity to the modelled South Island hydro generation and adding a range of generation capacity to the South Island reservoir (1, 2, 3 and 4 TWh), along with 24.5 TWh of additional renewable generation.

Alongside the Lake Onslow project emulation, the effect of increasing the HVdc Link's capacity is explored. The capacity levels considered are 1200 MW, 1400 MW, 1600 MW, 2000 MW and 2400 MW with the additional 1 TWh storage Lake Onslow case. For the base Lake Onslow simulations, the HVdc capacity is set to 1400 MW to reflect what its capacity will be in 2030 [Transpower New Zealand 2018b]. Lastly, a brief investigation into the effect of different ratios of wind and solar generation that make up the additional renewable generation is conducted. The Price Discovery and System Operation Simulation are applied with this 2030 system model variant in a similar manner as before.

6.1 ADDED RENEWABLE GENERATION

In the 2030 system, the additional renewable generation needs to fulfil the deficit in energy due to the increase in demand and reduction of thermal generation capacity.

The difficulty with determining the amount of renewable generation to install is the balance between supplying sufficient energy in low inflow years while not spilling excessive volumes of water in other years. As such the key relationships to examine with increasing the renewable generation are demand curtailment and spilt energy.

Figure 6.1 presents the demand curtailment in the low inflow years (left) and moderate to high inflow years (right) with increasing renewable generation. The demand curtailment shown consists of two components. In low inflow years (Figure 6.1a) at lower levels of added renewable generation, demand curtailment is dominated by the energy shortfall. The demand curtailment shifts to be capacity based at 22.25 TWh or more added renewable generation due to insufficient capacity during periods with high demand and low wind and solar generation. The capacity based curtailment is also present in the high inflow years for all levels of added renewable generation (Figure 6.1b). With increasing renewable generation, the reduction in energy based curtailment is more significant than capacity based curtailment given that the renewable generation does not always produce during high demand periods (aside from geothermal generation, which adds 18 MW of capacity per 0.75 TWh of additional renewable energy).

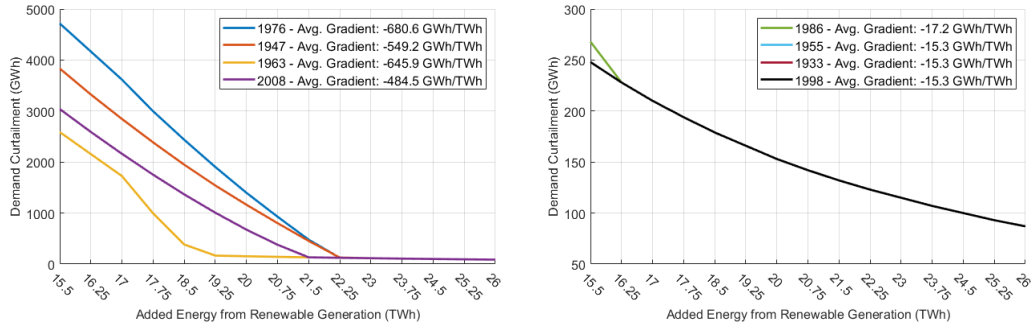

(a) Low inflow years

(b) Moderate to high inflow years

Figure 6.1 Demand Curtailment in Inflow Years over the added renewable generation range with average gradients

The demand curtailment in low inflow years changes from energy to capacity inadequacy with higher levels of added renewable generation. As mentioned, there is a 22200 GWh maximum deficit in the 2030 system in the lowest inflow year. To provide context for the dry years, they can be described as:

- 1976: Worst inflow sequence on record (17280 GWh Total)
- 1947: Expected once in every ~20 years (~5th worst, 19079 GWh Total)
- 1963: Expected once in every ~8 years (~10th worst, 19011 GWh Total)
- 2008: Expected once in every ~4 years (~20th worst, 20548 GWh Total)

The average and median annual inflows are 22283 GWh and 22038 respectively. The rank order of these years accounts for the timing of the inflows, not just the total energy. This is why 1947 is ranked as a worse year than 1963, even though total inflows are slightly greater. Refer to Appendix E for details.

Operationally, insufficient energy results in a hydro storage reservoir being empty for a portion of the year, rendering its hydro generation capacity unavailable. This is shown for the 1976 inflow with 15.5 TWh of added renewable generation with storage in both reservoirs (Figure 6.2a) being empty coinciding with demand curtailment (Figure 6.2b).

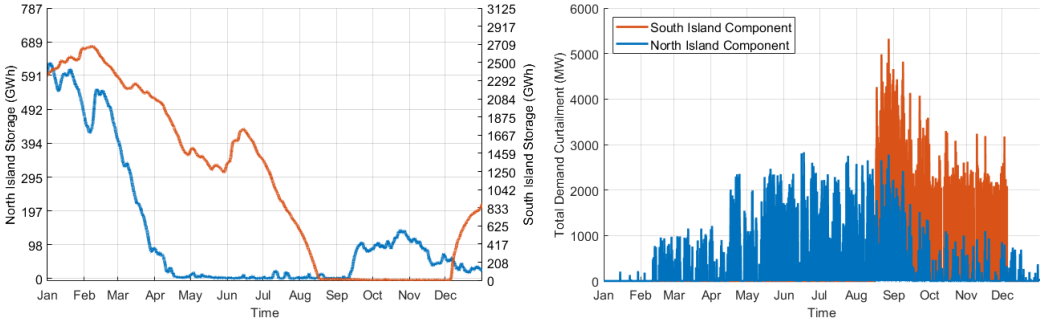

(a) Storage in both reservoirs

(b) Demand Curtailment

Figure 6.2 Storage and Demand Curtailment with the 1976 inflow year. 15.5 TWh of additional renewable generation.

Each increment of added renewable generation results in higher storage trajectories, eventually avoiding empty reservoirs and eliminating demand curtailment due to insufficient energy. The reduction in demand curtailment is not equal to the increase in energy from the renewable generation. This is due to:

- A portion of the renewable generation energy arriving after the empty storage period, highlighting the importance of accounting for the seasonality of the renewable generation, not just the total energy.
- With considerable penetration of non-dispatchable renewable generation, there are occasions where the renewable generation production is greater than demand or its production is restricted by transmission capacity, requiring some amount of spilt energy.
- There is a limit to the amount of water that can be conserved

Regarding the last point, during periods of high must-run renewable generation, hydro generation may be dispatched at its minimum flow level. An example of this occurring is shown in Figure 6.3. For three levels of additional renewable generation (15.5, 16.25 and 17 TWh, shown in Figure 6.3b), it can be seen that the combined North and South

Island hydro generation is reaching its minimum flow level. When this occurs, instead of conserving water, thermal generation is displaced (Figure 6.3c).

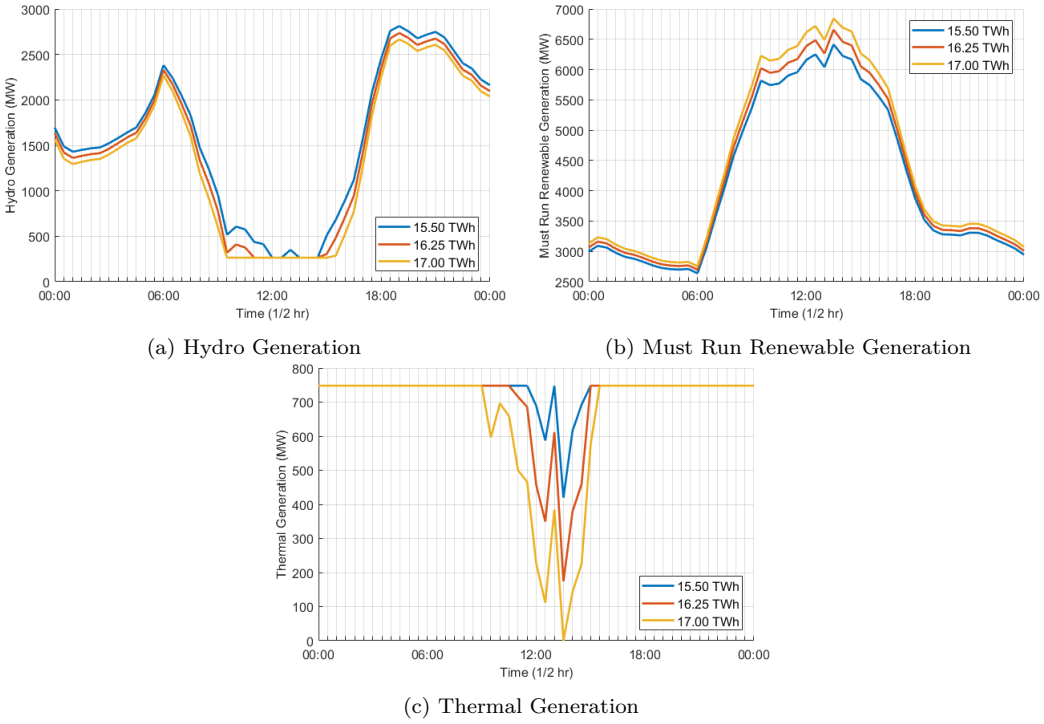

(a) Hydro Generation

(b) Must Run Renewable Generation

(c) Thermal Generation

Figure 6.3 New Zealand Thermal, Hydro and Must Run Renewable Generation on the 19th January. Four added renewable generation levels shown

Figure 6.4 shows the reduction in annual thermal generation with increasing renewable generation for the low inflow years. At lower levels (15.5 to 22.25 TWh), energy shortfall based demand curtailment is occurring (refer to Figure 6.1a) while thermal generation is reducing due to it being displaced by must run renewable generation.

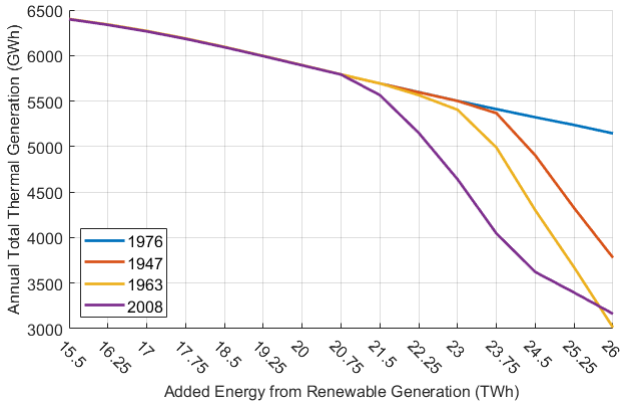

Figure 6.4 Storage in both reservoirs

Based on the demand curtailment relationship, a minimum of 22.25 TWh of added renewable generation is necessary to avoid demand curtailment in the worst dry year. However, a consequence of such a high addition of renewable generation is that in moderate to high inflow years, water will be spilt. Spilling water does not directly threaten security of supply, it is an inefficiency which devalues the investment. Also, if the renewable generation production exceeds demand or is restricted by a transmission capacity constraint, its output will be curtailed. Both the water spilt from reservoirs and the curtailed production over the range of added renewable generation for all inflow years is presented in Figure 6.5.

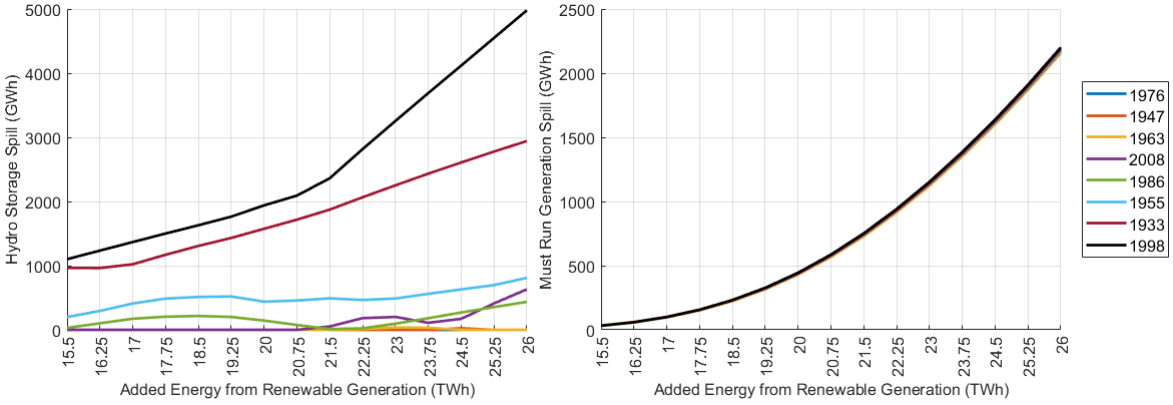

(a) Hydro Storage Spill (b) Renewable Generation Spill

Figure 6.5 Hydro Storage Spill and Renewable Generation Spill over the range of added renewable generation energy for all inflow years

Even at 15.5 TWh of additional renewable generation, 1 TWh is spilt in the first and second highest of the representative inflow years (1998 and 1933), while in the dry inflow years, there is considerable demand curtailment. In the 1986 (median) and 1955 inflow years, water spill is less than 1 TWh. With the 2008 inflow sequence, from 21.5 TWh to 22.25 TWh of added renewable generation, the system transitions from insufficient-energy based curtailment to spilling water highlighting the nature of New Zealand's inflows and limited storage capacity. As indicated by these hydro spill results, in order to cover dry years, some combination of additional generation capacity and storage is necessary. An example of this is explored in Section 6.2. Note that in some cases, must run spill is due to minimum flow hydro generation constraints taking precedence over wind and solar generation.

Figure 6.5b shows the amount of curtailed energy production from the renewable generation as its penetration increases. This can be influenced to some extent by varying the proportions between wind, solar and geothermal generation but is unavoidable at high renewable generation penetrations as is presented in Section 6.3. This is an inherent

inefficiency of high renewable generation penetration, though having flexible demand such as the Lake Onslow pumped hydro storage facility would allow this curtailed production to be used.

Another weakness of must-run renewable generation is that it does not reliably produce when needed, specifically during peak demand periods, meaning capacity-providing assets need to be invested in alongside the renewable generation. Figure 6.6a shows the demand curtailment time series with the 1998 inflow sequence and 24.5 TWh of added renewable generation. Demand curtailment predominantly occurs during the winter months with the peak curtailment being 1626 MW.

To determine the exact factors leading to the demand curtailment, its duration curve and coincident operational variables can be examined. Figure 6.6a presents the demand curtailment time series which when ordered from highest to lowest produces the demand curtailment duration curve. It indicates the percentage of the year that demand curtailment of a certain MW level occurs. For example, from 2.64% to 100% (96.36% of the year), demand curtailment is zero. For the remaining 2.64% of the year, demand curtailment is between 1626 MW and 0 MW. This portion of the duration curve is magnified in Figure 6.7a. The hydro, thermal and renewable generation and HVdc Link power flow values that occur alongside the demand curtailment value are presented in Figure 6.7b, Figure 6.7c and Figure 6.7d. For example, at the peak curtailment point, hydro and thermal generation are at capacity, while must run renewable generation is 1914 MW and power flow is 441.4 MW from the South Island to North Island.

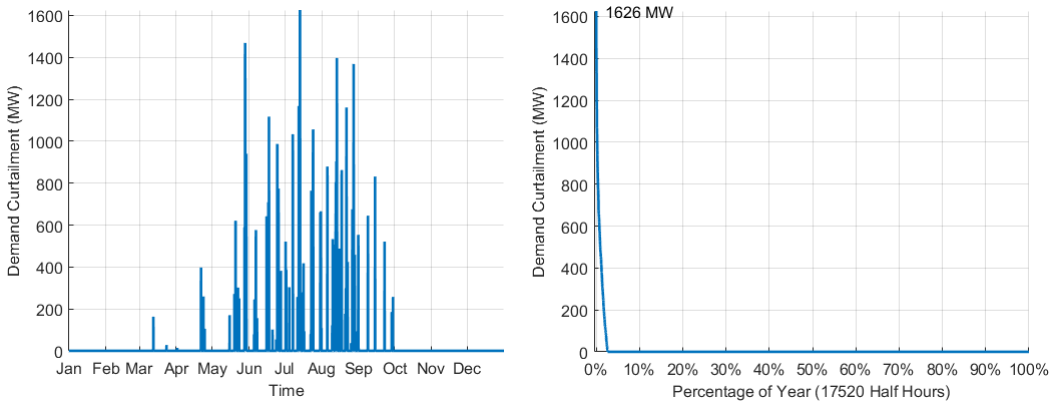

(a) Time Series

(b) Duration Curve

Figure 6.6 Demand Curtailment Time Series and Duration Curve

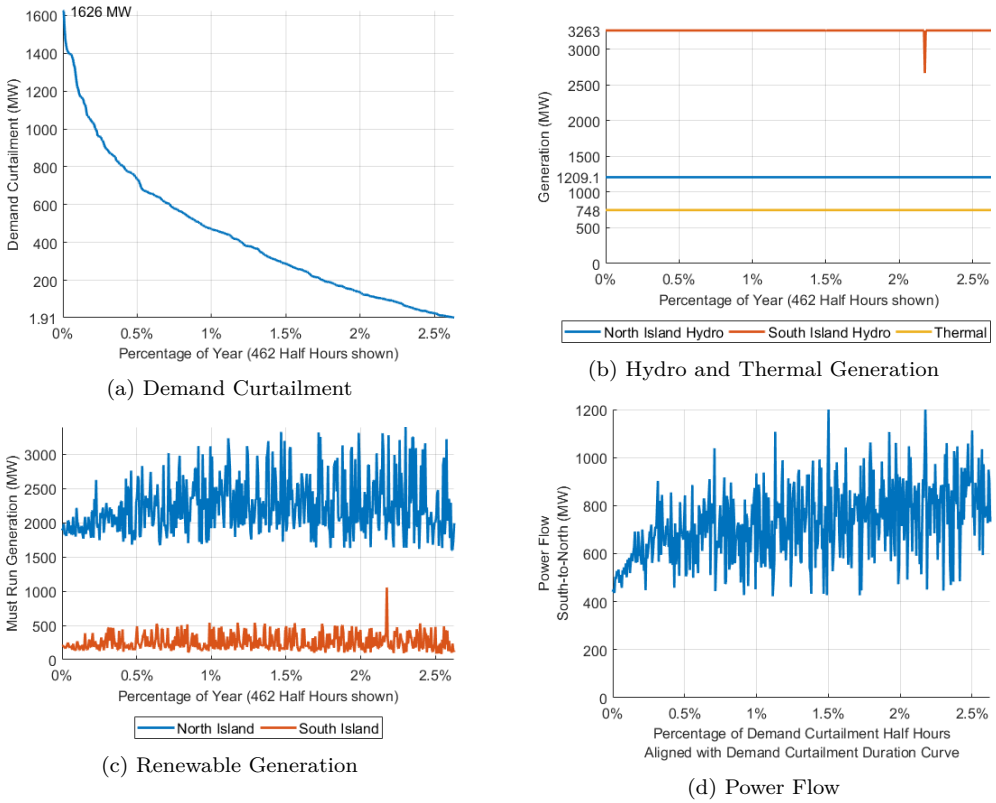

(a) Demand Curtailment

(b) Hydro and Thermal Generation

(c) Renewable Generation

(d) Power Flow

Figure 6.7 Demand Curtailment Duration Curve with corresponding Generation and Power Flow - 1998 Inflow Year

As can be seen, at high demand curtailment periods, must run generation is relatively low while all hydro and thermal generation is at capacity. For the majority of periods, the HVdc Link is unconstrained meaning the demand curtailment is due to a lack of generation capacity. The effect of Lake Onslow's 1 GW addition to South Island hydro generation capacity is shown in Section 6.2.

For reference, the distribution of demand curtailment during the day is presented in Figure 6.8. The majority of periods are during the evening demand peaks while solar generation is low.

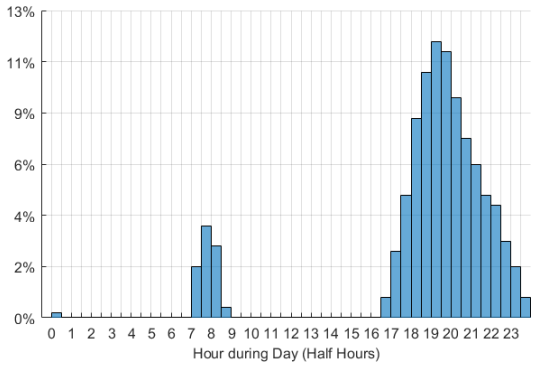

Figure 6.8 Intra-Day Distribution of when Demand Curtailment occurs

6.2 LAKE ONSLOW PROJECT

The emulation of the Lake Onslow project involves increasing the South Island hydro storage and generation capacity. This is in conjunction with 24.5 TWh of added renewable generation. Also, the effect of expanding the HVdc Link capacity and the change in thermal generation operation between the 2015 and 2030 system is briefly examined.

Figure 6.9 shows the hydro storage spill for each expansion of South Island storage capacity. Given that the majority of the selected inflow years had no spill or less than 1000 GWh of spill, the additional 1000 GWh of storage is sufficient to capture the excess water. In the wettest (1998) and 5th wettest (1933) inflow years, an additional 4000 and 3000 GWh extra storage would be required. For the 2030 system model, an additional 1000 GWh of storage is sufficient to cover the majority of inflow conditions. However expanding New Zealand's hydro storage to cater for the increase in must-run renewable generation beyond 2030 could be suitable from a reliability perspective.

To determine the impact of the additional 1000 MW of South Island hydro generation on the capacity based demand curtailment, Figure 6.10 presents the demand curtailment duration curve and accompanying dispatched generation levels, renewable generation and HVdc Link power flow plots as previously presented. The added capacity reduces the demand curtailment due to insufficient capacity by 931 MW from 1626 MW to 695 MW (comparing Figure 6.7a to Figure 6.10a). However, Figure 6.10b shows that the South Island hydro generation has between 1 MW and 797 MW of available capacity during the demand curtailment periods. The South Island hydro generation is limited due to the HVdc link power flow being at capacity for all demand curtailment periods.

Figure 6.11a shows the total demand curtailment if the HVdc Link's capacity is increased up to 2400 MW. The total demand curtailment reduces from 26 GWh to 6 GWh. However as shown in Figure 6.11b, the peak demand curtailment only has a minor decrease as the additional 1000 MW of South Island hydro generation capacity is not sufficient. To cater for the 2030 system scenario peak demand periods, more than the Lake Onslow capacity would be required. In particular, more capacity-providing assets in the North Island are preferable as this avoids the need to invest in more HVdc Link capacity and can contribute to reservoir requirements.

Increasing the HVdc capacity also results in a minor reduction in the must-run renewable generation spill as shown in Figure 6.12. The reduction is approximately 0.075 GWh per MW of added HVdc Link capacity which is highly unlikely to be adequate to justify doubling the current HVdc Link capacity.

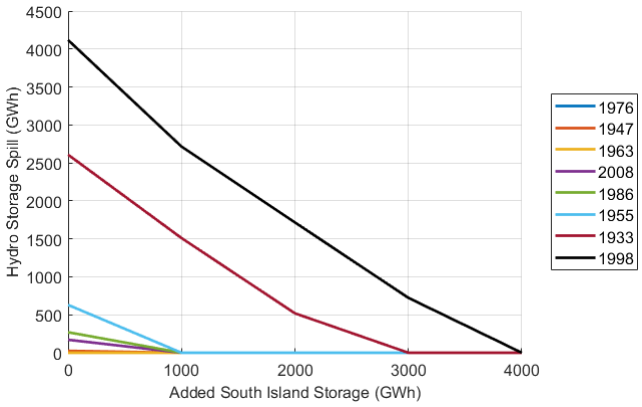

Figure 6.9 Reduction of spill with increasing South Island storage capacity for all inflow years

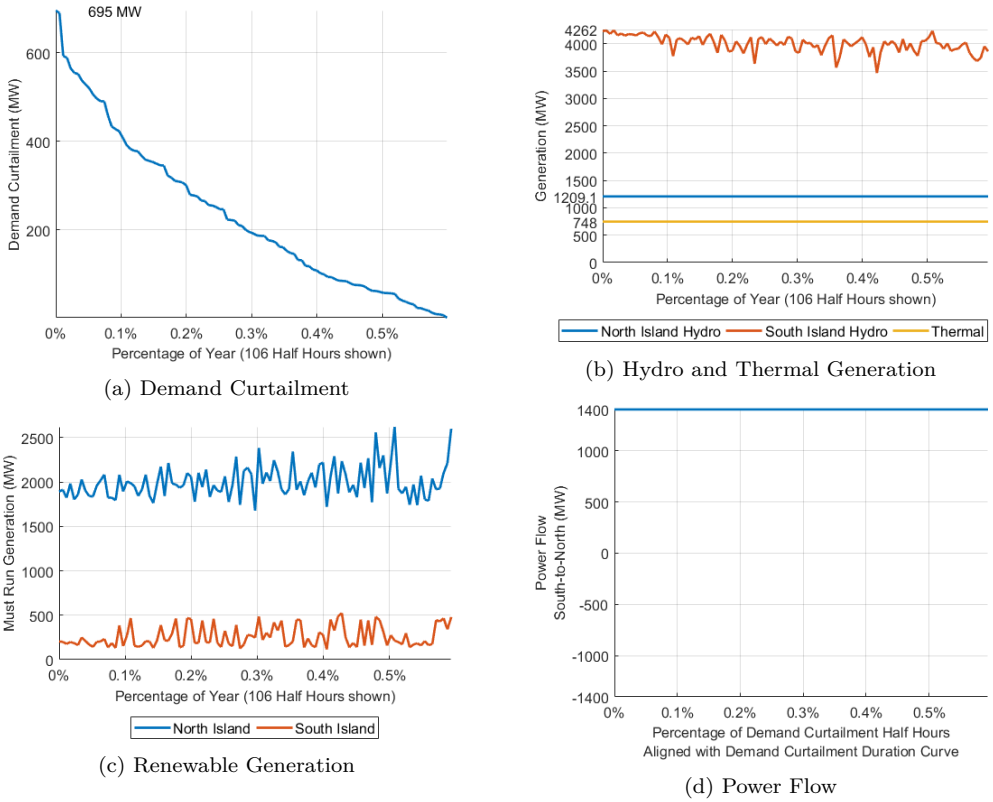

(a) Demand Curtailment

(b) Hydro and Thermal Generation

(c) Renewable Generation

(d) Power Flow

Figure 6.10 Demand Curtailment, Generation and Power Flow at time steps where demand curtailment occurs with additional 1000 MW South Island hydro generation capacity - 1998 Inflow Year

The last finding is how thermal generation operation changes from the 2015 system to the 2030 system. Figure 6.13 presents the thermal generation utilisation (or annual capacity factors) over the range of inflow years ordered from driest to wettest conditions for the 2015 (left) and 2030 (right) models. The 2030 system includes the Lake Onslow project with 1000 GWh of additional hydro storage. With the 2015 system, the variation in annual thermal generation is relatively linear with the inflow conditions where the drier the inflow year, the more thermal generation is used. In the 2030 system, there is

a stronger distinction between dry and wet years with thermal generation supplying baseload in dry years and peaks in wet years. The 2030 relationship highlights the criticality of timing the dispatch of thermal generation in dry years. With less thermal generation capacity, greater foresignt is required to effectively firm hydro storage and avoid empty reservoirs.

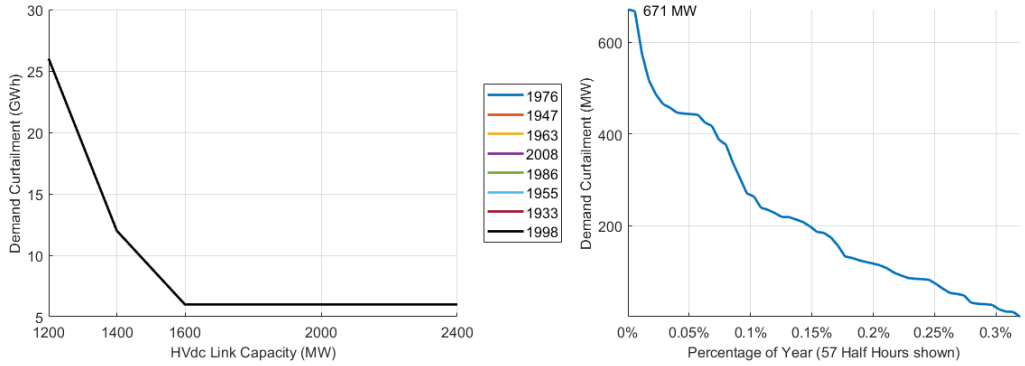

(a) Demand Curtailment (b) Demand Curtailment Duration Curve

Figure 6.11 Demand Curtailment over the range of HVdc Link Capacities and Demand Curtailment Duration Curve (Represents all Inflow Years, 1600-2400 MW HVdc Link Capacity)

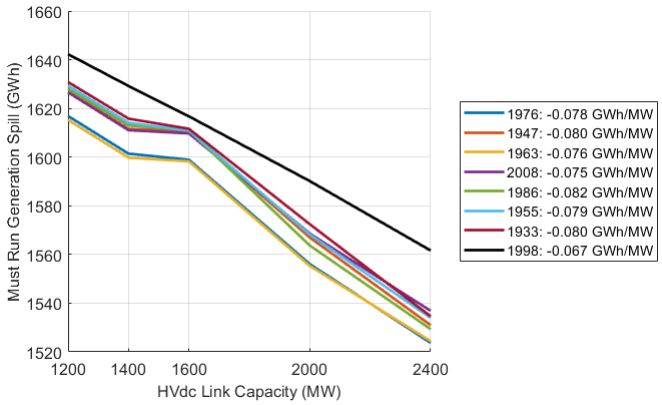

Figure 6.12 Must Run Renewable Generation Spill over the range of HVdc Link Capacities

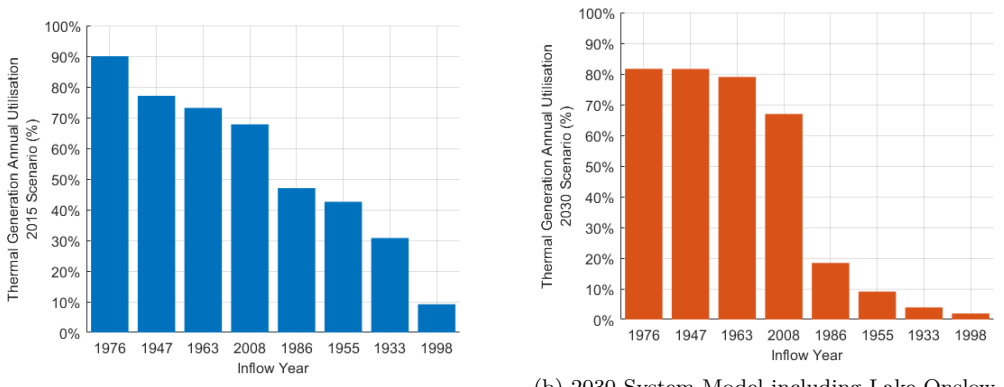

(a) 2015 System Model (b) 2030 System Model including Lake Onslow, 1000 GWh of added Storage case

Figure 6.13 Annual Thermal Generation Utilisation over the inflow years

6.3 WIND VS SOLAR

When investigating the added renewable generation and Lake Onslow project, a fixed ratio of geothermal, solar and wind generation was used. Given the different seasonality and patterns of wind and solar generation, it is worthwhile to briefly examine the impact of varying the ratio between them. No additional geothermal generation was considered as new geothermal capacity is limited.

To determine the effect of different mixes of wind and solar generation, the hydro scheduling tool is applied to the New Zealand system model including 21.5 TWh of additional renewable generation and a range of ratios of wind and solar generation. The chosen ratio was 4 Geothermal : 11 Solar : 6 Wind. The solar-to-wind ratios considered are: 11:6, 9:8, 7:10, 5:12, 3:14 and 1:16. 21.5 TWh of additional renewable generation is selected as, at the 11:6 base ratio across the inflow years, there is:

- Energy Based Demand Curtailment (1976, 1947, 2008)
- Capacity Based Demand Curtailment (1963, 1986, 1955, 1933, 1998)
- Moderate hydro storage spill (1998, 1933)
- Must-run renewable spill (all years)

Note that this investigation is not statistically representative given only the 2015 wind, solar and demand series are used. It primarily serves to demonstrate the hydro scheduling tool's capability to examine different combinations of renewable generation and quantify the differences.

Before examining the results Figure 6.14 presents the difference between solar and wind generation providing context for the investigation. Figure 6.14a shows the quantile range of the 16 years of solar generation data and the 2015 solar generation series. Figure 6.14b shows the same for wind generation data (41 years). Solar generation is highly dependent on sunlight hours, producing more energy during summer (November-Jan) than during winter (June to August). Wind generation is far more variable and shows no consistent seasonality over the years of data. Note the 2015 wind profile has low production during the early months of the year and high production during winter and spring. Ideally the average combined renewable generation pattern would be similar to the demand profile, which in New Zealand is high during winter and low during summer, to reduce the dependence on New Zealand's limited storage.

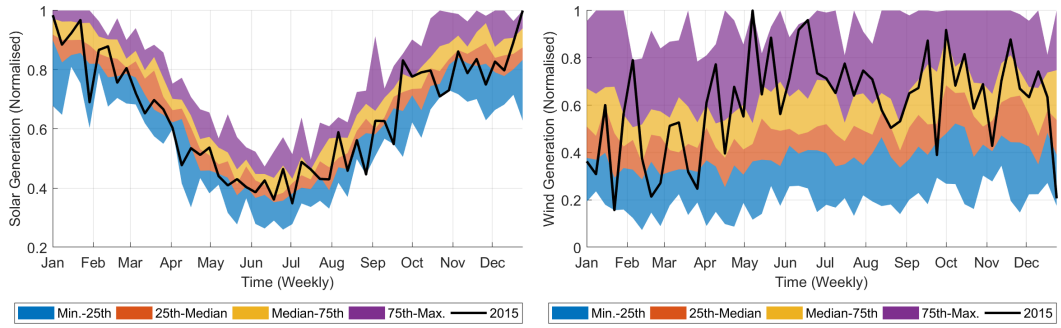

(a) Normalised Solar Generation (b) Normalised Wind Generation

Figure 6.14 Normalised Solar and Wind Generation Patterns

Figure 6.15 presents the demand curtailment of low inflow years and must-run generation spill annual totals over the range of solar-to-wind ratios. The x-axis shows the solar-to-wind energy ratio (<Solar #>:<Wind #>). The main conclusion that can be drawn from Figure 6.15 is that having 1.4 to 2.4 times more wind generation than solar generation provides the best diversity in terms of demand curtailment and must-run generation spill reductions.

At a high proportion of wind generation (1:16), less energy is supplied during the early months of the year (January-March). This leads to more hydro generation being dispatched resulting in lower storage leading into winter. Although the 2015 wind series has high output over winter, it is insufficient. Note that the water value for both the North and South Island is such that thermal generation is effectively baseloaded. With a high proportion of solar generation (11:6), there is insufficient energy provided during winter leading to empty reservoirs and demand curtailment.

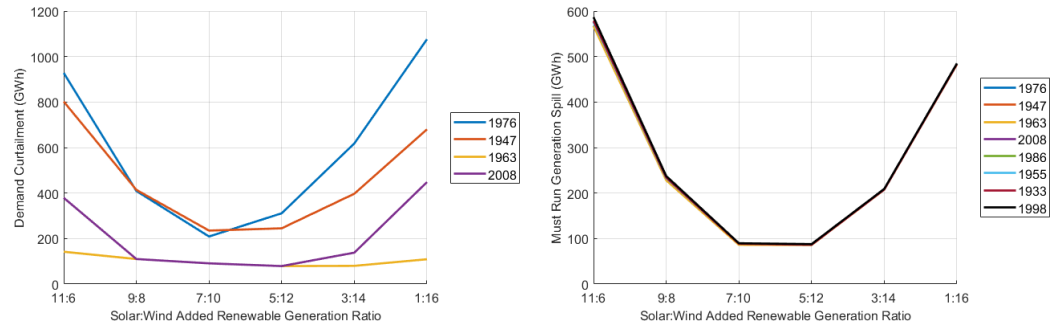

(a) Demand Curtailment - Low Inflow Years (b) Must-Run Generation Spill

Figure 6.15 Low Inflow Year Demand Curtailment and Must-Run Generation Spill across all inflow years over a range of solar and wind generation ratios providing 21.5 TWh

Figure 6.16 shows the demand curtailment in moderate-to-high inflow years and hydro storage spill. The total demand curtailment over the solar-wind ratios shown in Figure 6.16a is due to insufficient capacity with a trough of 79 GWh at 5:12 and high end point values of 142 GWh at 11:6 and 109 GWh at 1:16. There is a preference of wind

generation since solar generation is low during the evening demand peaks whereas wind generation is more likely to be producing. Although as wind generation is intermittent, its alignment with demand peaks is inconsistent as shown with the increase in demand curtailment from 3:14 to 1:16 with increased wind generation.

As presented in Figure 6.16b, there is no consistent relationship between hydro spill and the ratio between solar and wind generation. In the 1998 inflow year, the more wind generation, the higher the spill whereas in the 1933 inflow year, spill reduces. As such, spill depends largely on the inflow pattern over the year, more so than on the ratio between wind and solar generation.

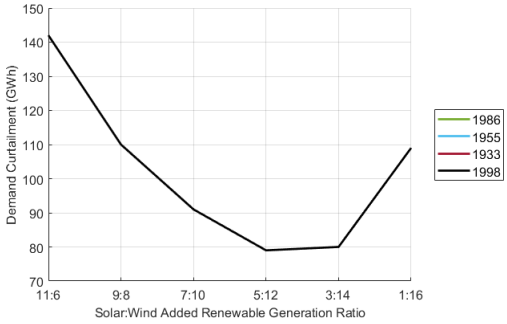

(a) Demand Curtailment - Moderate to High Inflow Years

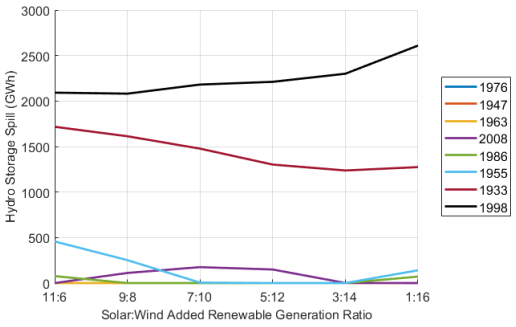

(b) Hydro Storage Spill

Figure 6.16 Demand Curtailment and Spill over a range of solar and wind generation ratios providing 21.5 TWh.

6.4 STUDY CONCLUSIONS AND HYDRO SCHEDULING TOOL REVIEW

The study involves investigating a 2030 scenario for New Zealand's electricity system using the hydro scheduling tool to quantify the value of various system investments for reducing demand curtailment and spilt energy. These investments consist of additional must-run renewable generation (wind, solar and geothermal), hydro generation and storage capacity and transmission capacity. The investments are needed to supply the 2030 system increase in demand and reduction of thermal generation capacity. The two study questions are:

1. Determine the amount of additional must run renewable generation required to avoid demand curtailment, focusing on dry inflow years

2. Determine the capability of New Zealand's existing hydro storage capacity to manage the additional intermittent renewable generation, and the benefits of increasing its capacity

Initially the 2030 system was simulated with a range of renewable generation penetrations from 15.5 TWh to 26 TWh supplied by a fixed proportion of geothermal, solar and wind generation (4 : 11 : 6 respectively) for a selection of representative inflow years. Following this, the Lake Onslow Project was emulated by increasing the South Island's hydro generation capacity by 1 GW, the HVdc link capacity to 1400 MW, a range from 1 TWh to 4 TWh of additional South Island hydro storage and 24.5 GWh of additional renewable generation. Further, the effect of varying the HVdc capacity from 1200 MW to 2400 MW and the impact of changing the ratio between solar and wind generation was explored.

It was found that demand curtailment arose from two factors: insufficient energy and inadequate capacity. With insufficient energy, the hydro reservoirs are inevitably emptied, removing hydro generation capacity, resulting in demand curtailment. This primarily occurs in low inflow years such as 1976 and 1947. With a minimum of 22.25 TWh of additional must run renewable generation, empty reservoirs are avoided. A consequence of this penetration is that in high inflow years such as 1998 and 1933, hydro storage spill is significant being around 2800 GWh and 2000 GWh over the year.

Demand curtailment due to inadequate capacity is unavoidable across all inflow years. It decreases with increasing renewable generation, but this is marginal given the intermittency of wind and solar generation and whether their production aligns with demand peaks. Peak demand curtailment coincides with low renewable generation production periods. The only means explored to reduce this demand curtailment was increasing the South Island hydro generation capacity by 1 GW which heavily reduced it.

Regarding the second study question, hydro storage spill was less than 500 GWh across 6 of the 8 representative inflow years. Significant spill occurred in the high inflow years (1998 and 1933) for the majority of the added renewable generation range. As found with the Lake Onslow Project study, an additional 1000 GWh of hydro storage would manage the majority of inflow years with the 2030 system scenario. To both minimise demand curtailment due to insufficient energy in dry years and eliminate spill in wet years, at least 3000 GWh of additional storage would be required.

Other findings of the study were:

- In the Lake Onslow Project, the additional 1 GW of hydro generation capacity is inadequate to eliminate capacity based demand curtailment. Although this is specific to the chosen 2030 demand profile, it does highlight the need for capacity-providing or shifting assets such as controllable generation capacity, demand

response and battery storage.

- In the 2030 model, with increased renewable generation and reduced thermal generation capacity, the annual utilisation of thermal generation changes dramatically depending on hydro inflows. During moderate-to-high inflow years, thermal generation capacity factors were less than 20% as they were operating as peaking plants. In low inflow years thermal generation is effectively baseloaded with capacity factors above 70%.
- From examining how the proportion of wind and solar generation changing the demand curtailment and spill in the system, there is value in coordinating their overall proportions to capitalise on their diversity.

The major weakness of the study is the use of only 2015 data particularly with solar and wind generation profiles. As such, none of the results or findings can be used directly. However, the study does present useful preliminary findings. In particular the tool's ability to determine the value of investing to meet the system energy and capacity requirement by increasing generation capacity, storage capacity and transmission capacity. The tool also clarifies probable dispatch landscapes for system scenarios such that storage management and utilisation of thermal generation can be gauged. Given this, the hydro scheduling tool can be used to inform government policy and investment decisions.

Chapter 7

CONCLUSION

The hydro scheduling problem is concerned with the management of hydro schemes in an optimal manner. The complexity of the hydro scheduling problem is in part due to the current decision influencing all future decisions. Methodologies have been developed, aiming to make the problem computationally tractable while representing the system with a sufficiently detailed model. Practices such as aggregating hydro schemes and systems to reduce dimensionality, spatially and temporally decomposing the problem and incrementally changing and experimenting with solution techniques has contributed to the broad range of methodologies developed to model a diverse range of systems. Studies have investigated changes to electricity systems, such as deregulation and, at present and pressingly, the transition away from fossil fuel thermal generation.

To study this transition, a medium term (one year time horizon) deterministic Dynamic Programming modelling tool was developed (the Price Discovery) which produced optimal water value functions. Typically medium term tools employ weekly time intervals given the computational burden higher resolutions impose. The developed modelling tool is capable of using time intervals from a half hour to one day, which allows the impacts of the electricity system capacity constraints to influence the water value functions. A high temporal resolution captures the impact of renewable generation's high frequency intermittency and variability.

During the development of the Price Discovery, a range of water value boundary conditions were tested at a high temporal resolution. It is shown that the boundary condition (empty and full storage) water values play a critical role in forming the water value function. When boundary values are based on system dispatch, they end up narrowly bounding the water value range in a way that is strongly dependent on the temporal resolution. For Dynamic Programming based tool, boundary values should not be dynamically updated but fixed at spill and demand curtailment costs.

New Zealand's electricity system serves as the case study to demonstrate the capability

of the hydro scheduling tool. A two-node, two-reservoir model was developed which, although simple, captures the major constraints and dynamics of the system while limiting the computational load on the modelling tool. The two-node model incorporates the major transmission constraint, the HVdc Link which connects the North Island and South Island, and the mismatch between the majority of demand being in the North Island while the majority of hydro generation and storage is in the South Island. The two-reservoir hydro model captures the different inflow seasonality between the islands.

The principle guiding the development of the modelling tool and system model was to minimise the computational intensity while capturing the hydrological dynamics and major constraints in New Zealand's system. This parsimonious approach was taken as the value of the modelling tool is to examine a large number of potential future systems and compare their performance, rather than a small number in detail.

Two sensitivity studies were conducted to determine an appropriate Price Discovery time interval and the number of discrete levels to use for the storage state space. The Price Discovery time interval determines what temporal variations are captured in the water value functions. On short time intervals, peak demand and the high frequency changes in renewable generation are apparent hence capacity constraints are active more often. On long time intervals, the emphasis is on balancing energy demand and supply with only extreme mismatches activating the capacity constraints. The time intervals investigated were 0.5, 1, 2, 6, 12 and 24 hours. In general, the higher the temporal resolution, the higher water is valued which leads to higher operating storage trajectories and longer computation times. As a compromise between the computational load and capturing the variations in demand and renewable generation, a 6 hour time interval was selected.

The second sensitivity study examined the storage state space discretisation with three options: 6x12, 9x16 and 12x21 (number of <North Island> x <South Island> levels). The Price Discovery produces an approximation of the water value functions, hence the higher the resolution, the closer the approximation. Since linear interpolation was used in the modelling tool and water value functions are monotonic non-increasing, the approximate water value function is an overestimate and the error is reduced for higher resolutions. With the 6x12 resolution, in a dry (low) inflow year, water was spilt due to the approximation being too course. Further, the 12x21 resolution, although the most accurate option, was too computationally intensive. As such the 9x16 option was selected.

To demonstrate the modelling tool's ability to conduct system studies examining the

integration of renewable generation, it was applied to a 2030 scenario of the New Zealand system model. The relationships that were determined include:

- The efficiency of additional renewable generation for providing energy and capacity
- The volume of unavoidable spill with the additional renewable generation
- The value of additional hydro storage capacity to capture excess generation leading to demand curtailment and spill being reduced
- The impact of various combinations of wind and solar generation

It was also found that the thermal generation operational mode in the modelling shifted from a relatively consistent relationship with the inflow year condition for the present day system, to a far more binary mode where in dry years they were baseloaded and in wet years they primarily supplied peaks. This highlights the difficulty of ensuring there is sufficient energy available in dry years by either maintaining the operational viability of thermal generation or replacing them with another resource.

7.1 FUTURE WORK

This thesis presents a hydro scheduling modelling tool and New Zealand system model and showcases the tool's capability to study the transition to a more climate friendly electricity system, namely shifting from fossil fuel thermal generation to renewable generation. However there is still room for further development.

First focusing on extensions to the thesis development process, deterministic inflows and a simple system model were opted for to allow reasonable computation times with the Price Discovery using a half hour time interval. This is very useful, as it provides an upper bound for how well the system can meet its energy supply commitments. However, the Price Discovery would ideally be extended to encompass uncertain inflows and the system model needs to have at least three reservoirs. With three reservoirs, one of the hydro schemes in either island could be separated and studied in more detail. A more detailed transmission system representation is possible as well. Given that pumped hydro storage is a potential investment, adapting the tool to incorporate these types of facilities would be useful.

Clutha and Waikaremoana schemes have dynamics and constraints not accounted for that influence their operation. For the Clutha scheme, a reasonable portion of inflows do not flow into the major storage reservoir, but into a smaller reservoir that only offers intra-day flexibility, effectively leading to the Clutha scheme having a significant

run-of-river generation component. For the Waikaremoana scheme, there is a range of storage and flow constraints that also lead to run-of-river style operation. As it stands, the hydro system model does not capture these behaviours, hence refining the aggregate hydro system model to account for these dynamics and determine whether it makes a significant difference relative to the operation of the existing aggregate model would be a good test of the latter's appropriateness.

As mentioned in Chapter 3, demand response and battery storage will likely play an integral role in managing the intermittency of renewable generation in future electricity systems. Integrating these and others (e.g. pumped hydro storage) into the modelling tool will allow a more detailed examination of future system scenarios.

As shown in Chapter 3 Section 3.6, the simulated dispatch of thermal generation is far less variable than the market based operation, in part due to the model's crude thermal generation price tranches. In terms of actual system operation, experimenting with methods to better approximate the more variable dispatch of thermal generation would assist in proving the modelling tool's applicability to the real world system. This could involve using a more granular thermal price curve.

With the advantage of modern day computing resources, conducting a direct comparison of a temporally decomposed modelling suite (long, medium and short term tools) versus a single high temporal resolution would be worthwhile to determine how well the dominant decomposition approach compares to an all-in-one tool. This is not to invalidate the temporal decomposition, but strictly to determine whether there is any significant cost to decoupling short, medium and long term dynamics.

Finally, to add to the exploration of renewable generation integration, conduct a statistically representative study to refine the future system relationships (such as wind versus solar generation) would add to the global effort to plan for this needed transition. Such a study would involve using a range of high temporal resolutions to capture the intermittency of renewable generation.

Appendix A

SMALL HYDRO SCHEMES AS RUN-OF-RIVER GENERATORS

Table A.1 presents the hydro generation and storage capacities of New Zealand's schemes. The New Zealand system model includes Waitaki, Waikato, Manapouri, Clutha and Waikaremoana and the smaller remaining schemes were excluded. By aggregating the large reservoirs together, there is the assumption that they are coordinated to achieve the optimal dispatch while managing their individual reservoirs. By extension, the smaller schemes could be coordinated with the larger reservoirs, for example dispatching the smaller schemes to conserve water in large reservoirs, even on an intra-day time scale. However, storage in the smaller schemes is relatively small, and they are usually dispatched to broadly match their inflow sequences.

Table A.1 Hydro Scheme's Generation and Hydro Storage Capacities

Scheme Name	**Island**	**Generation Capacity (MW)**	**Hydro Storage (GWh)**
Waitaki	South	1723	2388
Waikato	North	1071.7	633
Manapouri	South	800	438
Clutha	South	740	299
Waikaremoana	North	138	154
Coleridge	South	35	39
Cobb	South	32	29
Tongariro	North	360	11
Mangahao	North	19	2
Matahini	North	72	1

Appendix B

CLUTHA SCHEME INFLOW SEQUENCE DETERMINATION

Figure B.1 presents the functional Clutha scheme layout of reservoirs, generation and waterways. The red and green arrows indicate the availability of the inflow data at various points in the scheme. The issue with the Clutha scheme is that the Wakatipu outflow data is not available. As such the Roxburgh outflow data is used as the aggregate reservoir input. The error with this is that it includes the Manuherikia River flows which does not pass through Lake Dunstan and the first hydro generator (Clyde). Manuherikia River is a relatively minor tributary flow.

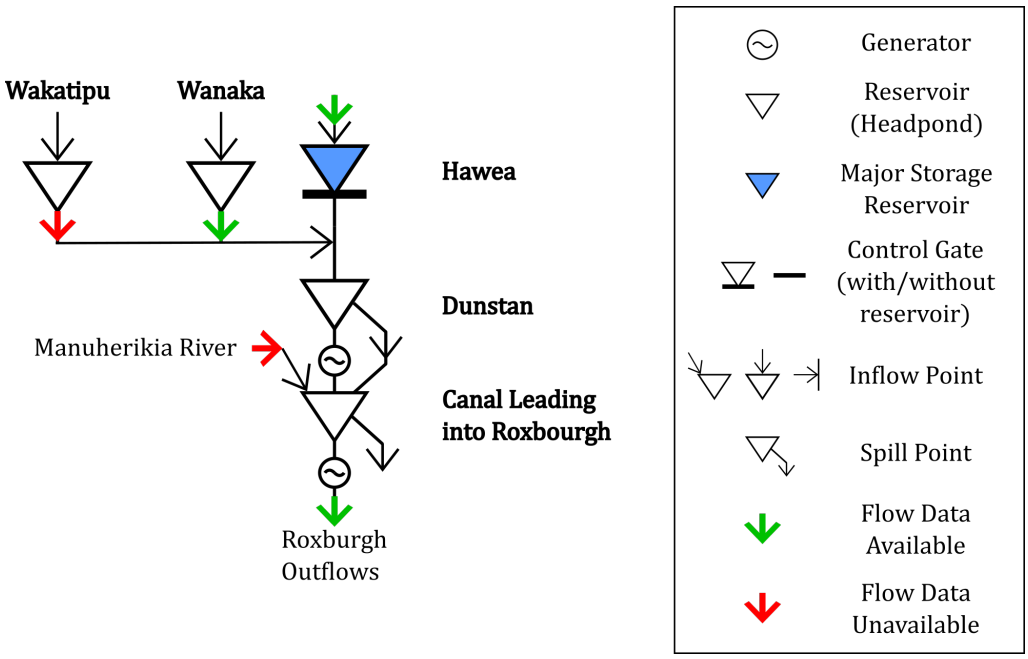

Figure B.1 Clutha Scheme - Detailed

Appendix C

NEW ZEALAND TRANSMISSION SYSTEM AND GENERATION MAP

Figure C.1 presents the geographical distribution of generation and Figure C.2 shows the transmission system. Both figures were sourced from Electricity Authority [2018].

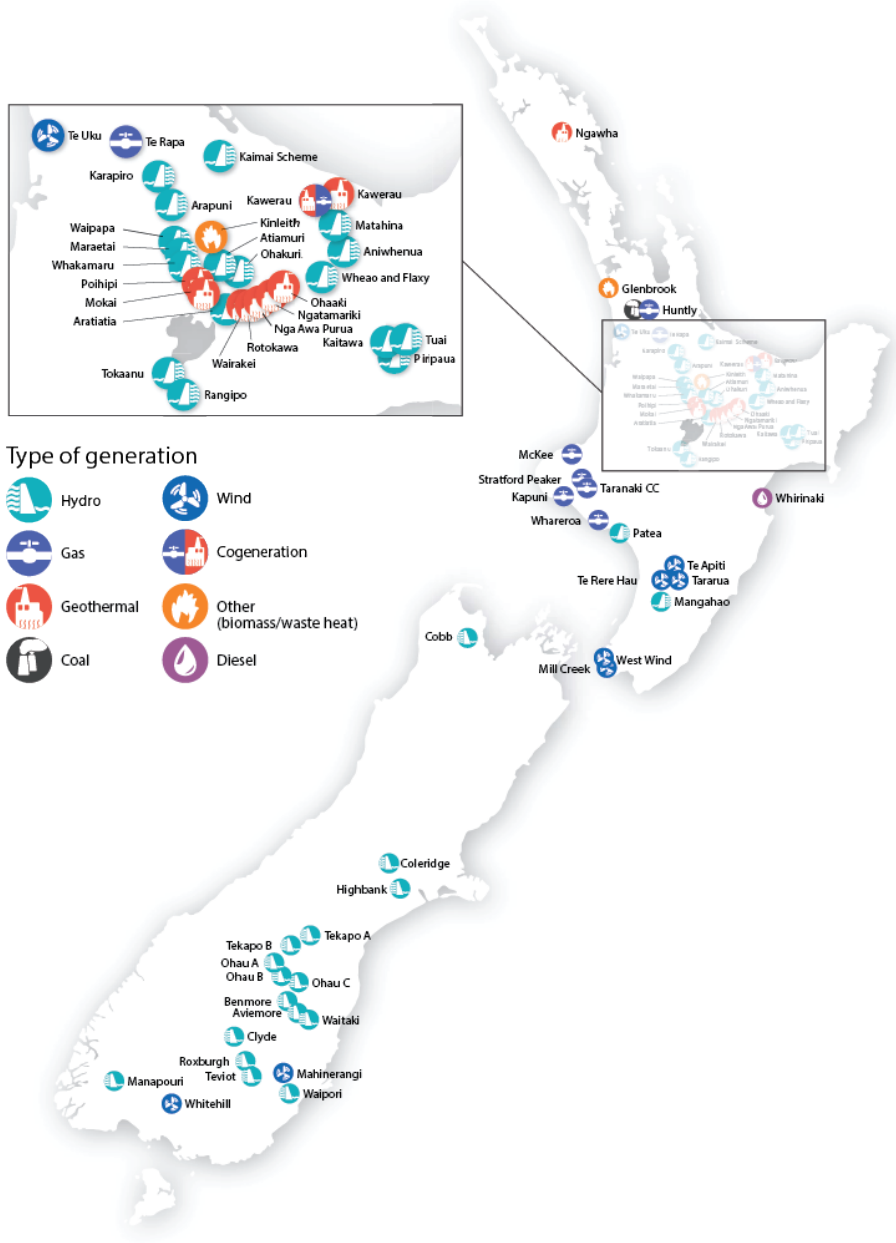

Figure C.1 New Zealand Generation Map

Figure C.2 New Zealand Transmission Map

Appendix D

THERMAL GENERATION PRICING VERIFICATION

In New Zealand's electricity system, generation is offered into the spot market. The offers are allowed to consist of five tranches with increasing prices and variable MW capacity allocations. The typical form of an offer is one or two low priced tranches (~$0.01) that are essentially guaranteed to be dispatched for the generation-retail companies contracted demand followed by high priced tranches that are generally aimed to sell electricity to their competitors.

Table D.1 presents the thermal generation prices use in the New Zealand system model. Given that much of the fuel data for the prices are out-of-date, distributions of thermal generators' tranches' prices and capacities are presented to verify whether the prices were adequately representative. Note that the price axis are all log based and the tranche data is from 2016.

Table D.1 Thermal Generation Capacities and Prices. McKee's and TCC's heat rates were from the manufacturer's specifications

Thermal Generator	**Capacity (MW)**	**Heat Rate (GJ/MWh)**	**Fuel Type**	**Price ($/GJ)**	**Price ($/MWh)**
Huntly Coal	500	10.3	Coal	5.72	58
Huntly e3p	400	7.2	Gas	7	50
Huntly p40	48	9.8	Gas	7	68.6
McKee	100	9.127	Gas	7	63.9
Stratford Peaker	200	8.362	Gas	7	58.5
TCC	385	7.6	Gas	7	53.2

Across all distributions, the prices of the second to fourth tranche are between $50 and $100, which contains the thermal generation prices used.

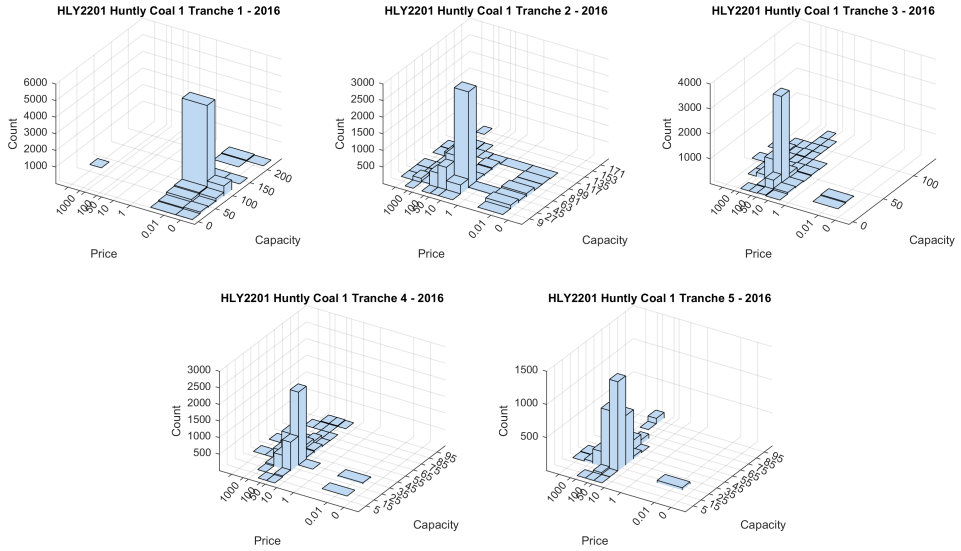

Figure D.1 Huntly Coal Unit 1

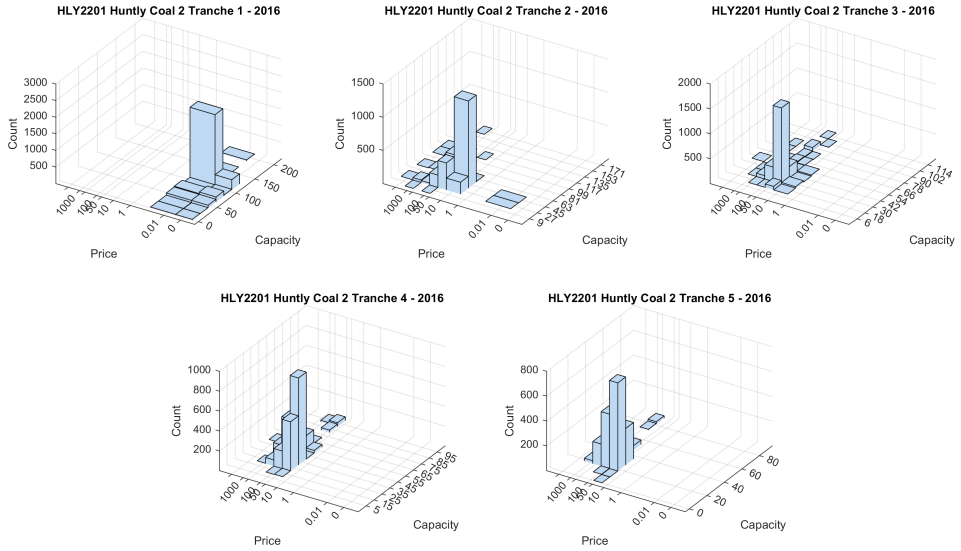

Figure D.2 Huntly Coal Unit 2

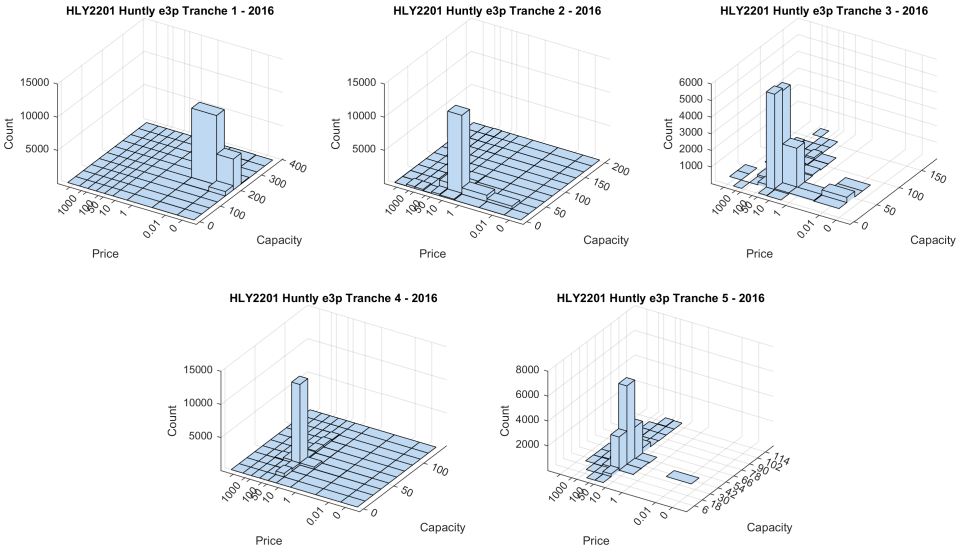

Figure D.3 Huntly Gas e3p Unit

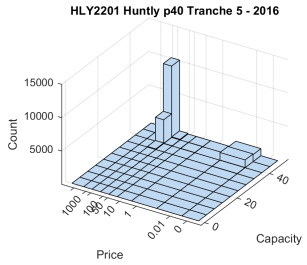

Figure D.4 Huntly Gas p40 Unit

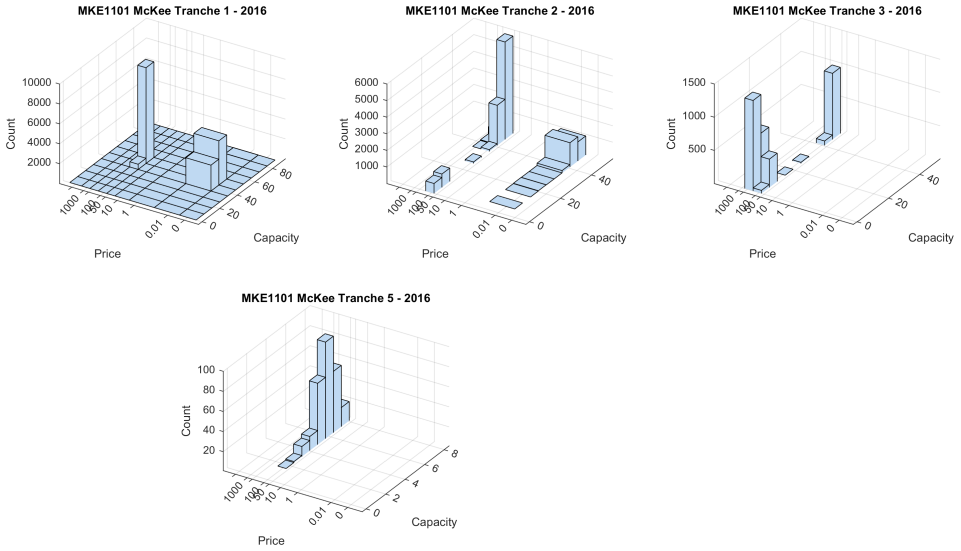

Figure D.5 McKee Gas

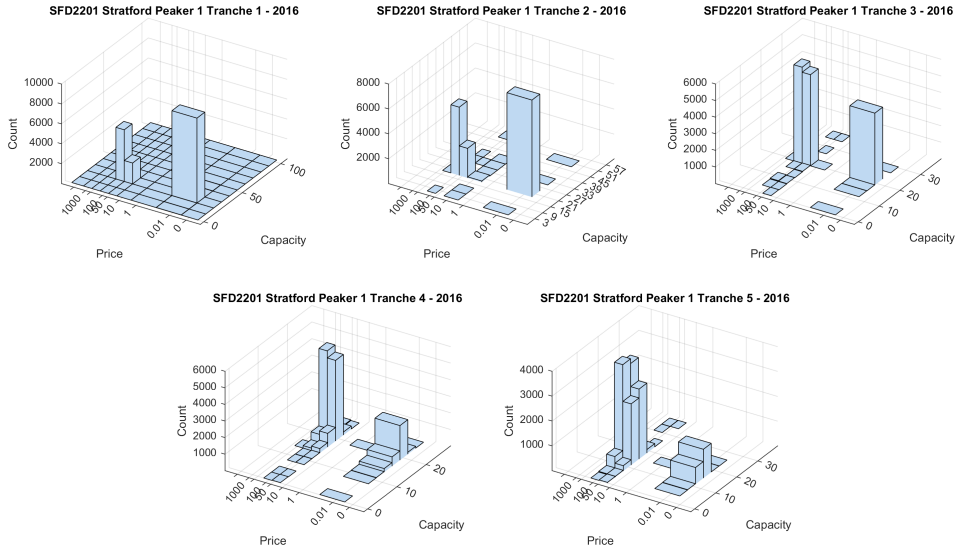

Figure D.6 Stratford Peaker Unit 1

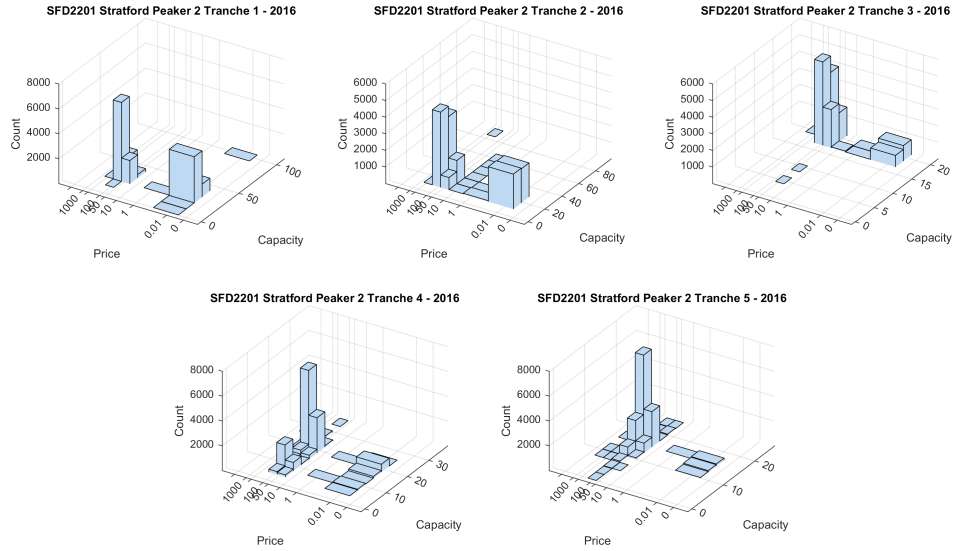

Figure D.7 Stratford Peaker Unit 2

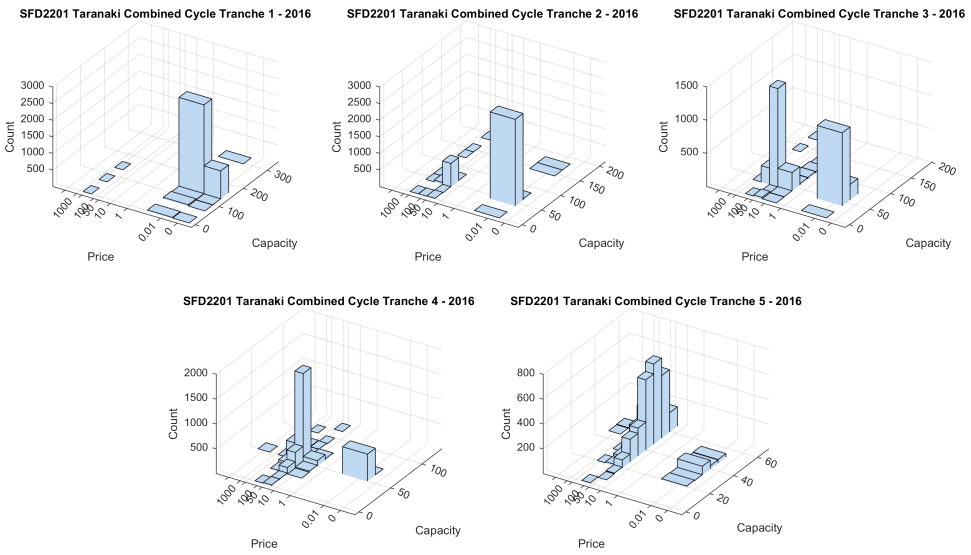

Figure D.8 Taranaki Combined Cycle

Appendix E

REPRESENTATIVE INFLOW SELECTION

The representative inflow sequences used in Chapter 5 and Chapter 6 were determined by simulating the 2015 year with 85 inflow sequences (1932 to 2016), examining the annual renewable generation percentage distribution and then selecting the years that are the 0th (minimum), 5th, 10th, 20th, 50th (median), 90th, 95th and 100th (maximum) percentile renewable generation percentages. Figure E.1 presents the distribution.

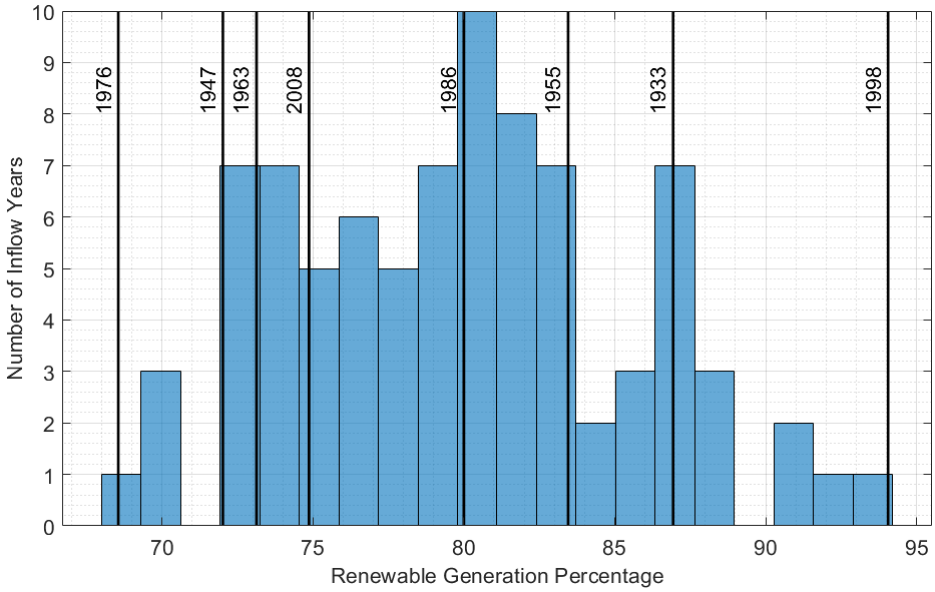

Figure E.1 Renewable Percentage Distribution of inflow years from 1932-2016 and the representative selections

Appendix F

SIMULATION COMPUTER SPECIFICATIONS

Table F.1 Average computer and software specifications

Specification	**Value**
Processor:	Intel Core i7-8700 3.20 GHz
RAM:	16 GB
Optimisation Tool:	IBM ILOG CPLEX Optimisation Studio 12.8.0
Modelling Development Tool:	MATLAB 2018b, 2019b

Appendix G

NEW ZEALAND ELECTRICITY MARKET AND SIMULATED OPERATION DATA DISCREPANCY

There are two apparent components contributing to the data discrepancy between operation by New Zealand's Electricity Market (NZEM) and the simulated operation. The first component is the difference in annual demand values as shown in Table G.1. The demand data for the simulated operation was based on the nodal level demand data sourced from the Electricity Authority's (EA) Electricity Market Database [Electricity Authority 2021], specifically via the dataset portal. These nodal demand series were then aggregated together. The NZEM demand data is presumably based on the same EA EMI demand but is processed by EA's system and presented via a reporting portal (which is separate to the dataset portal). As a consequence of this demand difference, the total simulated hydro and thermal generation is greater than that of the NZEM. The additional demand value is from the Ministry of Business Innovation and Employment [2020] (MBIE) data is present to show another value of demand. Note the simulated demand value is approximately halfway between the NZEM and MBIE values.

The second apparent component of the discrepancy is from the conversion of the hydrological data to energy values. Table G.2 presents the water (energy) balance of the simulated and NZEM systems. The simulated operation balances with the storage and inflow-generation difference (net energy into the system) being equal whereas the NZEM has 0.76 TWh of missing energy. For both the simulated and NZEM calculations, the inflows and storage values are based on the hydro system scaling outlined in Chapter 3. This water balance comparison appears to show that the water-to-energy conversion overestimates the amount of energy. Note, although spill is not presented here, the NZEM did not spill 0.76 TWh worth of water.

Table G.1 Comparison of New Zealand Demand Values from the Simulated, New Zealand Electricity Market (NZEM) and the Ministry of Business, Innovation and Employment. Values are in GWh

	Simulated	NZEM	MBIE
Demand	41324	39439	43349
Hydro Generation	17851	16790	-
Thermal Generation	21883	20951	-

Table G.2 Comparison of the Simulated and New Zealand Electricity Market (NZEM) water balance. Values are in TWh

	Starting Storage	Total Inflows	Total Hydro Generation	Ending Storage	Storage Difference	Inflow, Generation Difference
Simulated	2.53	21.62	21.88	2.27	-0.26	-0.26
NZEM	2.53	21.62	20.95	2.45	-0.09	0.67

REFERENCES

Becker, L. and Yeh, W.W.G. (1974), 'Optimization of real time operation of a multiple-reservoir system', *Water Resources Research*, Vol. 10, No. 6, pp. 1107–1112.

Bellman, R. (1954), 'The theory of dynamic programming', *Bull. Amer. Math. Soc.*, Vol. 60, No. 6, pp. 503–515.

Brandi, R.B.S., Ramos, T.P., Dias, B.H., Marcato, A.L.M. and da Silva Junior, I.C. (2015), 'Improving stochastic dynamic programming on hydrothermal systems through an iterative process', *Electric Power Systems Research*, Vol. 123, pp. 147–153.

Celeste, A., Curi, W. and Curi, R. (2009), 'Implicit Stochastic Optimization for deriving reservoir operating rules in semiarid Brazil', *Pesquisa Operacional*, Vol. 29.

Celeste, A.B. and Billib, M. (2009), 'Evaluation of stochastic reservoir operation optimization models', *Advances in Water Resources*, Vol. 32, No. 9, pp. 1429–1443.

Chong, E.K.P. and Zak, S.H. (2013), *An Introduction to Optimization*, John Wiley & Sons, Incorporated, Somerset, UNITED STATES.

Concept Consulting Group Limited (2013), 'Gas Supply and Demand Scenarios 2012 - 2027: March 2013 update including Maui pipeline analysis', Tech. rep., Wellington.

Côté, P. and Leconte, R. (2016), 'Comparison of Stochastic Optimization Algorithms for Hydropower Reservoir Operation with Ensemble Streamflow Prediction', *Journal of Water Resources Planning and Management*, Vol. 142, No. 2, p. 4015046.

Covec (2014), 'Coal Prices in New Zealand Markets: 2013 Update', Tech. rep., Ministry of Business Innovation and Employment, Wellington.

de Matos, V. and Finardi, E. (2012), 'A computational study of a stochastic optimization model for long term hydrothermal scheduling', *International Journal of Electrical Power & Energy Systems*, Vol. 43, pp. 1443–1452.

Dias, B., Marcato, A., Souza, R., Soares, M., Junior, I., Oliveira, E., Brandi, R. and Ramos, T. (2010), 'Stochastic Dynamic Programming Applied to Hydrothermal Power Systems Operation Planning Based on the Convex Hull Algorithm', *Mathematical Problems in Engineering*, Vol. 2010.

Duenas, P., Ramos, A., Tapia-Ahumada, K., Olmos, L., Rivier, M. and Pérez-Arriaga, J.I. (2018), 'Security of supply in a carbon-free electric power system: The case of Iceland', *Applied Energy*, Vol. 212, pp. 443–454.

Electricity Authority (2018), 'Electricity in New Zealand', Tech. rep., Wellington.

Electricity Authority (2021), 'Electricity Market Information', .

Farias, C., Celeste, A., Sakata, Y., Kadota, A. and Suzuki, K. (2006), 'Use of Monte Carlo optimization and artificial neural networks for deriving reservoir operating rules', *PROCEEDINGS OF HYDRAULIC ENGINEERING*, Vol. 50, pp. 25–30.

Flatabø, N., Haugstad, A., Mo, B. and Fosso, O. (2002), 'Short-term and Medium-term Generation Scheduling in the Norwegian Hydro System under a Competitive Power Market Structure', .

Fredo, G.L.M., Finardi, E.C. and de Matos, V.L. (2019), 'Assessing solution quality and computational performance in the long-term generation scheduling problem considering different hydro production function approaches', *Renewable Energy*, Vol. 131, pp. 45–54.

Grygier, J.C. and Stedinger, J.R. (1985), 'Algorithms for Optimizing Hydropower System Operation', *Water Resources Research*, Vol. 21, No. 1, pp. 1–10.

Henao, F., Rodriguez, Y., Viteri, J. and Dyner, I. (2019), 'Optimising the insertion of renewables in the Colombian power sector', *Renewable Energy*, Vol. 132.

Howard, R.A. (1960), *Dynamic programming and Markov processes.*, John Wiley, Oxford, England.

IBM (2018), 'CPLEX Optimisation Studio V12.8', .

Johnson, S.A., Stedinger, J.R., Shoemaker, C.A., Li, Y. and Tejada-Guibert, J.A. (1993), 'Numerical Solution of Continuous-State Dynamic Programs Using Linear and Spline Interpolation', *Operations Research*, Vol. 41, No. 3, pp. 484–500.

Kelman, J., Stedinger, J.R., Cooper, L.A., Hsu, E. and Yuan, S.Q. (1990), 'Sampling stochastic dynamic programming applied to reservoir operation', *Water Resources Research*, Vol. 26, No. 3, pp. 447–454.

Kirk, D.E. (1970), *Optimal Control Theory: An Introduction*, Prentice-Hall, Englewood Cliffs.

Labadie, J.W. (2004), 'Optimal Operation of Multireservoir Systems: State-of-the-Art Review', *Journal of Water Resources Planning and Management*, Vol. 130, No. 2, pp. 93–111.

Lee, J.H. and Labadie, J.W. (2007), 'Stochastic optimization of multireservoir systems via reinforcement learning', *Water Resources Research*, Vol. 43, No. 11, pp. 1–16.

Lindqvist, J. (1962), 'Operation of a Hydrothermal Electric System: A Multistage Decision Process', *Transactions of the American Institute of Electrical Engineers. Part III: Power Apparatus and Systems*, Vol. 81, No. 3, pp. 1–6.

Little, J.D.C. (1955), 'The Use of Storage Water in a Hydroelectric System', *Journal of the Operations Research Society of America*, Vol. 3, No. 2, pp. 187–197.

Littman, M.L., Dean, T.L. and Kaelbling, L.P. (1995), 'On the Complexity of Solving Markov Decision Problems', pp. 394–402.

Mariño, M.A. and Mohammadi, B. (1983), 'Reservoir Operation by Linear and Dynamic Programming ', .

MATLAB (2019), *Version 9.6 (R2019a)*, The MathWorks Inc., Natick, Massachusetts.

McQueen, D. (2016), *Quantifying the benefits from the spatial diversification of wind power in New Zealand.*, Doctor of philosophy, University of Canterbury.

Ministry of Business Innovation and Employment (2020), 'Data tables for electricity', Tech. rep., Ministry of Business Innovation and Employment, Wellington.

Moreira, R. and Celeste, A. (2017), 'Performance evaluation of implicit stochastic reservoir operation optimization supported by long-term mean inflow forecast', *Stochastic Environmental Research and Risk Assessment*, Vol. 31, pp. 1–8.

Newham, N. (2008), *Power System Investment Planning using Stochastic Dual Dynamic Programming*, Doctor of philosophy, University of Canterbury.

Pereira, M.V.F. and Pinto, L.M.V.G. (1983), 'Application of Decomposition Techniques to the Mid - and Short - Term Scheduling of Hydrothermal Systems', *IEEE Transactions on Power Apparatus and Systems*, Vol. PAS-102, No. 11, pp. 3611–3618.

Pereira, M.V.F. and Pinto, L.M.V.G. (1991), 'Multi-stage stochastic optimization applied to energy planning', *Mathematical Programming*, Vol. 52, No. 1-3, pp. 359–375.

Pérez-Arriaga, I.J. (2007), 'Security of electricity supply in Europe in a short, medium and long-term perspective', *European Review of Energy Markets*, Vol. 2, No. 2, pp. 1–28.

Philbrick Jr., R.C. and Kitanidis, P.K. (1999), 'Limitations of Deterministic Optimization Applied to Reservoir Operations', *Journal of Water Resources Planning and Management*, Vol. 125, No. 3, pp. 135–142.

Philpott, A., Guan, Z., Khazaei, J. and Zakeri, G. (2010), 'Production inefficiency of electricity markets with hydro generation', *Utilities Policy*, Vol. 18, No. 4, pp. 174–185.

Read, E. and Hindsberger, M. (2010), 'Constructive Dual DP for Reservoir Optimization', In *Handbook of Power Systems I*, pp. 3–32.

Read, R.A. (2014), *Developing alternative SCDDP implementations for hydro-thermal scheduling in New Zealand*, Masters of commerce, University of Canterbury.

Ryan, K. and Bardsey, E. (2020), 'Lake Onslow hydro project: Pros and cons', .

Santos-Martin, D. and Lemon, S. (2015), 'SoL – A PV generation model for grid integration analysis in distribution networks', *Solar Energy*, Vol. 120, pp. 549–564.

Scott, T.J. and Read, E.G. (1996), 'Modelling hydro reservoir operation in a deregulated electricity market', *International Transactions in Operational Research*, Vol. 3, No. 3, pp. 243–253.

Srdjević, B. (1985), 'The Successive Approximations DP Method for Preliminary Development of the Operating Rules for Multiple Purposes Reservoirs', .

Stage, S. and Larsson, Y. (1961), 'Incremental Cost of Water Power', *Transactions of the American Institute of Electrical Engineers. Part III: Power Apparatus and Systems*, Vol. 80, No. 3, pp. 361–364.

Stedinger, J.R., Sule, B.F. and Loucks, D.P. (1984), 'Stochastic dynamic programming models for reservoir operation optimization', *Water Resources Research*, Vol. 20, No. 11, pp. 1499–1505.

Tejada-Guibert, J.A., Johnson, S.A. and Stedinger, J.R. (1993), 'Comparison of two approaches for implementing multireservoir operating policies derived using stochastic dynamic programming', *Water Resources Research*, Vol. 29, No. 12, pp. 3969–3980.

Transpower New Zealand (2018a), 'Scheduling and Dispatch', .

Transpower New Zealand (2018b), 'Te Mauri Hiko - Energy Futures', Tech. rep., Transpower New Zealand, Wellington.

Transpower New Zealand (2021), 'Software Specifications: RMT Specification', .

Turgeon, A. (2005), 'Solving a stochastic reservoir management problem with multilag autocorrelated inflows', *Water Resources Research*, Vol. 41, No. 12, pp. 1–9.

Turgeon, A. and Charbonneau, R. (1998), 'An aggregation-disaggregation approach to long-term reservoir management', *Water Resources Research*, Vol. 34, No. 12, pp. 3585–3594.

Wallace, S.W. and Fleten, S.E. (2003), 'Stochastic Programming Models in Energy', In *Stochastic Programming*, Vol. 10 of *Handbooks in Operations Research and Management Science*, pp. 637–677, Elsevier.

Warland, G. and Mo, B. (2016), 'Stochastic Optimization Model for Detailed Long-term Hydro Thermal Scheduling Using Scenario-tree Simulation', *Energy Procedia*, Vol. 87, pp. 165–172.

Willis, R., Finney, B.A. and Chu, W.S. (1984), 'Monte Carlo Optimization for Reservoir Operation', *Water Resources Research*, Vol. 20, No. 9, pp. 1177–1182.

Wolfgang, O., Haugstad, A., Mo, B., Gjelsvik, A., Wangensteen, I. and Doorman, G. (2009), 'Hydro reservoir handling in Norway before and after deregulation', *Energy*, Vol. 34, pp. 1642–1651.

WSP Opus (2018), 'Hydrological Modelling Dataset Report 2: Flow Series Description and Methodology', Tech. rep., Electricity Authority, Wellington.

Yang, Z., Liu, P., Cheng, L., Wang, H., Ming, B. and Gong, W. (2018), 'Deriving operating rules for a large-scale hydro-photovoltaic power system using implicit stochastic optimization', *Journal of Cleaner Production*, Vol. 195.

Yeh, W.W., Becker, L., Hua, S., Wen, D. and Liu, J. (1992), 'Optimization of Real-Time Hydrothermal System Operation', *Journal of Water Resources Planning and Management*, Vol. 118, No. 6, pp. 636–653.

YOUNG, G.K. (1967), 'Finding Reservoir Operating Rules', *Journal of the Hydraulics Division*, Vol. 93, No. 6, pp. 297–322.